Association of Local Immune Suppression in Skin with HPV-Induced Epithelial Hyperplasia

Paula Ting-Yu Kuo

Bachelor of Biomedical Sciences/ Master of Biochemistry and Molecular Biology

A thesis submitted for the degree of Doctor of Philosophy at

The University of Queensland in 2018

Faculty of Medicine

The University of Queensland Diamantina Institute

Abstract

Persisting high-risk human papillomavirus (HPV) infection is a major cause of cervical cancer, which develops from cervical intraepithelial neoplasia (CIN). "High-risk" HPVs, in particular HPV16 and HPV18, are able to evade immunosurveillance in some patients, and create a suppressive local immune environment. Expression of viral protein E7 causes a dysregulated cell cycle, a result of E7 and Rb protein interaction, leading to epithelial hyperplasia of the infected area. A suppressive local immune environment has been observed in E7-expressing mouse skin with a thickened epithelial layer. Previously, animal studies on immune responses against persisting high-risk HPV infection have not separated the effects of expression of viral protein E7 from the effects of the accompanying skin hyperplasia. However, hyperproliferative epithelium can contribute to the change of immune responses by secreting a unique profile of cytokines and chemokines. In this project, mice expressing the HPV16 E7 protein as a transgene in keratinocytes, with (K14.E7xRb$^{\Delta L/\Delta L}$) or without (K14.E7) disrupted interaction of E7 with Rb in keratinocytes are utilised. The epithelial transcriptome, subsets of skin-infiltrating/ residing immune cells, and immune responses are analysed in these mice, and compared with non-transgenic mice. I have thus investigated separately the contribution of E7 protein expression, and of E7-Rb interaction-associated skin hyperplasia, to the suppressive local immune environment.

Suppressed peripheral immune responses were observed in the K14.E7 transgenic animals. These correlated with up-regulated regulatory cytokine secretion, infiltration of regulatory immune cells and ineffective antigen presentation, and comparison with K14.E7xRb$^{\Delta L/\Delta L}$ mice allowed me to establish that these were a consequence of hyperproliferative epithelium, rather than of E7 expression. Further, keratinocytes of K14.E7xRb$^{\Delta L/\Delta L}$ were able to present both exogenous E7 peptide, and endogenous (transgenic) E7 antigen, enabling antigen-specific T cell lysis *in vitro*, whereas keratinocytes of K14.E7 mice were only able to present exogenous E7 peptide effectively to T cells. To understand the changes induced by E7-Rb interaction and its associated epithelial hyperplasia, whole skin RNA sequencing was utilised. A unique profile of cytokine/ chemokine secretion that associated with epithelial hyperplasia alone was identified. In particular, chemokines CXCL9 and CXCL10 were highly upregulated in non-haematopoietic cells in the hyperproliferative epithelium and recruit CXCR3$^+$ lymphocytes to the hyperplastic skin. Overexpression of CXCL9 and CXCL10 is not observed in K14.E7xRb$^{\Delta L/\Delta L}$ skin, and CXCR3$^+$ T cells are preferentially recruited by

CXCL9 and CXCL10 in supernatants of K14.E7 but not K14.E7xRb$^{\Delta L/\Delta L}$ skin cultures *in vitro*. CXCR3 signalling promotes infiltration of a subset of effector T lymphocytes that enables rejection of donor lymphocyte deficient, E7-expressing skin grafts. This suggests that recruitment of CXCR3$^+$ T cells can be an important factor in the rejection of precancerous skin epithelium providing they can overcome local immunosuppressive mechanisms driven by skin-resident lymphocytes. In comparison to the suppressive local immunity of K14.E7 skin, skin immune responses were induced normally in the K14.E7xRb$^{\Delta L/\Delta L}$ transgenic mouse. It was therefore expected that the K14.E7xRb$^{\Delta L/\Delta L}$ skin, unlike K14.E7 skin, would be rejected when transplant onto syngeneic non-transgenic recipients. However, rejection was not observed, even when the skin was grafted onto transgenic recipients with E7-specific cytotoxic T cells and E7 specific immunisation. Skin-derived CD11b$^+$ DCs were present in reduced numbers in the skin draining lymph node of K14.E7xRb$^{\Delta L/\Delta L}$ skin graft recipients, when compared with non-transgenic skin graft recipients. Thus, I hypothesise that this may contribute to impaired rejection of K14.E7xRb$^{\Delta L/\Delta L}$ skin. Taken together, the hyperplastic epithelium contributes to CXCR3$^+$ effector T cell recruitment. However, the CXCR3$^+$ T cell population is insufficient to overcome the locally suppressed immune environment generated by E7-Rb interaction and its associated epithelial hyperplasia. Disruption of the interaction can only partially restore the immune responses, as the skin without E7-Rb interaction was not rejected when transplanted.

In summary, this project provides evidence that highlights the differential role of HPV16E7 expression and E7-Rb interaction-associated hyperplasia and gains insights to the local immune responses against persistent HPV infection.

Declaration by author

This thesis is composed of my original work, and contains no material previously published or written by another person except where due reference has been made in the text. I have clearly stated the contribution by others to jointly-authored works that I have included in my thesis.

I have clearly stated the contribution of others to my thesis as a whole, including statistical assistance, survey design, data analysis, significant technical procedures, professional editorial advice, financial support and any other original research work used or reported in my thesis. The content of my thesis is the result of work I have carried out since the commencement of my higher degree by research candidature and does not include a substantial part of work that has been submitted to qualify for the award of any other degree or diploma in any university or other tertiary institution. I have clearly stated which parts of my thesis, if any, have been submitted to qualify for another award.

I acknowledge that an electronic copy of my thesis must be lodged with the University Library and, subject to the policy and procedures of The University of Queensland, the thesis be made available for research and study in accordance with the Copyright Act 1968 unless a period of embargo has been approved by the Dean of the Graduate School.

I acknowledge that copyright of all material contained in my thesis resides with the copyright holder(s) of that material. Where appropriate I have obtained copyright permission from the copyright holder to reproduce material in this thesis and have sought permission from co-authors for any jointly authored works included in the thesis.

Publications during candidature

Peer-reviewed articles

1. HPV16E7-Induced Hyperplasia Promotes CXCL9/10 Expression and Induces CXCR3+ T-Cell Migration to Skin.
   Kuo P, Tuong ZK, Teoh SM, Frazer IH, Mattarollo SŒ, Leggatt GR.
   J Invest Dermatol. 2017 Dec 23. doi:10.1016/j.jid.2017.12.021. [Epub ahead of print]

2. Murine HPV16 E7-expressing transgenic skin effectively emulates the cellular and molecular features of human high-grade squamous intraepithelial lesions
   Z.K. Tuong, K. Noske **P. Kuo**, A.A. Bashaw, S.M. Teoh, I.H. Frazer
   Papillomavirus Research, 2018 Jun 5: 6-20 ISSN 2405-8521,
   doi.org/10.1016/j.pvr.2017.10.001. [Epub ahead of print]

3. HPV16-E7-Specific Activated CD8 T Cells in E7 Transgenic Skin and Skin Grafts.
   Jazayeri SD, **Kuo PT**, Leggatt GR, Frazer IH.
   Front Immunol. 2017 May 4;8:524. doi: 10.3389/fimmu.2017.00524. eCollection 2017

4. Batf3 selectively determines acquisition of CD8+ dendritic cell phenotype and function.
   Chandra J, **Kuo PT**, Hahn AM, Belz GT, Frazer IH.
   Immunol Cell Biol. 2017 Feb;95(2):215-223. doi: 10.1038/icb.2016.83. Epub 2016 Nov 29

5. A Mouse Model of Hyperproliferative Human Epithelium Validated by Keratin Profiling Shows an Aberrant Cytoskeletal Response to Injury.
   Zhussupbekova S, Sinha R, **Kuo P**, Lambert PF, Frazer IH, Tuong ZK. EBioMedicine. 2016 Jul;9:314-323.
   doi: 10.1016/j.ebiom.2016.06.011. Epub 2016 Jun 7

Conference abstracts

1. The Australasian Society for Immunology 2017 Annual Scientific Meeting,
    27 November- 01 December 2017, Brisbane Convention and Exhibition Centre,
    Brisbane, Queensland
    HPV16E7-induced Hyperplasia Promotes CXCL9/10 Expression and Induces CXCR3+
    T Cell Migration to Skin
    Paula Kuo, Kelvin Tuong, Siok-Min Teoh, Graham Leggatt, Stephen Mattarollo, Ian
    Frazer
    University of Queensland Diamantina Institute

2. Immunotherapy@Brisbane 2017 Conference, 10-12 May 2017,
    Brisbane Convention and Exhibition Centre
    Pre-Malignant Immune Suppressive Environment Is Dependent on HPV16E7-Rb
    Interaction Induced Epithelium Hyperplasia
    Paula Kuo, Kelvin Tuong, Graham Leggatt, Stephen Mattarollo, Ian Frazer
    University of Queensland Diamantina Institute

3. Keystone Symposia- Cancer Immunology and Immunotherapy: Taking a Place in
    Mainstream Oncology, 19-24 March 2017, Whistler, Canada
    Pre-Malignant Immune Suppressive Environment Is Dependent on HPV16E7-Rb
    Interaction Induced Epithelium Hyperplasia
    Paula Kuo, Kelvin Tuong, Graham Leggatt, Stephen Mattarollo, Ian Frazer
    University of Queensland Diamantina Institute

4. International Congress of Immunology 2016, 21-26 August 2016
    Melbourne Convention & Exhibition Centre, Victoria, Australia
    Pre-Malignant Immune Suppressive Environment Is Dependent on HPV16E7-Rb
    Interaction Induced Epithelium Hyperplasia
    Paula Kuo, Kelvin Tuong, Stephen Mattarollo, Ian Frazer
    University of Queensland Diamantina Institute

Publications included in this thesis

HPV16E7-Induced Hyperplasia Promotes CXCL9/10 Expression and Induces CXCR3+ T-Cell Migration to Skin.

Kuo P, Tuong ZK, Teoh SM, Frazer IH, Mattarollo SR, Leggatt GR.

J Invest Dermatol. 2017 Dec 23. doi:10.1016/j.jid.2017.12.021. [Epub ahead of print]

– incorporated as Chapter 2.

Contributor	Statement of contribution
Paula Kuo	Designed experiments (80%) Performed experiments (95%) Analysed results (90%) Interpreted results (85%) Wrote and edited the paper (75%)
Kelvin Z. Tuong	Designed experiments (5%) Analysed results (10%) Wrote and edited the paper (10%)
Siok-Min Teoh	Performed experiments (5%)
Ian Frazer	Designed experiments (5%) Interpreted results (5%) Wrote and edited the paper (5%)
Stephen Mattarollo	Designed experiments (5%) Interpreted results (5%) Wrote and edited the paper (5%)
Graham Leggatt	Designed experiments (5%) Interpreted results (5%) Wrote and edited the paper (5%)

Contributions by others to the thesis

Prof. Ian Frazer, A/Prof. Graham Leggatt, Dr. Stephen Mattarollo and Dr. Kelvin Zewen Tuong contributed significantly to the conception and design of the project, as well as critical revision of the thesis. Siok-Min Teoh contributed to the process of animal experiments and sample handling.

Statement of parts of the thesis submitted to qualify for the award of another degree

None

Research Involving Human or Animal Subjects

Animal work included in this research was approved by the Animal Ethics Committee-Health Sciences group under ethics number 367/13 and 452/16. A copy of the ethics approval letter is attached in the thesis appendix. No human subjects were involved in this research.

Acknowledgements

Keywords

HPV16E7, Rb, hyperplasia, chemokine, chemokine receptor, skin grafting, suppressive local immunity, dendritic cells, T cells, keratinocytes

Australian and New Zealand Standard Research Classifications (ANZSRC)

ANZSRC code: 111107, Immunology, 80%

ANZSRC code: 111112, Oncology and Carcinogenesis, 20%

Fields of Research (FoR) Classification

FoR code: 1107, Immunology, 80%

FoR code: 1112, Oncology and Carcinogenesis, 20%

Table of Contents

CHAPTER 1

CHAPTER 4

CHAPTER 5-APPENDIX

List of Figures

Chapter 5

List of Tables

List of Abbreviations

ANOVA: Analysis of variance

APC: Antigen-Presenting Cell

Arg: Arginine

CAMERA: Correlation Adjusted MEan RAnk

CCL: CC Chemokine Ligands

CCR: CC Chemokine Receptor

CFSE: Carboxyfluorescein succinimidyl ester

CIN: cervical intraepithelial neoplasi

CTL: Cytotoxic T Lymphocyte

CXCL: CXC Chemokine Ligand

CXCR: CXC Chemokine Receptor

DAMP: Damage-Associated Molecular Patter

DAVID: Database for Annotation, Visualization and Integrated Discovery

DC: Dendritic Cell

DNCB: 2,4-Dinitrochlorobenzene

E: early proteins

EGFR: epidermal growth factor receptor

FACS: Fluorescence-Activated Cell Sorting

GF001: E7 protein MHCI peptide

GSEA: Gene Set Enrichment Analysis

GVHD: Graft-Versus-Host-Disease

HPV: Human Papillomavirus

HSP: Heat Shock Protein

IDO1: Indoleamine 2,3-Dioxyehnase

IFN: Interferon

IL: Interlukin

IRF: Interferon Regulatory Factor

K14: Keratin 14

K5: Keratin 5

KC: keratinocyte

KO: Knock Out

L: late proteins

LC: Langerhans Cell

LCR: long control region

LDH: lactate dehydrogenase

LIMMA: Linear Models for Microarray and RNA data

LN: Lymph Node

MFI: Mean Fluorescence Intensity

MHCII: Major Histocompatibility Complex II

migDC: Migratory DC

mOVA: Membrane OVA

nAb: neutralising Antibody

NK: Natural Killer Cell

NKT: Natural Killer T cell

NOD SCID: Nonobese diabetic/severe combined immunodeficiency

OCT: Optimal Cutting Temperature compound

OT-1: OVA-specific $CD8^+$ T cell

OVA: Ovalbumin

PAMP: Pathogen-Associated Molecular Pattern

Pathway Interaction Database: PID

qPCR: quantitative Polymerase Chain Reaction

RAG: Recombination Activating Gene

Rb: retinoblastoma protein

ResDC: Resident DC

RNAseq: RNA sequencing

ROAST: Rotation gene set test

RPMI: Roswell Park Memorial Institute Medium 1640

SEM: Standard Error of the Mean

T_{EM}: Effector Memory T cells

Th: T helper cell

TNF: Tumour Necrosis Factor

T_{reg}: Regulatory T cell

TRI: Translational Research Institute

VIN: Vulvar Intraepithelial Neoplasia

ΔL: LXCXE

Chapter 1

Introduction

1.1   Literature Review

Human papillomavirus infection and cancer

Human papillomavirus (HPV) is a double-stranded DNA virus without viral surface lipid envelope. There are over 180 types of HPV identified. HPV infections are restricted to keratinocytes of the skin and mucosal tissues (Frazer, 2004). Infection by low-risk HPV types results in benign genital warts and benign warts on other parts of the body, while high-risk HPV type16 and 18 are responsible for 70% of cervical cancer (Durst et al., 1983). Moreover, increased incidence of head and neck cancers caused by high-risk HPV infection has been observed and the incidence rate has sharply increased during the past two decades (Gillison et al., 2012; Gillison et al., 2014; WORLD HEALTH ORGANIZATION International Agency for Research on Cancer Multicenter Cervical Cancer Study, 2007) Although preventative vaccination has been implemented widely and made the diseases preventable, therapeutic strategies for existing infections are not as prominent. Understanding how the high-risk HPV infection impacts on an individual is then thus critical to develop potent therapies for persistent infections.

The genome of HPV is about 8000 base pairs, encoding early viral proteins-E1, E2, E4, E5, E6, and E7, as well as late proteins-L1 and L2 (Figure 1), and is typically located extrachromosomally in an infected cell. The replication of the virus does not induce viraemia and cytolysis throughout the course of the infection cycle. This enables HPV to replicate in a silent manner and thus evade host immune surveillance (Kupper and Fuhlbrigge, 2004).
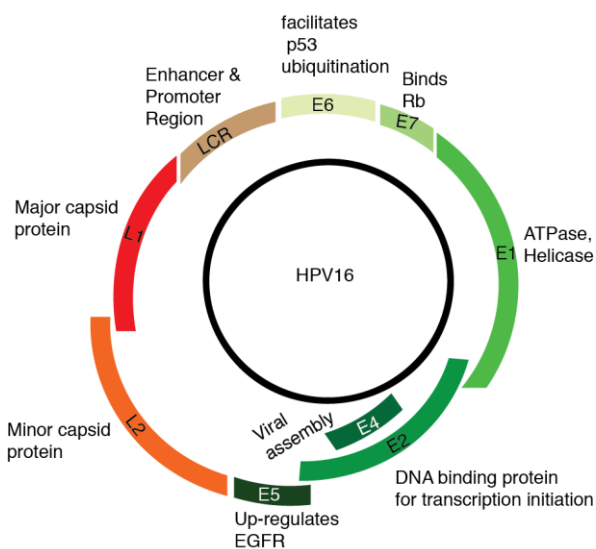
Figure 1.1. HPV16 genome structure (graph remade form (Stanley et al., 2007)). The genome structure of the double stranded DNA virus HPV16 includes long control region (LCR) as enhancer and promoter region, early proteins (E1-E7) that sustain viral replication and late proteins (L1 and L2) for viral structure.

The HPV viral infection cycle is highly dependent on keratinocyte differentiation, where it establishes its replication niche in the proliferative basal layer of the epithelium and expresses low levels of early viral proteins. As the keratinocytes differentiate, the amount of early protein expression increases. The late

proteins (L1 and L2) encoding capsid proteins are only expressed in terminally differentiated keratinocytes. In contrast to the late proteins, the early proteins are responsible for the viral replication throughout all disease stages. E1 acts as an ATPase and helicase for viral genome replication (Ustav et al., 1991). E2 protein is a sequence-specific DNA binding protein that initiates transcription of viral genes (Bouvard et al., 1994). E4 protein induces productive infection (Foguel et al., 1998) and E5 induces proliferation by stimulating the transforming activity of epidermal growth factor receptor (EGFR) (zur Hausen, 2001). E6 facilitates ubiquitination of the p53 tumour suppressor protein and thus promotes its degradation (Huibregtse et al., 1993). E7 interacts with the retinoblastoma protein (Rb) and disrupts its interaction with E2F1. The unbound E2F1 then activates excessive transcription signals for cell proliferation and replication (Cobrinik et al., 1992; Nevins, 1992). The acute cellular defects of HPV infection, including dysregulated cell cycle progression, differentiation and DNA damage response, are dependent on the binding of E7 with Rb (Balsitis et al., 2003; Jacks et al., 1992; Slebos et al., 1994). Apart from Rb interaction-dependent mechanisms, epithelial expression of the E7 protein in both Rb-expressing and Rb-deficient mice showed the same hyperplastic skin phenotype, suggesting additional regulation carried out by E7 in an Rb-independent manner (Balsitis et al., 2003). Additionally, E7 has also been reported to interact with transcription factors and co-regulators, including c-Jun (Antinore et al., 1996), chromatin remodelling enzyme p300 (Bernat et al., 2003), SKI-interacting protein (Skip), (Prathapam et al., 2001) TATA-box binding protein (TBP) (Slebos et al., 1994) and proteasome (Wang et al., 2001).

The tumour-inducing effects of "high risk" HPVs are largely attributed to the expression of E6 and E7 proteins. The functional inactivation of both p53 and Rb by E6 and E7, respectively, are necessary for carcinogenesis, as disabling either of them alone does not enable malignant transformation of primary cells *in vitro* (Munger et al., 1992; Thomas et al., 1999). E6 and E7 proteins also interfere with interferon secretion by interacting with IRF3 (Ronco et al., 1998) and IRF9 (Arany et al., 1995) respectively, and thus inhibit IFNα transcription. E7 also binds to IRF1 and prevents IFNβ promoter activation via recruitment of histone deacetylase to the IFNβ promoter (Park et al., 2000). Collectively, the low replication profile, dysregulation of cell cycle, and interference with interferon secretion during persistent high-risk HPV infection contribute to the formation, progression and immune evasion of HPV-induced cancers. According to this study, despite the fact that E7 protein interacts with many cellular proteins other than Rb, it is very likely that E7-Rb interaction is the major cause of the suppressive local immunity.

Tumour microenvironment and immune suppression in epithelial cancer

Tumour growth is greatly influenced by the microenvironment, where it creates communication between tumour and the immune system. Elucidating the immune modulation of tumour microenvironments and the balance between active and repressive immune responses have become a major focal point of tumour immunotherapy research. Several lines of evidence support that cancer patients have better prognosis when they present with tumour infiltrating lymphocytes (Clark et al., 1989; Clemente et al., 1996; Zhang et al., 2003). Tumour infiltrating T lymphocytes were shown to correlate with better prognosis in ovarian cancer (Zhang et al., 2003), melanoma (Clark et al., 1989; Clemente et al., 1996) and breast cancer (Mulligan et al., 2016). The anti-tumour immunity of T cells have been demonstrated in UV light-induced tumour, where the absence of T cells promoted their progressive growth (Ward et al., 1990). However, as tumours develop, they secrete factors to "educate" or prime infiltrating lymphocytes and alter their differentiation in favour of tumour development. In this case, tumour infiltrating T lymphocytes do not necessarily help eradicate tumour, but instead facilitate tumour growth and metastasis. For instance, transfer of antigen-specific CD4$^+$ T cells into mutant *Ras* oncogene mice did not improve tumour eradiation but instead promoted tumour growth (Siegel et al., 2000). Depletion of intra-tumoural CD4$^+$ T cells was shown to be beneficial for tumour regression accompanied by improved cytotoxic CD8$^+$ T cell activity (Awwad and North, 1988). In the study by Christopher T. et al., CD4$^+$ T cells were shown to be responsive for peptide recognition when mutant *Ras* oncogene mice, which are cancer-prone mice, were immunised with mutant peptide. However, these mice failed to eradicate oncogene-expressing tumour cells (Siegel et al., 2000). In an ovarian cancer study, tumour cells secrete CCL22 to recruit Foxp3$^+$CD4$^+$CD25$^+$ T$_{reg}$, which suppress tumour-specific T cell immunity and foster cancer growth (Curiel et al., 2004). These studies suggest an existing regulatory CD4$^+$ T cell (T$_{reg}$) population is either recruited or being induced in the tumour microenvironment.

In addition to T lymphocytes, myeloid cells infiltrate tumours and promote tumour progression though supporting tumour proliferation, angiogenesis and evading immune surveillance (Shojaei et al., 2009; Shojaei et al., 2007; Yang et al., 2004). Tumour infiltrating myeloid cells are immature CD11b$^+$ myeloid cells differentiated from common myeloid precursors (CMP). Types of tumour infiltrated myeloid cells include: 1) tumour-associated macrophages (TAM), 2) Tie-2 expressing monocytes (TEM), 3) immature myeloid cells, and myeloid derived suppressor cells (MDSC) that show suppressive activities. More recently, tumour infiltrating myeloid cells are gaining better recognition as targets for cancer research

as they play important regulatory roles in bridging the tumour microenvironment and effective T cell responses. Thus, modulating the recruitment signals or blocking the downstream factors of these infiltrated cells may be important targets of cancer immunotherapy.

Current development of HPV therapeutic vaccines: the promises and the needs

Although prophylactic HPV vaccines are available, therapeutic vaccines for high risk HPV16 and HPV18 are still in need to treat persistent infection and to prevent it from developing into cancer. To date, HPV therapeutic vaccination is aimed at boosting IFNγ secretion and cytotoxicity of CD8$^+$ T cells by immunising with HPV viral antigens. Current therapeutic vaccine trials include three platforms: the protein/peptide based, viral vector based and the E7-DNA based platform. In all three platforms, pre-cancerous cervical intraepithelial neoplasia (CIN) patients showed more effective responses than cervical cancer patients (Morrow et al., 2013). The strategies and outcomes for each platform are discussed in this section.

The general strategy of the protein/peptide vaccine platform involves linking the E7 antigen to different pathogen proteins, such as *Haemophilus influenza* protein D (Corona Gutierrez et al., 2004), and HSP65 from *Mycobacterium bovis (Einstein et al., 2007; Hallez et al., 2004)*. This is thought to invoke a greater response as a result of increased immunogenicity. After immunised with linked E7 antigen, vaccine-induced IFNγ production is increased in CD4$^+$ and CD8$^+$ T cells and lesion size is reduced by 50% (Einstein et al., 2007). However, the total percentage of vaccinated patients that presented with regression is similar to the unvaccinated cohort (spontaneous regression). In a clinical study conducted by van der Burg and Melief et al. showed all recruited stage 3 vulvar intraepithelial neoplasia (VIN3) patients had IFNγ-associated proliferative CD4$^+$ T cell responses and increased IFNγ production by CD8$^+$ T cells after immunised with HPV16E6/E7 peptide (Kenter et al., 2009). At 12-months follow-up, 15 out of 19 patients had clinical responses. Although, similar approach was utilised for CIN2 and CIN3 therapeutic vaccine development, the vaccine response was mainly dominated by CD4$^+$FOXP3$^+$CD25$^+$ regulatory T cells, suggested a necessity to overcome the inhibitory effects (Welters et al., 2008).

One viral vector (modified vaccinia ankara, MVA) based therapy, targeting E2 antigen of HPV16 and 18, showed 37.5% of enrolled patients were HPV DNA negative after

treatment (Garcia-Hernandez et al., 2006). However, those patients also developed antibodies against the viral vector and recurrence of lesions was observed after the end point of treatment. The E7-DNA based platform showed a more promising effect with high percentage of patients with significant regression. Patients were immunised with plasmid DNA encoding similar sequence to E7 of HPV16. In these patients, there was no detectable HPV DNA and no histological disease phenotype upon completion of the therapy (Sheets et al., 2003). However, a major drawback in this trial was presented; the effects were restricted to patients expressing HLA-A2 haplotype. Another trial that targeted both E6 and E7 of HPV16/18 showed 18 out of 18 patients with antigen-specific antibody production in serum, as well as 10 out of 11 patients with increased cytotoxic T lymphocytes (Bagarazzi et al., 2012). However, $CD4^+FOXP3^+CD25^+$ T_{reg} cells were also increased after receiving the vaccine, suggesting a possible factor that may impact on the therapeutic outcome. More recently, a DNA plasmid based therapeutic vaccine targeting HPV16/18 E6 and E7 (VGX-3100) has shown promising results in a double-blind phase 2b clinical trial (NCT01304524) (more discussion on this vaccine can be found in chapter 4). The vaccine, although is significantly effective, having 40% of responders, there is 60% of participants who do not respond to the vaccination. This suggests that a general suppressive immune response plays important role in controlling the efficiency of immunotherapy and also that the individual variance may accounts for degree of responsiveness.

As persistent HPV infection alters the epithelial environment and perturbs lymphocyte functions as a result of continuous antigen stimulation, it may be worth targeting suppressive/inhibitory factors or boosting positive immune responses induced in the altered epithelial environment as an alternative or complimentary therapeutic approach. This study focuses on the persistent high-risk HPV type 16 infection. The following chapters concentrate on the observations and impacts of E7 protein of the HPV16.

K14.E7 transgenic mouse as a model for persistent HPV infection

Due to the lack of a representative *in vitro* model of HPV16 infection, animal models that exhibit the traits of persistent HPV16 infection were developed. Because HPV infection is highly species specific, an animal model that represents human HPV infection requires to circumvent this species specificity and to reflect the localised infection in the clinical setting. To mimic the tissue specific infection of HPV16, Lee et al. delivered HPV virus with LoxP flanking by adenovirus to create extrachromosomal viral replication after Cre recombinase excision (Lee et al., 2004). However, the LoxP flanking sites disrupted the long control region of the virus genome and thus was unable to rule out the possible effect that this region has on viral replication. The Frazer Lab utilizes a transgenic K14.E7 mouse, where expression of HPV16 E7 protein is driven by the keratin 14 promoter, as a study model for persistent HPV16 infection. The K14.E7 transgenic mice express E7 protein in both skin and thymus without the presence of autoimmunity to E7 (Malcolm et al., 2003) and show hyper-proliferative epithelium with increased skin thickness (Herber et al., 1996). Although exhibiting increased epidermal thickness and lymphocyte infiltration in the skin, the hyperplastic K14.E7 transgenic mice do not progress to cancer in a C57BL/6 background. In fact, according to our RNA sequencing data, the mRNA expression profile in K14.E7 mice skin resemble the profile of human cervical intraepithelial neoplasia grade 3 (CIN3) (Tuong et al., 2018). Thus, the K14.E7 mouse model serves as a useful tool to study epithelial pre-malignancy and the discovery and improvement of potential therapeutic strategies.

K14.E7xRb$^{\Delta L/\Delta L}$ as E7-expressing non-hyperplastic model

The observed hyperplasia in K14.E7 skin is caused by the interaction between E7 and Rb, leading to dysregulated cell cycle control and hyper-proliferation. Deletion of Rb gene resulted in dysregulated cell cycle progression and failed to restore E7-expressing skin to normal physiology (Balsitis et al., 2005). Frederick et al. (Dick et al., 2000) first generated the mutated LXCXE motif of Rb protein (Rb$^{\Delta L/\Delta L}$) and showed that this mutation keeps normal Rb function intact and does not interrupt E2F1-Rb interaction. The mutation mainly disrupts Rb-E7 interaction (Dick et al., 2000). Crossing Rb$^{\Delta L/\Delta L}$ mice with K14.E7 transgenic mice allows the identification of whether Rb-dependent or Rb-independent effect is required for E7-induced deregulation (Balsitis et al., 2005) (Figure 1.2). Inhibited proliferation of suprabasal cells in the skin of K14.E7xRb$^{\Delta L/\Delta L}$ was observed when compared with K14.E7, suggesting that E7 accelerates epithelial proliferation in an Rb-binding-dependent manner (Balsitis et al., 2005). Moreover, infiltration of CD3$^+$ T cell in the skin of K14.E7xRb$^{\Delta L/\Delta L}$ was

reduced to a comparable level to syngeneic non-transgenic mouse (Choyce et al., 2013). This finding also suggests that T cell skin infiltration is an Rb-dependent function of HPVE7 protein and possibly a result of epithelial hyperplasia.
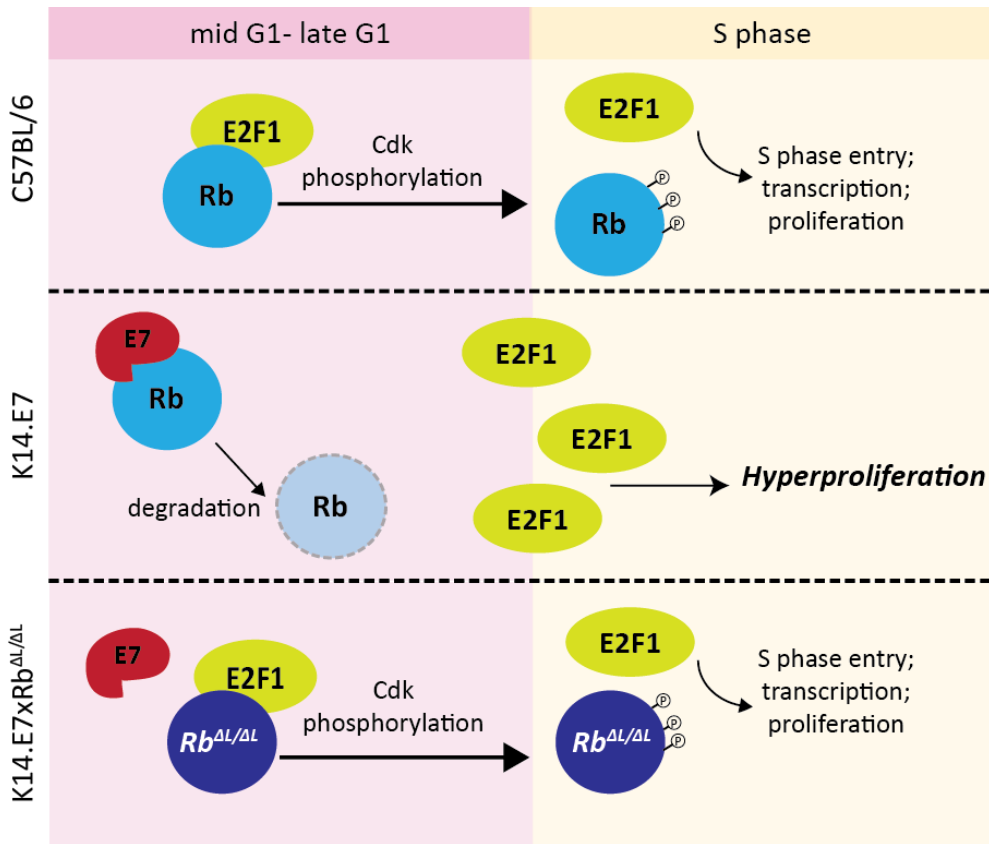
Figure 1.2. E7-Rb interaction disrupts normal cell cycle control
(graph remade from (Brown et al., 2012; Dick et al., 2000)).
In a normal cell cycle (C57BL/6), Rb protein interacts with transcription factor E2F1 during mid G1 phase to late G1 phase. Rb protein is gradually phosphorylated by cyclin-dependent kinases and will eventually release E2F1 after tri-phosphorylation. As a result, E2F1 can activate transcription and allow S phase entry for cell proliferation. The interaction between E2F1 is disrupted in the presence of E7 (K14.E7). E7-Rb interaction leads to Rb degradation and uncontrolled cell cycle progression. In the K14.E7xRb$^{\Delta L/\Delta L}$ model, where the E7-Rb interacting site is mutated, Rb remains its normal function and therefore allows normal cell cycle progression even in the presence of E7.

Syngeneic immunocompetent mice do not reject K14.E7 skin grafts

In response to general acute virus infection, antigen presenting cells migrate to drain lymph node where they present viral antigens and/or damage-associated molecular pattern (DAMP) as well as pathogen-associated molecular pattern (PAMP) to naïve lymphocytes. Primed T cells undergo activation and differentiation, which contribute to virus clearance and generate long-lived effector memory T cells (T_{EM}) for tissue surveillance. DAMP and PAMP molecules can also serve as T cell attractants. Tissue resident T cells and T_{EM} can be primed locally and will either proliferate or generate counteracting suppressive T cell subsets upon second or long-term infection.

The Frazer lab utilises a skin grafting model to emulate persistent HPV infection. This is achieved by grafting the skin of K14.E7 mice onto syngeneic immune competent mice. Immune competent mice do not reject K14.E7 skin while rejection was observed for K5mOVA-expressing skin grafts, where a membrane-bound chicken ovalbumin is expressed under the control of keratin 5 promoter (Broom et al., 2010). Furthermore, rejection of K5mOVA skin grafts, but not K14.E7, can be accelerated with either transfer antigen-specific CD4+ T cells or substitution with CD40 co-stimulation (Broom et al., 2010). Rejection of E7-expressing skin graft can be enabled by *Listeria monocytogenes* infection (Frazer et al., 2001) or in combination with active immunisation plus transferring antigen-specific CD8+ T cell (Matsumoto et al., 2004). These results indicate that the ability of effective CD8+ T cell responses and memory are either impaired or ineffective during persistent HPV16 infection.

Mechanisms that contribute to K14.E7 skin graft tolerance

Ongoing efforts in the Frazer lab are focused on elucidating the underlying immunological mechanisms that prevent K14.E7 skin graft clearance. The main findings to date will be summarised in a concise fashion in the sections hereafter. A summary table of the current findings from the Frazer lab is shown below.

Table 1.1. Summary of current findings that contribute to suppressive immune environment in K14.E7 skin

Inducer/ recruiting signal	Infiltrating and residing cells	Secreted Factors	Skin grafts rejected	References
IL-23; IL-1β	CD4; γδT cells	IL-17	K14.E7xIL-17$^{-/-}$	(Gosmann et al., 2014b)
IL-18	NKT	IFNγ	K14.E7xJα18$^{-/-}$ K14.E7xCD1d$^{-/-}$ K14.E7x IFNγ $^{-/-}$	(Gosmann et al., 2014a; Mattarollo et al., 2010a; Mattarollo et al., 2011)
IFNγ	IFNγR-expressing migratory DC	Indoleamine 2,3-Dioxyehnase (IDO1)	Inhibitor of IDO1 (1-D/L-MT) accelerates K14.E7 skin graft rejection	(Mittal et al., 2013)
CCL2, CCL5 from Keratinocyte	Mast cells		K14.E7xKit $^{w-sh/w-sh}$	(Bergot et al., 2014)
Ccr6	CD4^{+} T cells		K14.E7xRAG$^{-/-}$	(Choyce et al., 2013)

?	CD4$^+$CD25$^+$ T$_{reg}$		K14.E7xFoxP3$^{-/-}$ (K14.E7xDEREG) **NOT REJECTED**	(Mattarollo et al., 2011; Narayan et al., 2009)
?	CD8$^+$ T cells		K14.E7xRAG$^{-/-}$	(Choyce et al., 2013)

Regulation of innate immunity of the K14.E7 skin

Innate immunity mediates the first response towards foreign antigens through inducing inflammation. Secretion of pro-inflammatory cytokines such as IL-1β, IL-6 and TNFα is the main inducer of inflammatory responses. K5mOVA skin grafts were spontaneously rejected when grafted onto syngeneic background mice and accompanied with high level of IL-1β secretion (Hadis et al., 2010). Moreover, IL-1β signalling pathway was shown to be critical for K14.E7 skin graft rejection, as depleting the naturally occurring IL-1R antagonist, IL-1Ra, enabled rejection of K14.E7 skin grafts (Hadis et al., 2010). Despite the abundance of pro-inflammatory cytokine secreted in K14.E7 skin, regulatory cytokine-IL-10 mRNA and protein expression are increased in cervical biopsies in association with cervical cancer progression (Bermudez-Morales et al., 2008). These findings suggest that pro-inflammatory cytokines and the balance between effector and regulatory cytokines are necessary to induce skin graft rejection in the context of keratin promoter driven antigens.

Arginase is identified as a pro-inflammatory factor, contributing to allergic asthma (Maarsingh et al., 2009), retinal inflammation (Zhang et al., 2009), and the clearance of arthritogenic alphavirus (Stoermer et al., 2012). Acute inflammation after topical 2,4-Dinitrochlorobenzene (DNCB) application was observed in the E7-expressing skin (Tran et al., 2014). Inhibiting arginase activity by N^{ω}-hydroxy-nor-^{L}-arginine ameliorates DNCB-induced hyper-inflammation. Consistent with the previous finding, DNCB-induced hyper-inflammatory skin exhibited higher level of IL-1β secretion. Infiltration of $CD45^{+}CD11b^{+}$ myeloid cells, and amplified Th2 cytokine production were observed after DNCB treatment, suggesting that myeloid cell activation contributes to arginase mediated inflammatory responses. Further identification showed a subset of myeloid cells, $CD11b^{+}$ $Gr1^{int}$ $F4/80^{+}$ $Ly6C^{+}Ly6G^{low}$, is responsible for Arg-1 production in DNCB-treated skin (Tran et al., 2014). Arg-1 production is independent of T and B lymphocytes, as evidenced by no significant difference in Arg-1 expression between K14.E7 and $K14.E7xRag^{-/-}$ mice, where no T cells and B cells exist in the latter (Tran et al., 2014). Depletion of IL-17 abolished DNCB-induced Arg-1 production and hyper-inflammation, indicating that IL-17 is the key inducer of Arg-1 (Tran le et al., 2015). Taken together, local determinants, such as IL-1β, Arg-1 and IL-17, control the outcome of K14.E7 skin grafts and inflammatory response towards topical immune therapies.

In addition to myeloid cells, mast cells were recruited by CCL2 and CCL5 in the K14.E7 skin and displayed increased degranulation (Bergot et al., 2014). Skin grafts from

K14.E7 mice crossed with mast cell depleted Kit [w-sh/w-sh] mice were rejected within three weeks (Bergot et al., 2014). This suggested that mast cells play an immune suppressive role in HPV16E7-expressing skin.

NKT cells mediate the outcome of K14.E7 skin grafts

Cells that control the bridging between innate and adaptive immune activation were also identified to play inhibitory roles in K14.E7 skin. These cells include Natural Killer T cell (NKT) and dendritic cells. NKT cells are T cells that can only be activated by antigens presented on CD1d molecule and have been shown to have profound impact towards immune regulation in both inducing cytotoxic immune responses and protection against foreign antigens (Godfrey and Kronenberg, 2004 and references therein).

NKT cells act as an immune response suppressor in the persistent HPV16 infection model. E7-expressing but NKT-deficient (CD1d[KO] or Jα18[KO]) skin grafts were rejected by immune competent mice (Mattarollo et al., 2010a). In contrast to the known cytotoxic function, IFNγ produced by NKT cells was found to be critical for K14.E7 skin graft tolerance. CD1d-expressing CD11C^{+}F4/80^{hi} population are responsible for activation of the NKT cells and secretion of IFNγ in the skin graft (Mattarollo et al., 2010a). However, the signals that recruit CD11C^{+}F4/80^{hi} population to the site of skin graft have not yet been characterised. Further investigations demonstrated that the secretion of IFNγ in E7-expressing skin is induced by IL-18, rather than IL-12 (Gosmann et al., 2014a). Taken together, in the K14.E7 mouse model, NKT cells contribute to the immune suppressive environment by secreting IFNγ and impair effective antigen-specific CD8^{+} T cell function (Mattarollo et al., 2010b).

Impaired antigen presenting ability of dendritic cells and keratinocytes in K14.E7 skin

Skin dendritic cells (DCs) serve as a first line responsive cell type that present pathogens and control the immunogenicity of vaccines to induce either effector immune response or tolerance. Upon activation, dendritic cells migrate to draining lymph node and present antigens along with co-stimulatory molecules to antigen-specific T cells. In normal skin, Langerin (CD207)-positive Langerhans cells (LCs) are the predominant dendritic cell type in the epidermis. In the dermis layer, migrating LCs, CD11b^{+} DC, CD103^{+} DC and CD207/CD11b double negative DCs comprise the whole dermal DC population (Heath and Carbone, 2009). Cutaneous expression of HPV16E7 alters the proportion and the ability of antigen presenting cell (APC) subtypes in the skin and thus contributes to differential

adaptive immune responses (Chandra et al., 2016). Migratory DC populations (CD11c$^+$MHCII^{hi}) were found to have increased IFNγR expression, receiving the elevated IFNγ signal from the E7-expressing skin, and to produce indoleamine 2,3-Dioxyehnase (IDO1) that induces K14.E7 graft tolerance (Mittal et al., 2013). DCs in the K14.E7 skin were demonstrated to have enhanced migration to the draining lymph nodes but impaired antigen processing ability (Chandra et al., 2016). Moreover, LC in the K14.E7 skin showed reduced MHCII expression and increased immune modulatory factor secretion, including IDO1, Arg-1, IL-10, IL-6, IL-12 and IL-23p40 (Chandra et al., 2016). In addition to professional antigen presenting cells, the ability of keratinocyte to present antigens through MHCI to CD8$^+$ T cells was inhibited in E7-expressing keratinocytes (Zhou et al., 2011). While IFNγ stimulation enhanced the susceptibility of OVA-expressing keratinocytes to T cell lysis through up-regulated MHCI expression, E7-expressing keratinocytes failed to be lysed under the same stimulation (Zhou et al., 2011). Together, antigen presenting process in both professional antigen-presenting cells (APC)s and keratinocytes is dysregulated and impaired in the K14.E7 skin.

Suppressive adaptive immune response in K14.E7 skin

The K14.E7 hyperplastic skin is highly infiltrated with proliferative CD4$^+$ and CD8$^+$ T lymphocytes when compared with wild type non-transgenic mice, suggesting that the skin-infiltrating lymphocytes contributes significantly to the immune regulation. Therefore, the ineffective T cell responses in the K14.E7 skin has been largely attributed to irresponsiveness of peripheral CD8$^+$ T cells, elevated regulatory T cell responses and regulatory cytokines. In the transgenic K14.E7 mice, the responsiveness of peripheral CD8$^+$ T cells to E7 or to other antigens that are not related to E7 are dampened, while CD4$^+$ T cells and antibody production are not affected (Narayan et al., 2009). This suppressive CD8$^+$ T cell response could be mediated by CD4$^+$CD25$^+$ T$_{reg}$ cells as neutralising either CD4$^+$or CD25$^+$ restores CD8$^+$ T cell response (Narayan et al., 2009). However, as neutralising antibody used in the study was not specific to T$_{reg}$ cells but the whole CD4$^+$ or CD25$^+$ T cell population, contribution of T$_{reg}$ cells in mediating the ineffective response should be further evaluated. Moreover, depleting FoxP3$^+$ regulatory T cells in either K14.E7 donors or recipients did not enable graft rejection, suggesting that FoxP3$^+$ T$_{reg}$ cells alone is not sufficient to induce the immune suppressive environment in K14.E7 skin (Mattarollo et al., 2011).

Pro-inflammatory cytokine-IL-17, secreted by CD4^{+} T cells and γδ T cells under the stimulation of IL-23, plays a suppressive role in the context of E7-expressing epithelium. Skin grafts of K14.E7xIL-17^{-/-} mice were enabled for rejection (Gosmann et al., 2014b), suggesting IL-17 as a critical factor determining the suppressive local immune environment.

The chronic inflammation and the recruitment of innate immune cells to the inflammatory site were shown to be B lymphocyte-dependent in a K14-HPV16 (express both E6 and E7 protein of HPV16) mouse model (de Visser et al., 2005). Although there is no significant B lymphocyte infiltration in the hyperplastic skin, the immunoglobulin deposition was observed (de Visser et al., 2005). Repopulation of B cells into K14HPV16 Rag^{-/-} mice restored the malignancy phenotype, with skin hyperplasia and increased infiltration of mast cells and Gr1^{+} cells (de Visser et al., 2005).

In summary, K14.E7 model mimics the late stage of epithelial tumorigenesis, where innate, adaptive and regulations between innate-adaptive immunity all contribute to the immune suppressive environment. However, how lymphocytes are recruited to the skin and the initiator for suppressive immune response are not yet fully understood. To date, only one study has suggested a possible mechanism that may mediate the T cell recruitment to E7-expressing skin. In the study by Choyce et al., it was found that CD4^{+} T cells in the K14.E7 skin expressed higher levels of CCR6 when compared to CD4^{+} T cells within the draining lymph nodes (Choyce et al., 2013). Together with K14.E7xRb$^{\Delta L/\Delta L}$, this study aims to understand to what extend the E7-Rb interaction contributes to the immune responses in the context of cutaneous HPV16E7 expression.

Chemokine and Chemokine receptors

One focus of this study investigates on the recruitment of T lymphocytes to the hyperplastic K14.E7 skin. This line of study is based on the results of the whole skin RNAseq analysis presenting in Chapter 2. An overview of chemokines and the receptors is presented in this section.

Chemokines are small secreted chemotactic cytokines ranging from 8-14kDa and are classified into four groups based on the position of the conserved cysteine residues: CXC, CC, C and CX_3C (Zweemer et al., 2014). They typically interact with chemokine receptors, which are seven-transmembrane receptors (7TMR) of the GPCR superfamily (Proudfoot, 2002), and carry out diverse signal transmission to direct leukocyte migration, inflammation and differentiation (Luster, 1998; Stoolman, 1989). The importance of chemokines and chemokine receptors in regulating inflammatory processes is underpinned in their involvement in the pathogenesis of several autoimmune diseases, including rheumatoid arthritis (Koch, 2005; Yellin et al., 2012), inflammatory bowel disease (McGuire et al., 2011), type I diabetes (Frigerio et al., 2002; Shehadeh et al., 2009) and psoriasis (Antonelli et al., 2008; Harper et al., 2009)

Multiple chemokines can interact with the same chemokine receptor resulting in functional redundancy in some cases, in a phenomenon termed by Robert J. Lefkowitz as biased signalling (Reiter et al., 2012; Samama et al., 1993). However, there are exceptions to this: CXCR4, CXCR5, CXCR6, CCR6, CCR9 and CX_3CR1 only have one specific ligand (Zweemer et al., 2014). The selective ligand binding accounts for tissue specific and cell type specific lymphocyte recruitments. For example, CCR9 plays critical role in recruiting lymphocytes to the gut (McGuire et al., 2011) and CCR6 drives Th17 homing to the site of inflammation (Reboldi et al., 2009).

More recently, chemokines have been observed to have functions aside from being leukocyte attractants. Nathan Karin and Gizi Wildbaum termed chemokines that are able to alter the biological functions of the recruited lymphocytes as driver chemokines (Karin et al., 2015). Like cytokines, which are well-studied signals that direct T cell differentiation and polarisation, driver chemokines have been shown to have similar role. For example, CXCL12 polarizes $CXCR4^+$ macrophages to IL-10 secreting M2-like macrophages (Martinez et al., 2008) and $CXCR4^+CD4^+$ T cells to IL-10 producing regulatory T cells (T_r1) that suppress experimental autoimmune encephalomyelitis (EAE) (Meiron et al., 2008). Apart

from inducing immunosuppressive cell types, chemokine signallings can influence effector T cell polarization. For instance, CXCL10 has been demonstrated to direct effector T cell polarisation (Salomon et al., 2002; Wildbaum et al., 2002). CXCL9 and CXCL10 together drive Th1 and Th17 polarization through STAT1, STAT4 and STAT5 phosphorylation dependent pathway.

Previous studies in the Frazer lab have identified several chemokine and chemokine receptor signalling pathways to mediate the recruitment of infiltrating lymphocytes in the thickened skin of K14.E7 transgenic mice. We have established that the E7 induced epithelial hyperplasia is associated with i) increased epidermal secretion of Ccl2 and Ccl5 and consequent recruitment of mast cells (Bergot et al., 2014), ii) increased expression of potent neutrophil chemoattractants including Cxcl1, Cxcl2 and Cxcl5 in DNCB-treated K14.E7 skin (Tran le et al., 2015), and iii) expression of Ccr6, the receptor for chemokine Ccl20, on CD4$^+$ T cells in K14.E7 skin is higher than lymph node of K14.E7 (Choyce et al., 2013). Although we have explored the relationship between several chemokines and immunocyte recruitment in K14.E7 skin, the epithelial hyperplasia-directed, as well as the degree of contribution of the E7-Rb interaction to lymphocyte-recruiting signal have not yet been understood.

The remainder of this literature review will focus on CXCR3 and its interacting ligands as results (see Chapter 2) indicate their involvement in E7-Rb interaction-associated skin hyperplasia. As IFNγ production is enriched in K14.E7 skin environment and could serve as a potent inducer for CXCL9 and CXCL10 secretion by keratinocytes, we hypothesise that CXCR3 chemokine receptor pathway is important for the recruitment of T cells in the K14.E7 hyperplastic environment.

CXCR3 and ligands

CXCR3 is primarily expressed on activated T cells and NK cells (Qin et al., 1998). Co-expression of CXCR3 and CCR5 mark the Th1 subsets (Qin et al., 1998), while CCR3 and CCR4 are preferentially expressed on Th2 subsets (Sallusto et al., 1998). Examples of CXCR3 functions include: i) the recruitment of activated Th1 cells to inflamed tissues (Campanella et al., 2008; Khan et al., 2000; Xie et al., 2003), ii) the regulation of skin-homing autoreactive CD8$^+$ T cells in graft-versus-host-disease (GVHD) (Villarroel et al., 2014), and iii) the rapid recruitment of NK cells to antigen-stimulated lymph node and facilitation of Th1

subset priming (Martin-Fontecha et al., 2004). Transcription factor T-bet, the master regulator controlling Th1 and CTL polarization, is also a direct trans-activator of CXCR3 expression (Lord et al., 2005). T-bet deficient mice have limited Th1 infiltration to the inflamed tissue, while reconstitution of Cxcr3 expression in T-bet$^{-/-}$ mice was able to re-balance the defect (Lord et al., 2005). Apart from effector cells, Cxcr3 is also expressed on Foxp3-positive regulatory T cells. Foxp3 up-regulates T-bet and in turn induces the expression of Cxcr3 on Foxp3-positive regulatory T cells. This allows accumulation of T_{reg} at sites of Th1-mediated inflammation and maintains the homeostasis of Th1 responses (Koch et al., 2009).

CXCR3 ligands include CXCL9 (monokine induced by gamma interferon, MIG), CXCL10 (interferon gamma-induced protein 10, IP-10) and CXCL11 (interferon-inducible T-cell alpha chemoattractant, I-TAC). The expression of these three ligands depends on interferon induction (Groom and Luster, 2011). Furthermore, they have different binding affinity with CXCR3, where CXCL11 has the highest affinity and CXCL10 is higher than CXCL9 (Groom and Luster, 2011). This binding discrepancy among ligands may accounts for the counteracting and cooperating effects of the CXCR3 signalling pathway. In most cases, CXCL9 and CXCL10 induce effective immune response after interacting with receptors on T cells, while CXCL11 induces suppressive immune response (Groom and Luster, 2011). For example, CXCL11 was shown to be required for inducing FOXP3-IL-10^{hi} CD4^{+} T_r1 cells (Zohar et al., 2014). However, it should be noted that C57BL/6 mice are genetically deficient in *Cxcl11* gene expression due to the generation of a premature stop codon within the *Cxcl11* transcript. Thus Cxcl11 protein expression is attenuated in C57BL/6 mice (Groom and Luster, 2011).

The redundancy of Cxcr3 ligands for T cell-recruitment has been demonstrated in a murine model of obliterative bronchiolitis (Medoff et al., 2006). They showed that even though Cxcl9 and Cxcl10 are induced and are required in a different manner and the expression level peaked at different stages during allogeneic transplant, in which neither *Cxcl9$^{-/-}$* nor *Cxcl10$^{-/-}$* animal showed significant recovery of rejection (Medoff et al., 2006). Apart from redundancy, CXCR3 ligands have been shown to have synergistic and cooperative effects. For example, CXCR3 ligands cooperatively induce activated T cell recruitment and generation of CTLs (Yoon et al., 2009) and also the recruitment of NK cells and CTLs to the spinal cord during herpes simplex virus-2 infection (Thapa et al., 2008). In some cases, CXCR3 ligands showed counteracting effects. This is seen in a murine MHC-

mismatched cardiac transplantation model, where Cxcl9 and Cxcl10 showed antagonistic effect towards priming of the donor-reactive T cells (Rosenblum et al., 2010). The absence of Cxcl9, in recipient, donor or both, down-regulate the frequency of donor-reactive IFNγ-producing CD8 T cells. On the contrary, donor-reactive IFNγ-producing CD8 T cells increased in the absence of Cxcl10 in a Cxcl9-dependent manner (Rosenblum et al., 2010). Although the physiological effect of CXCR3 signalling pathway has been extensively studied, there are limited investigations on how this signal is involved in the context of persisting cutaneous HPV infection. This study aims to decipher the degree of involvement of this pathway in HPV infection using transgenic K14.E7 mouse model.

1.2   Project Significance

We have an established mouse model, K14.E7 that mimic the pre-cancerous lesions associated with persistent HPV16 infection. As the HPV16 E7 protein interacts with tumour suppressor gene Rb and disrupts normal cell cycle, E7 expression in keratinocytes is typically associated with hyperproliferation of the epithelium. Previous studies in the Frazer lab have shown that the hyperproliferative skin phenotype accompanied with increased number of immune cell infiltration, defective antigen presentation, increased regulatory cytokine secretion and suppressed immune response in K14.E7 skin (Gosmann et al., 2014a; Hadis et al., 2010; Mattarollo et al., 2010a; Mittal et al., 2013). However, whether these observed phenotypes and immune responses in K14.E7 skin are the result of viral oncogene E7 expression or the E7-Rb interaction-induced hyperplasia is not yet understood.

These effects may potentially be delineated using a mutant Rb expressing mouse model that results in the disruption of E7-Rb interaction, without affecting normal Rb function (Rb$^{\Delta L/\Delta L}$). Double transgenic mice bearing K14.E7 and mutant Rb expression (K14.E7xRb$^{\Delta L/\Delta L}$) will enable us to differentiate the effects caused by E7 expression and E7-Rb interaction-induced hyperplasia. With the K14.E7xRb$^{\Delta L/\Delta L}$ mouse model, we will be able to identify potential new and/or novel targets that are dependent on E7-Rb interaction. These findings may aid in facilitating the development of better HPV16 therapeutic vaccines for the treatment of pre-cancerous epithelial lesions.

1.3   Hypothesis and aims

HPV16E7-Rb interaction-induced hyperplastic skin environment is responsible for suppressive immune responses in HPV16E7 pre-cancerous lesion.

This study includes the following aims:
  Aim1: Characterization of K14.E7Rb$^{\Delta L/\Delta L}$ mice in the aspects of skin phenotypes and general immune responses
  Aim2: Investigate the mechanisms involved in K14.E7 skin infiltrating T cells and if the infiltration requires E7-Rb interaction-induced hyperplasia.
  Aim3: To find out if K14.E7Rb$^{\Delta L/\Delta L}$ skin graft can be rejected when grafted onto syngeneic background mice. If so, what are the mechanisms? If not, what are the

possible factors involved in the immune suppressive environment in addition to E7-Rb interaction-induced hyperplasia.

Chapter 2

HPV16E7 induced hyperplasia promotes CXCL9/10 expression and induces CXCR3$^+$ T cell migration to Skin

2.1 Preface

The results in this chapter cover aim one and two of the whole project. In this article, we characterized the skin of K14.E7x Rb$^{\Delta L/\Delta L}$ in terms of immune cell subsets, identified chemokines CXCL9/10 secreted from the hyperplastic K14.E7 skin using RNA sequencing and further functionally annotated the contribution this particular chemokine pathway to the fate of the K14.E7 skin graft. This article highlights, for the first time, a T lymphocyte population that contribute positively to skin graft rejection. This chapter was published as an original research article online on December, 2017 in Journal of Investigative Dermatology.

2.2 Article 1

Original Article

Journal of Investigative Dermatology

HPV16E7 INDUCED HYPERPLASIA PROMOTES CXCL9/10 EXPRESSION AND INDUCES CXCR3+ T CELL MIGRATION TO SKIN

Paula Kuo[1], Zewen K. Tuong[1], Siok Min Teoh[1], Ian H. Frazer[1]*, Stephen R. Mattarollo[1]*, Graham R. Leggatt[1]*

[1]The University of Queensland Diamantina Institute,

Translational Research Institute,

Woolloongabba, Queensland 4102, Australia

* These authors contributed equally and share last authorship

Correspondence:

Ian Frazer, The University of Queensland, Faculty of Medicine, The University of Queensland Diamantina Institute, Translational Research Institute

Short title:

CXCR3+ T cell migration to K14.E7 skin

2.3 Abstract

Chemokines regulate tissue immunity by recruiting specific subsets of immune cells. Mice expressing the E7 protein of HPV16 as a transgene from a *keratin 14* promoter (K14.E7) show increased epidermal and dermal lymphocytic infiltrates, epidermal hyperplasia and suppressed local immunity. Here, we show that CXCL9 and CXCL10 are overexpressed in non-haematopoietic cells in skin of K14.E7 mice when compared with non-transgenic animals, and recruit CXCR3^{+} lymphocytes to the hyperplastic skin. Overexpression of CXCL9 and CXCL10 is not observed in E7 transgenic mice with mutated Rb gene whose protein product cannot interact with E7 (K14.E7xRb$^{\Delta L/\Delta L}$) and in consequence lack hyperplastic epithelium. CXCR3^{+} T cells are preferentially recruited by CXCL9 and CXCL10 in supernatants of K14.E7 but not K14.E7xRb$^{\Delta L/\Delta L}$ skin cultures *in vitro*. CXCR3 signalling promotes infiltration of a subset of effector T lymphocytes that enables donor lymphocyte deficient, E7-expressing skin graft rejection. Taken together, this suggests that recruitment of CXCR3^{+} T cells can be an important factor in the rejection of precancerous skin epithelium providing they can overcome local immunosuppressive mechanisms driven by skin-resident lymphocytes.

2.4 Introduction

Cervical intraepithelial neoplasia (CIN) is caused by persisting infection of the cervix with high-risk human papilloma virus (HPV). HPV infection often evades immune surveillance by various mechanisms (Hasan et al., 2013; Natale et al., 2000; Pacini et al., 2015; Tindle, 2002). Although administration of therapeutic HPV vaccines, including peptide, protein or dendritic cell based vaccines, to patients with cervical intraepithelial neoplasia (CIN) have been associated with disease regression in several clinical trials (Hallez et al., 2004; Natale et al., 2000; Van Doorslaer et al., 2010), the rate of regression is not significantly greater than what occurs without intervention (Morrow et al., 2013). In addition, induction of CD4+ and CD8+ T cell responses after administration of HPV16 E6 and E7 peptides had been accompanied with a concomitant induction of inhibitory immune responses, negating potential therapeutic effects (Welters et al., 2008).

E7 is a papillomavirus encoded oncoprotein that disrupts regular cell cycle by interacting with and facilitating degradation of the Rb protein (Brown et al., 2012), leading to hyperproliferation of E7 expressing epithelial cells. A transgenic mouse model expressing HPV16 E7 viral protein under the control of keratin 14 promoter (K14.E7) has been generated to mimic persistent HPV epithelial infection (Herber et al., 1996). K14.E7 mouse skin shows disrupted keratinocyte differentiation with increased expression of stress keratins (6, 16 and 17) (Zhussupbekova et al., 2016) and high numbers of skin-infiltrating lymphocytes, resembling observations in human CIN lesions (Adurthi et al., 2008; Carrero et al., 2009; Kobayashi et al., 2008). Although K14.E7 skin graft is tolerated when grafted onto syngeneic immunocompetent recipients (Frazer et al., 2001; Matsumoto et al., 2004), removal of T cells from E7-expressing hyperplastic skin significantly enhances rejection of E7 transgenic skin grafts from immune competent recipients (Choyce et al., 2013) suggesting the presence of immunosuppressive lymphocytes within the K14.E7 skin environment.

Chemokines direct leukocyte migration and differentiation (Luster, 1998; Stoolman, 1989) and also direct cytotoxic lymphocyte infiltration to tumour sites (Balkwill, 2004; Chow and Luster, 2014; Mantovani et al., 2004; Spranger et al., 2017). However, tumour infiltrating lymphocytes may contribute to the immunosuppressive environment and thus facilitate tumour growth, survival and metastasis (Balkwill, 2003). Clinical trials targeting chemokine inhibition have reported promising results against HIV infection (Muniz-Medina et al., 2009; Watson et al., 2005; Wood and Armour, 2005) and peripheral and cutaneous T cell lymphoma (Ishii et al., 2010; Satoh et al., 2006). An increased expression of CCR6 by CD4^{+}

T cells (Choyce et al., 2013) and mast cell recruitment by CCL2 and CCL5 (Bergot et al., 2014) has been demonstrated in E7 transgenic skin.

Here, we show that immune cell infiltration to E7 transgenic skin is a consequence of epidermal hyperplasia, and that hyperplasia induces CXCL9 and CXCL10 production to recruit a subset of CXCR3$^+$ T cells, promoting rejection of grafted E7 transgenic skin depleted of immunosuppressive lymphocytes. Consequently, hyperplastic skin causes the infiltration of both suppressive and functional lymphocytes and the balance of these two subsets determines the fate of K14.E7 skin grafts.

2.5 Results

E7 interaction with Rb protein is necessary to attract T cells to E7 transgenic skin

K14.E7 transgenic mouse skin exhibits an immune cell infiltrate and regulatory cytokine production (Chandra et al., 2016; Choyce et al., 2013; Gosmann et al., 2014a; Gosmann et al., 2014b; Mattarollo et al., 2010b; Tran le et al., 2015). To determine whether the lymphocytic infiltrate observed in E7 transgenic skin requires interaction of E7 with Rb protein, we utilized a double transgenic mouse model expressing HPV16 E7 and a mutant Rb (K14.E7xRb$^{\Delta L/\Delta L}$) that fails to bind E7 and therefore lacks epithelial hyperplasia without perturbing other Rb functions (Balsitis et al., 2005; Dick et al., 2000). The double transgenic mouse has equivalent expression of E7 mRNA to K14.E7 mice (Figure 2.1a). We compared skin immunocytes from female K14.E7 and K14.E7xRb$^{\Delta L/\Delta L}$ mice (Rb$^{\Delta L/\Delta L}$ and C57BL/6 mice as controls). K14.E7 skin, but not K14.E7xRb$^{\Delta L/\Delta L}$ skin, demonstrated increased numbers of CD45$^+$ lymphocytes, CD11b$^+$ non-dendritic cell (DC) cells, CD4$^+$ and CD8$^+$ T cells (Figure 2.1b, d and e). Moreover, decreased numbers of epidermal and dermal Langerhans cells (LCs), and higher proportions of epidermal and dermal CD11b$^+$ DC, were observed in K14.E7 skin when compared with non-transgenic skin (Figure 2.1c). The numbers and types of antigen presenting cells in K14.E7xRb$^{\Delta L/\Delta L}$ skin were similar to skin from non-transgenic animals. Keratinocytes in K14.E7 skin showed increased major histocompatibility complex II (MHC II) expression, a finding consistent with keratinocyte activation in many inflammatory skin diseases (Bjerke, 1982; Gawkrodger et al., 1987; Lampert et al., 1982; Poulter et al., 1982), whereas this was not observed in K14.E7xRb$^{\Delta L/\Delta L}$ or non-transgenic skin (Figure 2.1f). In contrast to the skin findings, the percentages of lymphocyte subsets in the spleen of each transgenic line and non-transgenic animals were similar (Figure S2.1b).

Taken together, these results suggest that E7 induced hyperplasia is mediating the immune cellular infiltrates that typifies hyperplastic E7-transgenic skin.

Gene expression profiling of E7 transgenic skin

Transcriptome analysis of skin of C57BL/6, K14.E7 and K14.E7xRb$^{\Delta L/\Delta L}$ was performed to understand the signals produced in the hyperplastic skin environment that promote immune cell recruitment. Differentially expressed genes (Benjamini–Hochberg P-value<0.01 and log$_2$ fold-change>2) in K14.E7, K14.E7xRb$^{\Delta L/\Delta L}$ and non-transgenic animals (group A, B and

C) were identified using the LIMMA-voom R package (Figure S2.2e). Genes identified with group A and C but not group B (n=482) could thus be associated with skin hyperplasia.

Gene ontology analysis (DAVID 6.8, KEGG) identified that the immune cell recruitment signals associated with cell adhesion and chemokine signalling were highly correlated with skin hyperplasia (n=482) (Figure 2.2a). Expression of genes encoding chemokines and chemokine receptors was up-regulated in K14.E7 skin but not in C57BL/6 nor in K14.E7xRb$^{\Delta L/\Delta L}$ skin (Figure 2.2b). As elevated production of IFNγ is observed in E7 transgenic skin (Gosmann et al., 2014a), and chemokines CXCL9 and CXCL10 are induced by Type 1 and 2 interferons and attract CXCR3$^+$ T cells, we examined the correlation between the CXCR3 pathway signature in K14.E7 and non-transgenic skin using the Pathway Interaction Database (PID), curated for pre-ranked GSEA analysis. The transcription profile of K14.E7 skin was positively correlated with the CXCR3 pathway signature, while the transcription signatures of K14.E7xRb$^{\Delta L/\Delta L}$ and non-transgenic skin both showed a negative correlation (Figure 2.2c). Up-regulation of the CXCR3 gene set in K14.E7 skin was also observed in CAMERA and ROAST analysis (Table S2.1).

CXCL9 and CXCL10 are expressed on CD45- cells in hyperplastic K14.E7 epidermis

Gene expression analysis suggested that CXCL9/10 chemokine production might contribute to CXCR3$^+$ immune cell recruitment in hyperplastic skin. Consistent with this hypothesis, we observed that CXCR3$^+$ CD4$^+$ but not CXCR3$^+$ CD8$^+$ or CXCR3$^+$ CD4$^-$CD8$^-$ TCRβ$^+$ T cells were increased in skin but not spleen from K14.E7 animals, when compared to K14.E7xRb$^{\Delta L/\Delta L}$ animals (Figure 2.3a-d). CXCR3+ CD4+ T cells from skin draining lymph nodes from K14.E7 mice are not activated when compared with cells from non-transgenic mice (Figure 2.3e). qPCR confirmed up-regulation of *Cxcl9/10* mRNA expression in skin but not spleen from K14.E7 animals when compared with K14.E7xRb$^{\Delta L/\Delta L}$ or non-transgenic animals (Figure 2.4a). Flow cytometric analysis showed that cells in the epidermis of K14.E7 mice express more CXCL9/10 (Figure 2.4b and c) than epidermal cells from K14.E7xRb$^{\Delta L/\Delta L}$ and non-transgenic mice, and that the majority of CXCL9/10 expression in K14.E7 epidermis was by CD45$^-$ cells (Figure 2.4d and e) and was dependent on IFNγ signalling (Figure S2.3a and b). Similarly, whole skin RNAseq showed reduced expression of *Cxcl9* mRNA in E7 transgenic animals lacking the IFNγ receptor (Figure S2.3c). DCs (gated on CD11c$^+$MHCII$^+$CD45$^+$) of K14.E7 epidermis, express low to negative level of CXCL9 and CXCL10 when compared to the DCs from non-transgenic skin (Figure S2.4).

Immunofluorescent staining showed that in K14.E7 skin, the expression of CXCL10 was particularly prevalent at the basal layer of the epidermis and amongst fully differentiated keratinocytes, whereas CXCL9 was expressed uniformly in the suprabasal region of the epidermis (Figure 2.4f). Although some MHCII$^+$ cells from the dermis of K14.E7 express CXCL9 and CXCL10 (Figure 2.4g), most expression appeared to be in MHCII$^-$ cells in the epidermis.

CXCR3 promotes T lymphocyte recruitment to E7-associated hyperplastic skin

To assess whether T cell migration to hyperplastic skin was dependent on CXCR3, an *in vitro* chemotaxis trans-well assay was performed, using T cells induced to express CXCR3 (Nakajima et al., 2002). Supernatant from skin explants from K14.E7 mice attracted significantly more CXCR3$^+$ CD4 and CD8 T cells (Figure 2.5a and b) than supernatant from K14.E7xRb$^{\Delta L/\Delta L}$ or non-transgenic skin. Moreover, CXCR3$^+$ T cell migration was significantly reduced by a CXCL9/10 neutralising antibody (nAb) (Figure 2.5a-c), confirming a role for CXCL9 and CXCL10 in T cell migration in this assay. No significant CXCR3$^+$ T cell migration was observed with supernatant from mice unable to express IFN-γ (K14.E7xIFN$\gamma^{-/-}$; IFN$\gamma^{-/-}$), supporting the hypothesis that CXCL9 and CXCL10 production is IFN-γ dependent. Expression of CXCR3 on migrated CXCR3$^+$ T cells was lower on cells that migrated in response to K14.E7 skin supernatant (Figure 2.5c), suggesting internalization of ligand-engaged receptors.

CXCR3 signalling is required for T cell subset infiltration into K14.E7 skin grafts

To further assess the role of CXCR3 chemokine signals in the recruitment of lymphocytes to K14.E7 skin *in vivo,* CXCR3$^+$ T cells, derived from CD45.1$^+$ congenic B6.SJL.Ptprca mice, were transferred to non-transgenic CD45.2$^+$ animals bearing well healed CD45.2$^+$ K14.E7 grafts. Graft recipients were subsequently administered a CXCR3 antagonist-AMG487 or vehicle control (Figure 2.5d). Skin grafts harvested after four days of AMG-487 treatment had less TCRβ^+ CD45.1$^+$ cells (~30 cells per cm^2 of skin graft) when compared to vehicle controls (~60 cells per cm^2 of skin graft). Numbers of endogenous CD45.2 cells in the grafts were not altered by AMG-487 treatment (Figure 2.5e). Moreover, no significant difference in CD45.1$^+$ T cell infiltration was found in lymph node or spleen of grafted animals (Figure 2.5f). The data shows that engagement of CXCR3 is required for a subset of T cells to localize in K14.E7 transgenic skin.

Antagonizing CXCR3 signal does not enable K14.E7 skin graft rejection

Skin grafting was performed to investigate the function of skin infiltrating CXCR3+ T cells in the context of K14.E7 skin hyperplasia. K14.E7xRag$^{-/-}$ skin grafts were shown to be spontaneously rejected (Choyce et al., 2013) and produce chemokines CXCL9 and CXCL10 (Figure 2.6a). Interestingly, while the dominant CD45$^-$ cell population in the epidermis of K14.E7xRag$^{-/-}$ mice produces minimal CXCL9/10, a small CXCL9/10-producing subpopulation that is not seen in K14.E7xIFNγ$^{-/-}$ mice is observed. This, therefore, may not be IFNγ induced. B6.SJL.Ptprca mice receive K14.E7 and K14.E7xRag$^{-/-}$ skin 7 days after recipients were immunized with E7 peptide. Grafted mice were treated with the CXCR3 antagonist-AMG487 or vehicle control (Figure 2.6b). Host-derived CXCR3+ T cells were recruited to skin grafts in small numbers in vehicle control mice, but were largely absent in mice treated with the antagonist (Figure 2.6c). More CD4+CXCR3+ than CD8+CXCR3+ cells were recruited to K14.E7 skin graft (Figure 2.6d), consistent with the higher frequency of CD4+CXCR3+ cells found in the skin of K14.E7 (Figure 2.3a). K14.E7xRag$^{-/-}$ skin grafts were rejected (defined as 50% of skin graft shrinkage) when the recipient mice were administered with vehicle control, but were not rejected when treated with CXCR3 antagonist. K14.E7 skin grafts onto C57BL/6 recipients were tolerated in both groups as previously shown (Figure 2.6e-f). This suggests that infiltrating CXCR3+ T cells are an effector population that is required for graft rejection in donor lymphocyte deficient skin grafts. Therefore, in the absence of donor lymphocyte mediated suppression, CXCR3+ effector T cell populations are able to effect skin graft rejection.

2.6 Discussion

In this manuscript, we utilized K14.E7xRb$^{\Delta L/\Delta L}$ mice, which resembles normal skin in immune landscape and gene expression profile, to separate the hyperplastic phenotype from the local HPV16 E7 expression. We demonstrated that epithelial hyperplasia induced by HPV16E7 protein expression is required for the infiltration of immunocytes and the induction of CXCL9 and CXCL10 chemokines, which can attract CXCR3$^+$ T cells to the skin. These findings pose two questions: firstly, how does the epithelial hyperplasia impact on infiltrated lymphocytes; secondly, how do these chemokines contribute to the local immune responses that is a feature of E7 transgenic skin.

We demonstrated that the presence of E7-induced epithelial skin hyperplasia can also alter the expression profile of skin chemokines. Importantly, disruption of the E7-Rb interaction and epithelial hyperplasia in our study resulted in a reduction in CXCL9 and CXCL10 production within the skin. A change in skin chemokines is also seen in several other skin disorders and epithelial proliferation associated with wound healing (Gillitzer and Goebeler, 2001). For instance, CXCL9 and CXCL10, induced by wounding, facilitates epithelial repair through production of growth factors (Yates et al., 2009) and assists in preventing infection by promoting pathogen specific immune responses (Thapa and Carr, 2008). CXCL9/ and CXCL10 can be induced in damaged skin from myeloid cells and activated keratinocytes. This attracts CXCR3$^+$ immunocytes as a feature of many inflammatory skin disorders (Flier et al., 2001). Similarly, epithelial hyperproliferation, induced by deletion of the Mi-2β chromatin remodeler, results in CXCL9 and CXCL10 chemokine production in skin, and subsequently recruit both effector and regulatory CD4$^+$ T cell populations (Kashiwagi et al., 2017). Moreover, CXCR3$^+$ CD4 and CD8 T cells were found to be important in enhancing epidermal proliferation in a chemical skin tumorigenesis model (Winkler et al., 2011). The effect of hyperplasia on chemokine recruitment of immune cells can also be observed in murine hyperplastic cervix (mucosal) induced by either transgenic expression of HPV16 E7 or by treatment with estradiol, another commonly associated carcinogen for cervical oncogenesis. Genes associated with immune trafficking (*Cxcl13, Ccl3, Cxcr2*) and inflammatory responses (*IL-1α, TNFα, Irf1*) were the top up-regulated categories in both models of hyperplastic cervix (Cortes-Malagon et al., 2013). Whether there is an additive effect of the different causes of hyperplasia on immune cell trafficking and immune response was not explored but this effect is likely to be an important aspect for cervical disease progression. In support of this, neoplastic progression could be delayed when non-antigen specific inflammation was reduced by depleting CD4$^+$ T cells

(Daniel et al., 2003) in a different HPVE7-induced epithelial hyperplasia mouse model (Arbeit et al., 1994). Up-regulation of CXCR2 and its ligands CXCL1, 2, 3 and 5 in K14.E7 skin (Figure 2.2b) may contribute to increased keratinocyte proliferation as CXCR2 deficient animals showed a delayed wound healing process in terms of epithelialization and neovascularization (Devalaraja et al., 2000). Together, these findings support the idea that epithelial proliferation is the likely driver of elevated chemokine production and the latter is further required for progression of the disease.

Although expression of CXCL9 and CXCL10 was dramatically increased in K14.E7 skin, antagonizing CXCR3 did not change the outcome for K14E7 skin grafts on immunocompetent recipients. However, when local immunosuppression was removed by utilizing lymphocyte-deficient K14E7 grafts, these grafts were promptly rejected (defined as 50% of graft shrinkage) in a CXCR3 dependent manner. However, graft rejection was then prevented by blocking CXCR3 interactions, suggesting that CXCR3$^+$ T cells function as effector cells responsible for graft rejection in these circumstances. But how does this infiltrating CXCR3$^+$ effector population fail to reject K14E7 skin grafts on immunocompetent recipients? We hypothesise that insufficient CXCR3$^+$ effector cells are recruited to overcome local suppressive mechanisms and/or that the infiltrating population undergoes programming toward a phenotype ineffective for graft rejection. While CXCR3$^+$ T cells are clearly effector cells in our model, they represent only a small subset of the T cells within the skin, suggesting that other chemokines may be involved in epithelial hyperplasia-induced T cell recruitment. Recently, chemokine CXCL14 has been shown to be down-regulated in a HPV16E7-dependent manner and impacts on anti-tumour immune response. Restoration of *Cxcl14* expression in HPV-positive mouse oropharyngeal carcinoma cells enables the recruitment of NK, CD4$^+$ and CD8$^+$ T cells to tumour draining lymph node (Cicchini et al., 2016). Our previous studies have shown that CCR6$^+$ CD4 T cells can be recruited via CCL20 to the hyperplastic K14E7 skin (Choyce et al., 2013). CCR6 regulates the migration of regulatory T cells (Yamazaki et al., 2008) but depletion of Foxp3$^+$ regulatory T cells from either K14.E7 skin graft donor or graft recipients failed to reject K14.E7 skin (Mattarollo et al., 2011). In this study, the majority of CXCR3 expression was observed on TCRβ$^+$CD4$^-$CD8$^-$ T cells (CXCR3$^+$CD4$^+$ and CXCR3$^+$CD8$^+$ T cells comprised, 2.2% and 0.6%, of total T cells respectively, while the total population of CXCR3$^+$ T cell is 7.5%). This unusual CD4$^-$CD8$^-$ subset of αβT cells can represent NKT cells, conventional T cells that have downregulated CD8 expression to form pro-inflammatory effector cells or alternatively, a population of regulatory cells (Brandt et al., 2017; Godfrey et al., 2004; Zhang et al., 2001).

The presence of a regulatory T cell population in K14.E7 skin, most likely NKT cells, prevents rejection of E7 transgenic skin by immunocompetent graft recipients although the chemokine attracting NKT cells to K14E7 skin remains unknown (Mattarollo et al., 2010a). Although no differential expression of CXCR3 was observed in non-transgenic, K14.E7 and K14.E7xRb$^{\Delta L/\Delta L}$, this double negative T cell population could also potentially contribute to skin immunity in a MHC-independent manner (Tikhonova et al., 2012; Van Laethem et al., 2007).

Ideally, immunotherapeutic intervention targeting effector immune cell recruitment should induce more efficient immune responses to combat cancers. As chronic IFNγ stimulation has profound impact on i) CXCL9 and CXCL10 chemokine expression/signalling and ii) the fate of K14.E7 skin grafts, one possible strategy may be to increase the infiltration of CXCR3^{+} T cells to HPV-infected lesions and overcome the local suppressive environment.

2.7 Materials and Methods

Animals

Mice were maintained in Translational Research Institute Biological Research Facility under specific pathogen free conditions. Female mice were used at 8-12wk of age. C57BL/6, K14.E7 (Herber et al., 1996), Rag$^{-/-}$ and B6.SJL.Ptprca mice were obtained from Animal Resources Centre (Perth, Australia). IFNγ$^{-/-}$ and IFNγR$^{-/-}$ mice were purchased from The Jackson Laboratory (Bar Harbor, ME). Heterozygous Rb$^{\Delta L/\Delta L}$ transgenic mice (Isaac et al., 2006) were obtained from Dr. Fred Dick. Homozygous Rb$^{\Delta L/\Delta L}$ mice were generated by backcrossing C57BL/6 for 10 generations. K14.E7xIFNγ$^{-/-}$, K14.E7xIFNγR$^{-/-}$, K14.E7xRag$^{-/-}$ and K14.E7xRb$^{\Delta L/\Delta L}$ mice were generated by mating heterozygous K14.E7 with homozygous IFNγ$^{-/-}$, Rag$^{-/-}$ and Rb$^{\Delta L/\Delta L}$, respectively. All procedures were approved by the University of Queensland Animal Ethics Committee (UQDI/367/13/NHMRC and UQDI/452/16).

FACS and Antibodies

FACS analysis were undertaken as previously described (Mattarollo et al., 2010a). Foxp3 Fix/Perm Concentrate and Diluent kit was used for intracellular staining (eBioscience, San Diego, USA). CXCL9 and CXCL10 were stained intracellularly with unconjugated goat anti-mouse polyclonal Ab (R&D, MN, USA) followed by PE-conjugated secondary donkey anti-goat IgG H&L Ab (Abcam, Cambridge, UK). Anti-mouse monoclonal Abs to CD45.2 (104), CD45.1 (30-F11), CD8α (53-6.7), TCRβ (H57-597), CD11b (M1/70), EpCAM (G8.8), CD19 (6D5), MHCII (I-A/I-E) (M5/114.15.2), IFNγ (XMG1.2), CXCR3 (CXCR3-173), CXCR3 (Met1-Leu367), CD3 (145-2C11), CD4 (GK1.5), CD11c (HL3) and corresponding isotype controls were purchased from Biolegend (San Diego, USA), eBioscience (San Diego, USA), BD Bioscience (San Jose, USA) and R&D (MN, USA).

RNA extraction, reverse transcription and qPCR

RNA Extraction was performed as described (Zhussupbekova et al., 2016). For each reverse transcription, 1 µg of extracted RNA was processed using a SuperScriptIII kit (Life technology, MA, USA). Primers sequences can be found in Table S2. qPCR was carried out on Applied Biosystems™ QuantStudio™ 6 Flex Real-Time PCR System.

Sequencing and analysis, GSEA and gene ontology analysis

RNA sequencing and raw data processing were done as previously described (Zhussupbekova et al., 2016). Detailed methods for GSEA and gene ontology analysis can be found in the supplementary materials and methods.

Skin Grafting and Reagents

Grafting was done as previously described (Choyce et al., 2013). Animals were given CXCR3 antagonist-AMG487 (Tocris, No. 3387, Bristol, UK) 3 µg/g body weight in DMSO, or DMSO alone, subcutaneously. E7 peptide (RAHYNIVTF) was synthesized by Auspep Pty Ltd, (Melbourne, Australia), with purity >80%.

Transwell migration assay

Splenocytes were activated (supplementary methods), and 5×10^5 activated cells in 100 µl were seeded into a 5 µm pore trans-well insert (Corning, No. 3421, NY, USA). Supernatants from in vitro skin cultures (supplementary methods) were diluted with RPMI in 1:2 ratio, with a final volume of 750 µl. As controls, recombinant CXCL9 (250-18, Peprotech, NJ, USA), CXCL10 (250-16, Peprotech, NJ, USA), neutralizing antibodies for CXCL9 (AF-492-SP, R&D, MN, USA), CXCL10 (AF-466-SP, R&D, MN, USA) or goat IgG isotype control (AB-108-C, R&D, MN, USA) were added to the bottom well of the transwell culture. Cells were incubated at 37°C for 60 minutes and the cells in the bottom wells were collected for FACS analysis.

Statistical analysis

Prism 7 (GraphPad Software, La Jolla, CA) software was used for statistical analysis and to prepare the plots. Unless otherwise stated, all analyses were done using one-way ANOVA, with Bonferroni's multiple comparison test. Unpaired Student's t-test and two-way ANOVA were used in Figure 2.6e and Figure 2.6f and j, respectively. All plots show mean value with SEM. Result significance was shown, where *$p<0.05$, **$p<0.01$, ***$p<0.001$ and ****$p<0.0001$.

Other methods can be found in Supplementary Method section.

Conflict of interest

The authors state no conflict of interest.

37
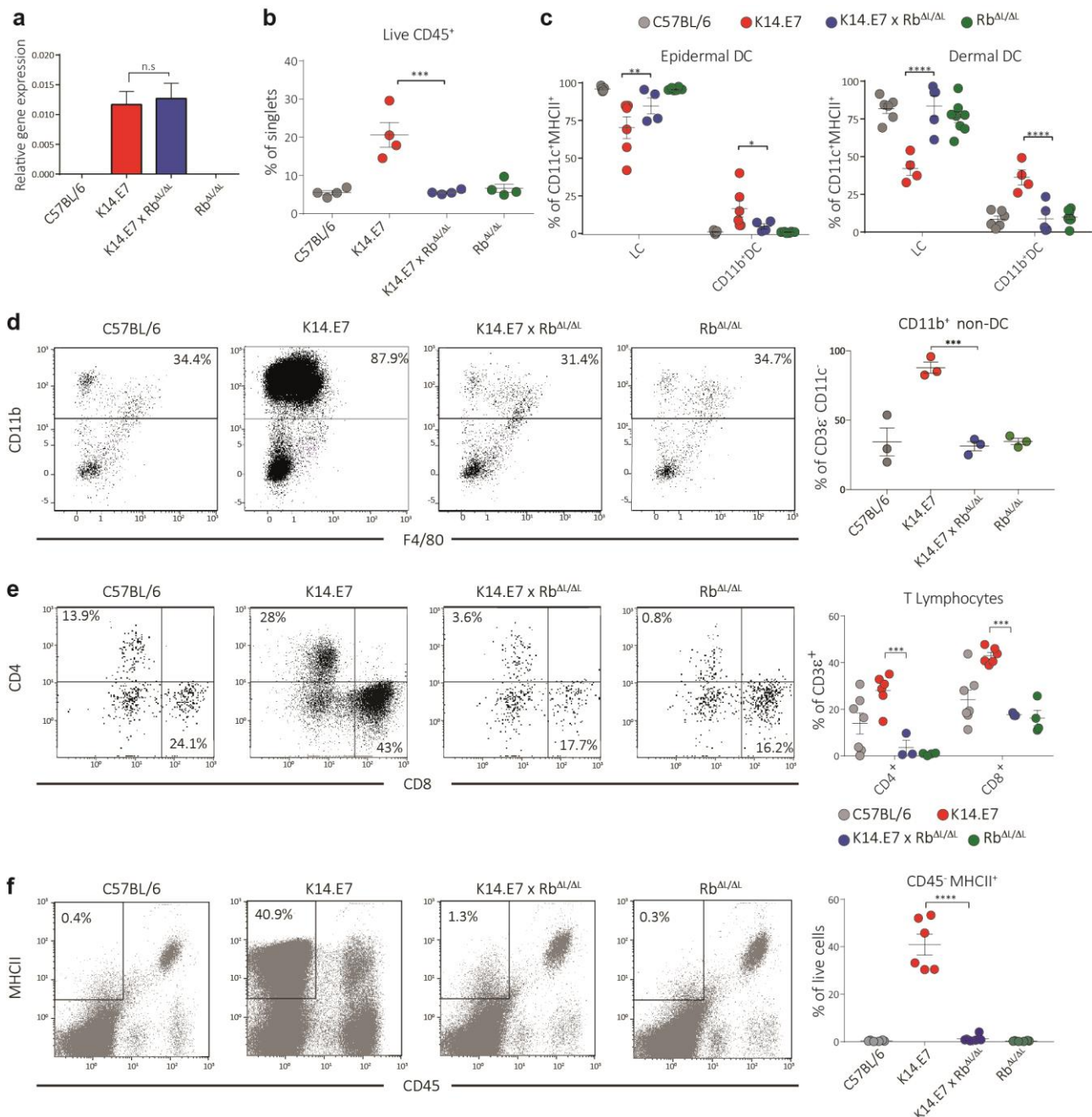
Figure 2.1. Effect of E7 expression on local immune responses is minimal in the absence of E7 induced epithelial proliferation

Skin from K14.E7 transgenic was compared with K14.E7xRb$^{\Delta L/\Delta L}$ and C57BL/6 mice. **(a)** Expression of *E7* mRNA relative to an internal control, Hprt. n>3 **(b-f)** FACS analysis of skin infiltrating immune cell populations. **(b)** live CD45$^+$ cells,; **(c)** epidermal and dermal antigen presenting cell populations- EpCAM$^+$CD11b$^+$ (LC) and EpCAM$^-$ CD11b$^+$ (CD11b$^+$ DC) as a percentage of CD11c$^+$MHCII$^+$ CD45$^+$ cells; **(d)** CD11b$^+$ non-DCs (as a percentage of CD3ϵ^- CD11c$^-$ CD45$^+$ cells); **(e)** CD4 and CD8 T cells under CD3ϵ^+ gate; **(f)** MHCII$^+$CD45$^-$ cells. Error bars showing mean+/-SEM of n>3.
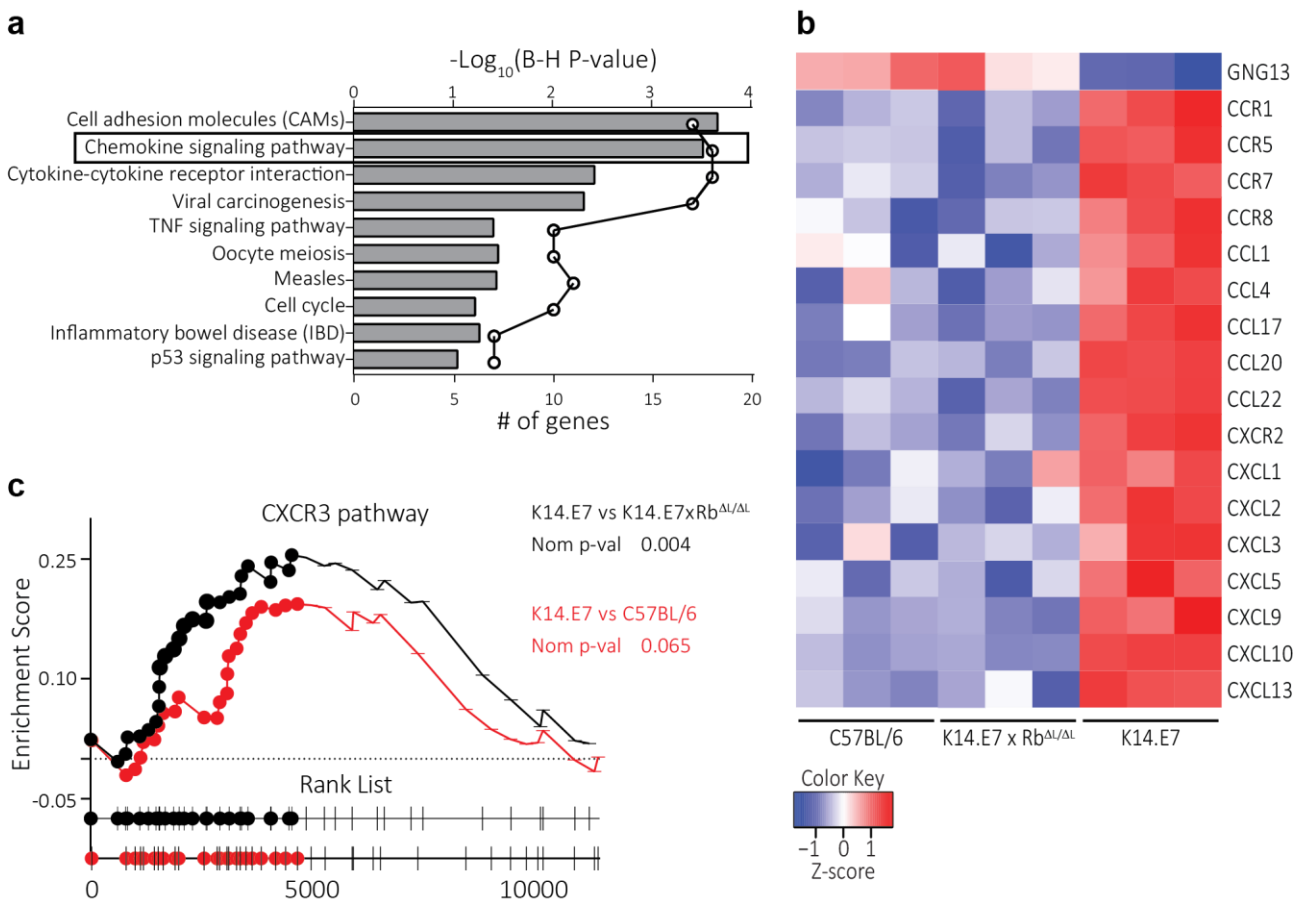
Figure 2.2. Overexpression of mRNA for chemokine receptors and ligands in E7 transgenic skin

(a) Pathway analysis of 482 genes differentially displayed in association with hyperplastic skin. Bars, top 10 pathways ranked by -log10 of B-H P-value; dots, number of genes in a particular gene ontology group. **(b)** Heat map of chemokine genes expression in C57BL/6, K14.E7 and K14.E7xRb$^{\Delta L/\Delta L}$ skin. **(c)** GSEA of CXCR3 pathway signature to the mRNA profile of K14.E7 vs. K14.E7xRb$^{\Delta L/\Delta L}$ and K14.E7 vs. C57BL/6. Black and grey dots, subset in the leading edge of the gene set, where 25/40 and 23/40 genes were identified, respectively.
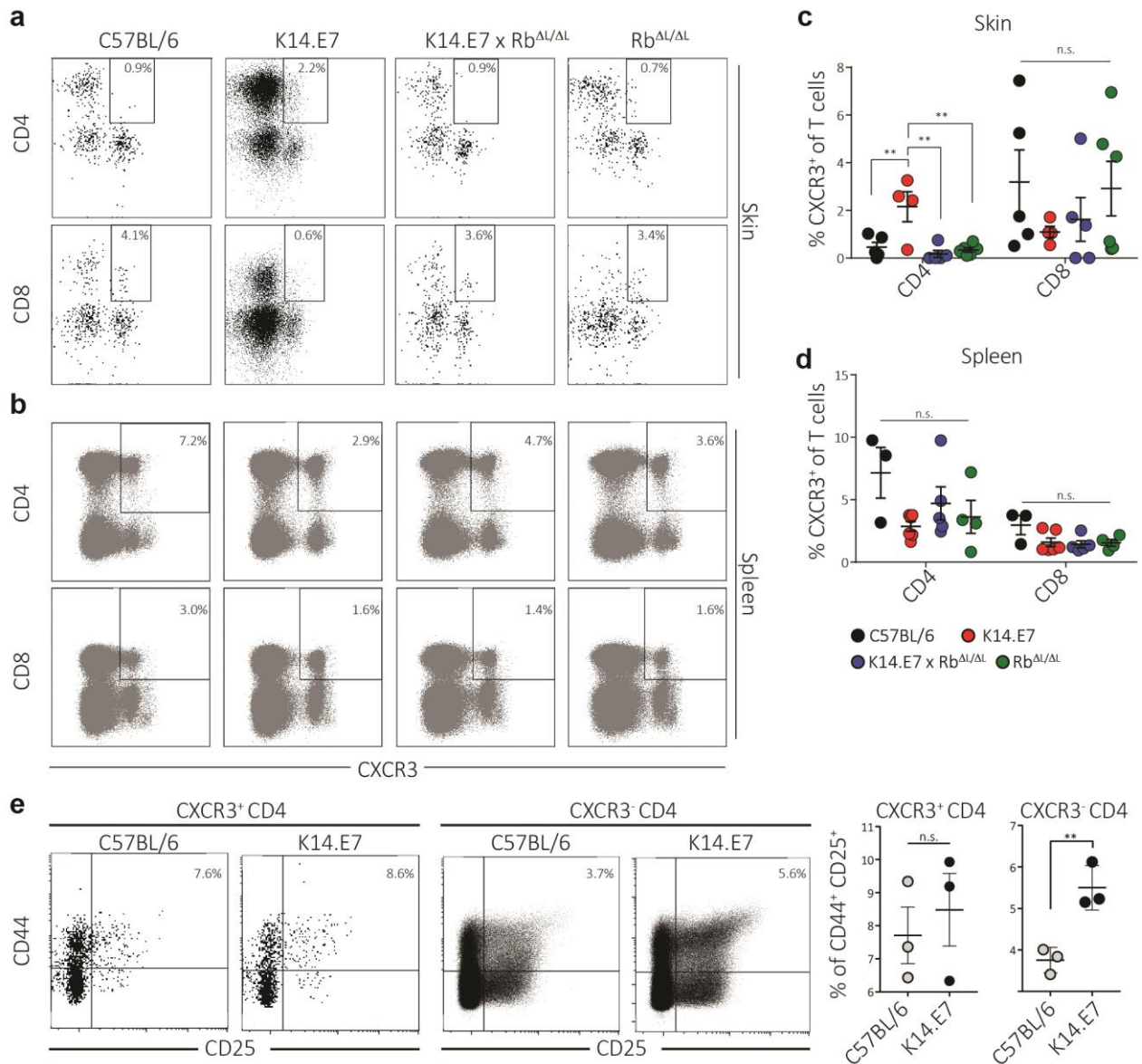
Figure 2.3. CXCR3 enriched on CD4 T cells in K14.E7 but not K14.E7xRb^{ΔL/ΔL} skin

CXCR3 expression on CD4$^+$ and CD8$^+$ T cells in skin and spleen. **(a and b)** Representative flow cytometry plots pre-gated on live CD45$^+$TCRβ$^+$ cells. a, skin; b, spleen. **(c and d)** Quantitative results from skin and spleen of 3-5 mice. **(e)** Representative plots showing expression of activation markers by CXCR3$^+$ and CXCR3$^-$ CD4 T cells from lymph nodes.
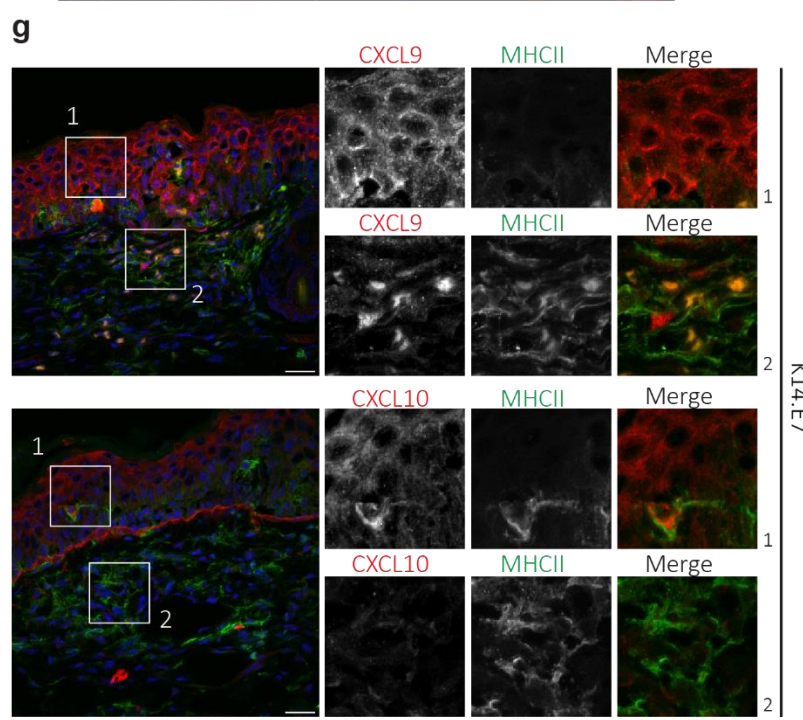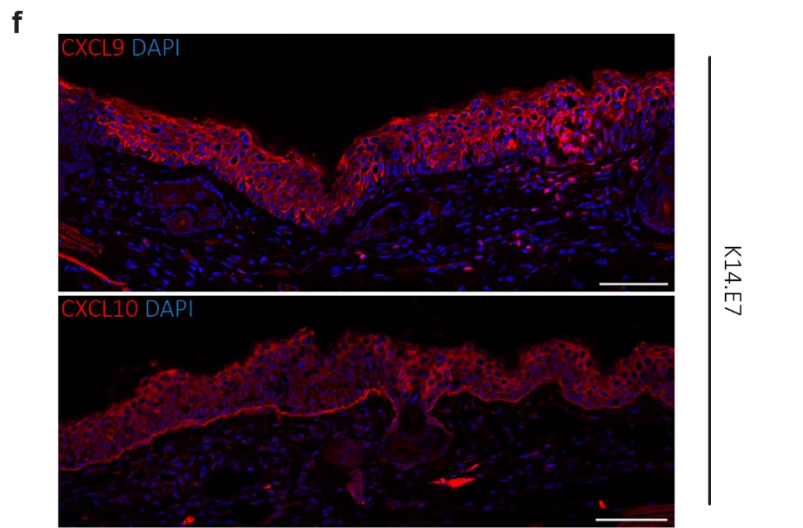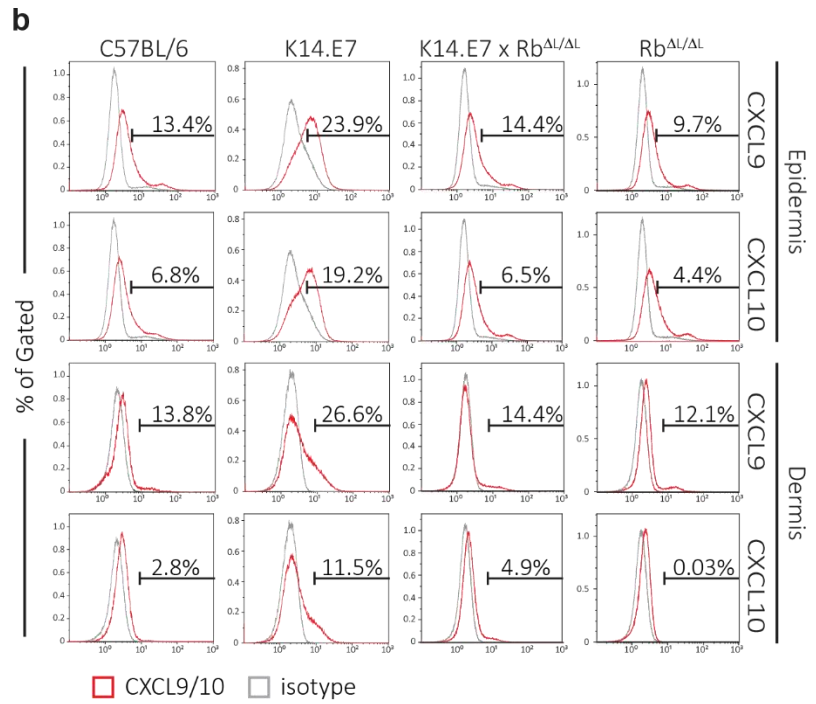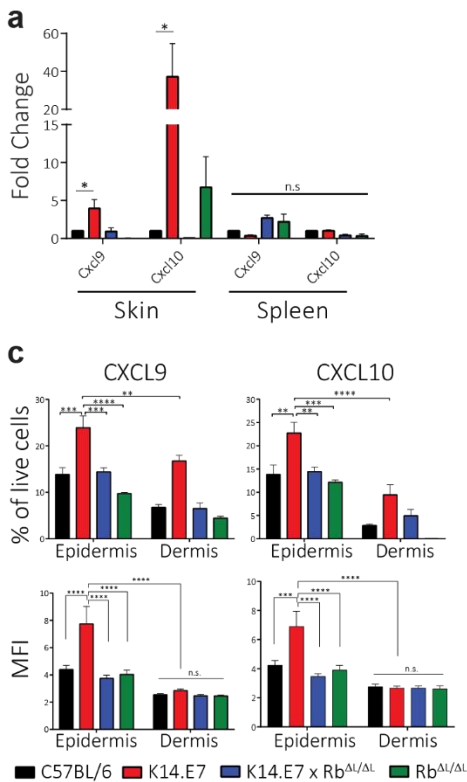
Figure 2.4. CXCL9/10 expression in skin is mostly by epidermal CD45⁻ cells

(a) Expression of *Cxcl9/10,* normalized with *Hprt,* relative to C57BL/6, in skin and spleen. **(b)** Intracellular CXCL9/10 were assessed for live cells from epidermis and dermis of K14.E7 and compared with K14.E7xRb$^{\Delta L/\Delta L}$ and C57BL/6 mice. **(d)** Expression of CXCL9/10 on CD45⁻, DCs (CD11c⁺MHCII⁺) and T cells (TCRβ⁺) in K14.E7 epidermis. **(c and e)** Quantitative data showing mean percentage and ΔMFI of (b) and (d), respectively. ΔMFI calculated by subtracting signal MFI from isotype control MFI. **(a-e)** Error bars showing mean+/-SEM with n>3 of each sample. **(f and g)** Immunofluorescent staining of CXCL9/10 (red) within K14.E7 skin. Blue, DAPI; green, MHCII. Scale bar= 200 μm in (f) 100 μm in (g).
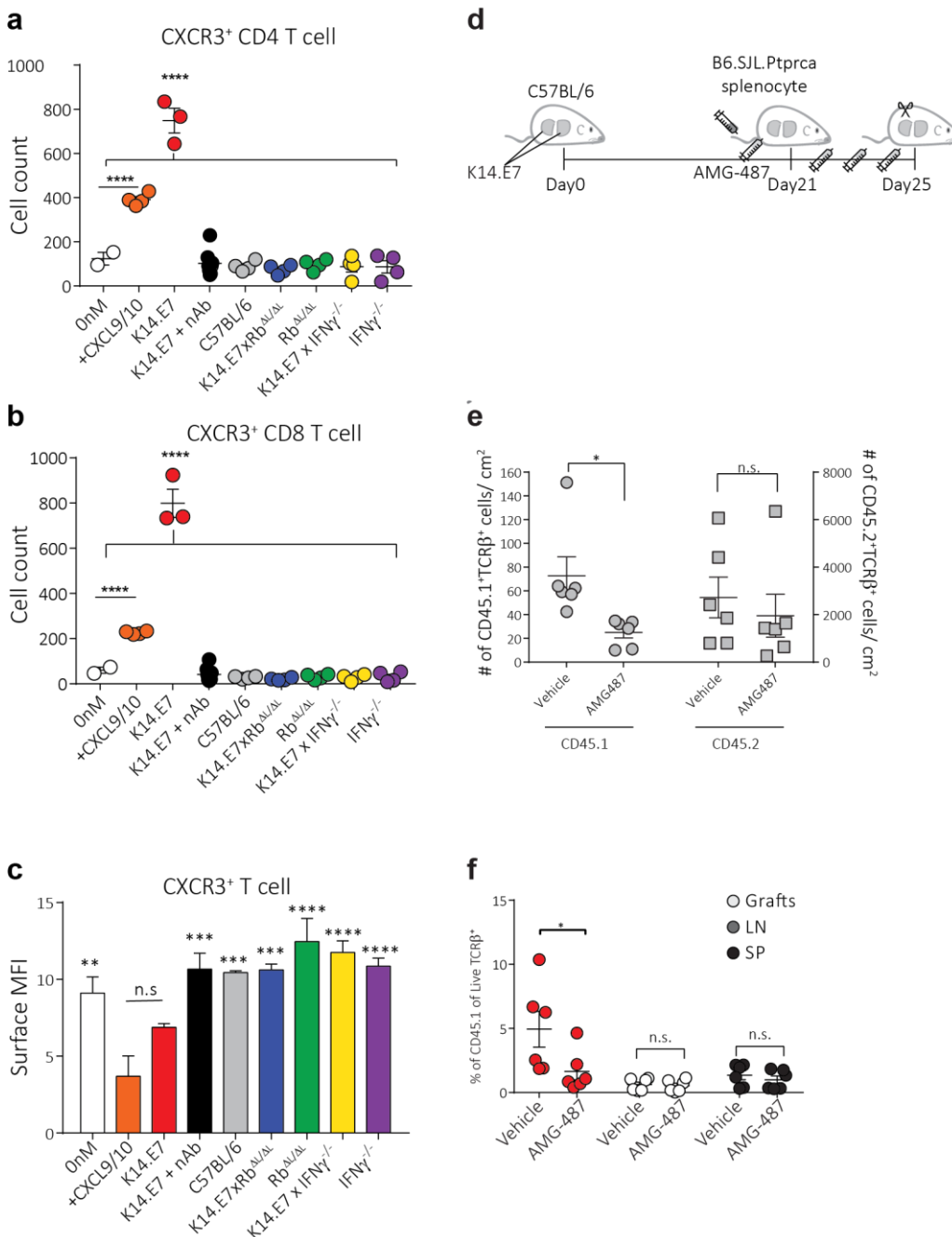
Figure 2.5. CXCR3+ T cells migrate to hyperplastic skin environment *in vitro* and *in vivo* [1]

(a-c) T cell migration assay. 0mM, medium control; +CXCL9/10, 50nM CXCL9; 10nM CXCL10; nAb[2], neutralizing antibody to CXCL9/10 at 200 ng/ml. Isotype Ab was included in K14.E7 supernatant. **(c)** MFI of surface CXCR3 on migrated T cells with. All compared to +CXCL9/10. **(d-f)** K14.E7 skin grafts were placed onto C57BL/6 (CD45.2) recipient. On day 21, $5*10^6$ activated B6.SJL.Ptprca (CD45.1) splenocytes were transferred intravenously.

---

[1] See Chapter 5 section 2 for full optimisation process of induction of CXCR3 expression on enriched T cells

[2] Procedures of establishing the use of neutralising antibody concentration is outlined in Chapter 5 section 3 and 4.

CXCR3 antagonist-AMG487 or vehicle control was injected subcutaneously for four days. On day 25, skin grafts were excised and lymph node and spleen were harvested for FACS analysis. **(e)** Number of CD45.1/ CD45.2 cells found in grafts on day 25. **(f)** Percentage of TCRβ$^+$CD45.1 cells found in different tissues. **(d-f)** Pooled result from two-independent experiments. All error bars showing mean+/-SEM with n>3.
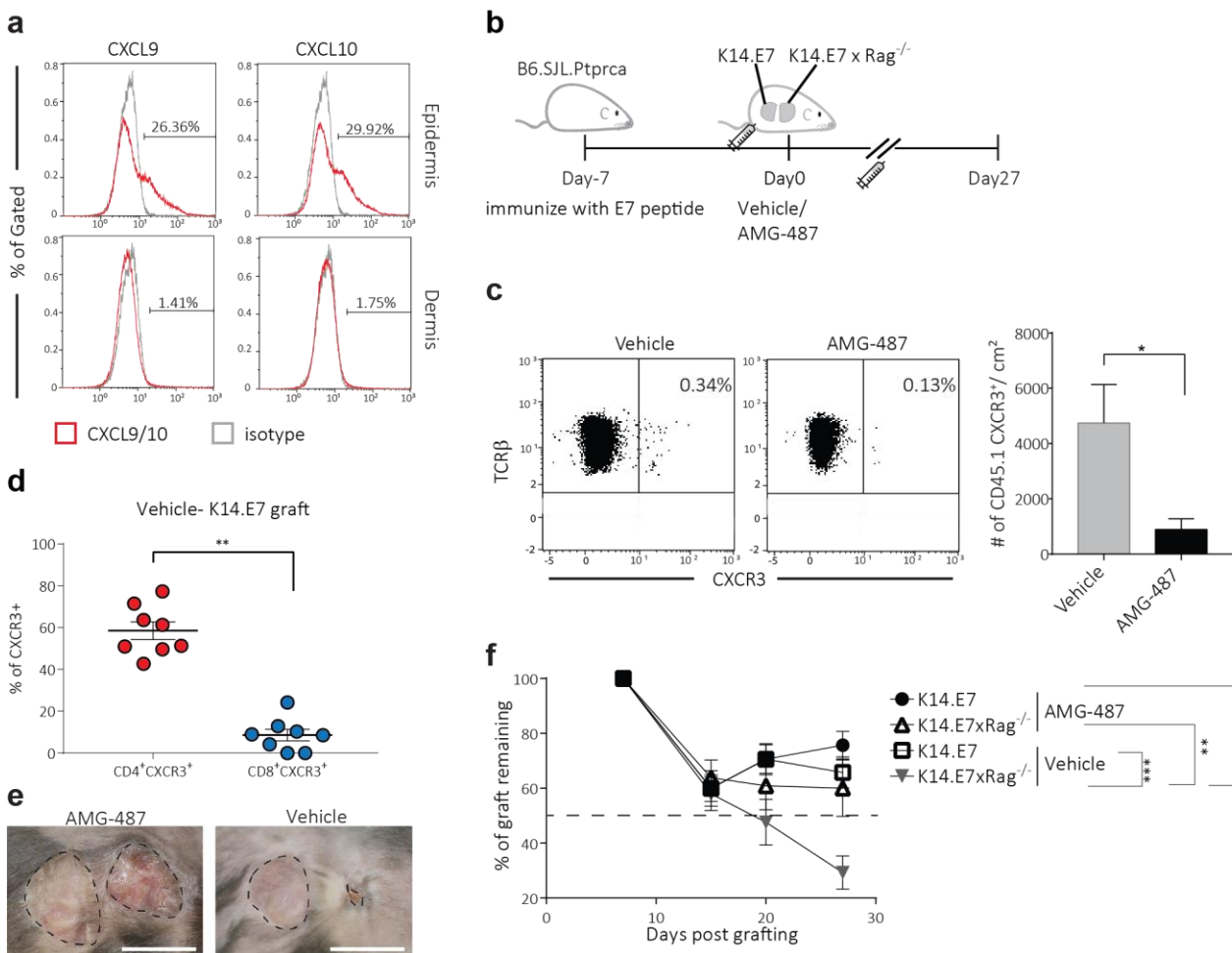
Figure 2.6. CXCR3⁺ T cells influence on graft rejection

(a) CXCL9/10 expression level in epidermis and dermis from K14.E7xRag^-/- mouse expressed as percentage compared to K14.E7. Representative plot showed from n>3. **(b-f)** Skin graft recipients received E7-peptide (50µg) subcutaneously 7 days before grafting. Recipients were grafted with K14.E7 (left) and K14.E7xRag^-/- (right) ear skin and treated with either vehicle control or AMG487 daily. N>5 per treatment group. All error bars showing mean+/-SEM. **(c)** CXCR3⁺ T lymphocytes (TCRβ⁺CD45.1) in K14.E7 skin grafts treated with vehicle control or AMG487. Cell numbers were normalized by skin graft size (per cm^2). Unpaired student t-test with *p<0.05 performed. **(d)** Percentage of CXCR3⁺CD4⁺ and CXCR3⁺CD8⁺ cells in K14.E7 skin graft treated with vehicle control. **(e)** Skin grafts on day 27, scale bar= 10 mm. **(f)** Percentage of graft survival.

Supplementary Methods

Histology sample preparation

For hematoxylin and eosin staining, ear skin was harvested and fixed in 4% paraformaldehyde solution overnight. Tissues were embedded in paraffin, sectioned and stained following standard protocol. For immunofluorescence staining, tissues were embedded in OCT and cryosectioned at 7 mm.

Isolation of cells from ear skin, lymph node and spleen

Ear skin was split into dorsal and ventral parts and incubated with 2.5 µg/µl Dispase II (Roche, Basel, Switzerland) for 1 hour at 37°C. Epidermis and dermis were separated with closed forceps and homogenized. Skin was further digested with 1 µg/µl, of collagenase D (Roche, Basel, Switzerland) and 0.2 µg/µl of DNase, (Roche, Basel, Switzerland) for 1hour at 37°C. Lymph node and spleen were mashed with syringe plunger and passed through 0.7 µm filter (BD Falcon, San Jose, USA). For each spleen, red blood cells were lysed with 1 ml of ACK buffer (0.15 M NH_4Cl, 1 mM $KHCO_3$, and 0.1 mM Na_2EDTA) for 30 seconds at room temperature and the reaction was stopped by adding 10 ml of FACS buffer (2 mM EDTA, 2% FCS in PBS).

Immunofluorescence staining

Skin tissue was embedded in OCT and cryosectioned at 7 µm onto Superfrost™ Plus slides (4951PLUS4, ThermoFisher, MA, USA). All procedures were done at room temperature. Samples were fixed in acetone for 5 minutes and blocked with 10% donkey serum in TBS buffer for 1 hour. Primary antibodies against CXCL9 and CXCL10 were diluted with TBS in 1:40 ratio and incubated with samples for 1 hour followed by 30 minutes of secondary Ab (Donkey Anti-Goat, Alexa Fluor 488, Abcam, Cambridge, UK) incubation. Samples were blocked again with 10% goat serum in TBS buffer for 1 hour. Primary Ab against MHCII (107628, Biolegend, San Diego, USA,) was diluted with TBS in 1:200 ratio and incubated with samples for 1 hour followed by 30 minutes of secondary Ab (Goat Anti-Rat IgG (H+L), FITC) incubation. All secondary antibodies were prepared in TBS in 1:200 ratio.

Skin Explant Culture

Skin explant culture was performed as previously described (Gosmann et al., 2014b). Briefly, ear skin was split into dorsal and ventral part and spread flat in 24-well plate with 1 ml of complete RPMI. Culture medium was changed after 1 hour and changed again after another 2 hours. Skin was further cultured with 1 ml medium for 20-24 hours and supernatant was collected.

Sequencing and analysis, Gene Set Enrichment Analysis (GSEA) and gene ontology analysis

Standard analysis procedure was performed following previous protocol (Subramanian et al., 2005).

The gene signatures of K14.E7 (n=3) and K14.E7 x Rb$^{\Delta L/\Delta L}$ (n=3) were curated from the RNAseq data processed as mentioned above. Genes were pre-ranked based on the significance of differential expression to C57BL/6 (n=3) and the top ~300 genes from the pre-ranked gene list were set as signature. Stage 1, 2 and 3 CIN patient RNA expression profile was extracted from de Boon et al., 2015 GSE643. CXCR3 pathway signature was adopted from PID (version: BioPAX3).

Candidate genes identified (hyperplastic gene list) were uploaded as input (482 genes) for functional annotation using Database for Annotation, Visualization and Integrated Discovery (DAVID) 6.8. Fisher exact probability with P<0.05 to determine significantly enriched gene set (Huang da et al., 2009).

T cells enrichment assay

Single cell suspension from spleen was incubated (1 x 10^8 cells/reaction) with 5% rat serum and biotin-labelled antibodies- CD19 (clone 6D5, Biolegend, San Diego, USA), CD11b (clone M1/70, Biolegend, San Diego, USA) and CD11c (clone N418, Biolegend, San Diego, USA) in 1:200 dilution in 1 ml of FACS buffer for 15 minutes at room temperature. Strepavidin beads (EasySep™ Streptavidin RapidSpheres™ 50001, STEMCELL technologies, Canada) were mixed thoroughly and 75 µl was added into each 1ml reaction and let sit at room temperature for 2 minutes. FACS buffer was added to top up the volume to 2.5 ml/reaction before placed in the EasySep™ Magnet (STEMCELL technologies, Canada). Enriched T cells were poured out from the tube and counted for further use.

T cell in vitro activation

To achieve optimal CXCR3 expression, T cells were stimulated with immobilized antibodies - αCD3 (3 µg/ml, clone 17A2, eBioscience, San Diego, USA) and αCD28 (3 µg/ml, clone 37.51, eBioscience, San Diego, USA) in 1M Tris-HCL (pH9.4) overnight at 4°C. Enriched T cells were seeded at a density of 2×10^6 cells/well in complete RPMI following with centrifugation of the whole plate. Cells were cultured at 37°C for 2 days then washed with PBS before re-plating in complete RPMI without activating antibodies for 1 day.

Supplementary Figures

a
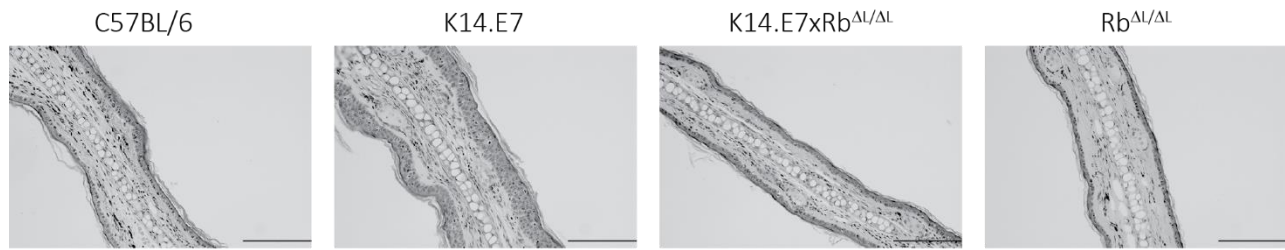
b
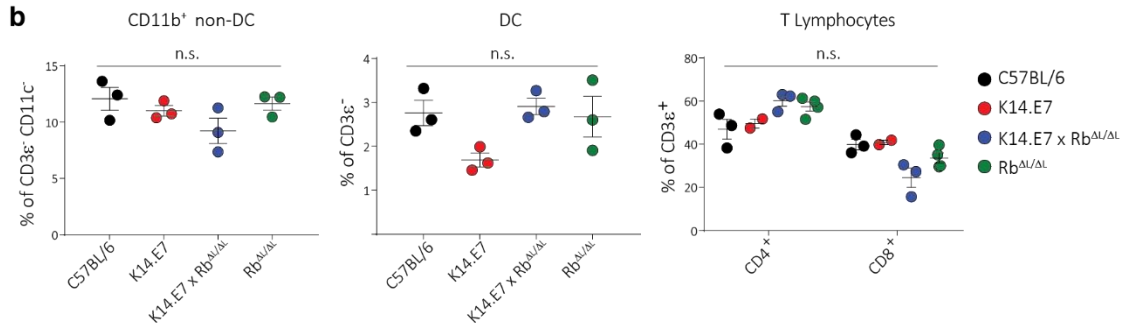
Figure S2.1.

a) Histological analysis of ear skin sections with haematoxylin and eosin (H&E) staining from indicated animals. Scale bar = 500 μm. b) FACS analysis of CD11b⁺ non-DCs, DCs, CD4⁺ and CD8⁺ T cells in spleens of indicated animal strains.
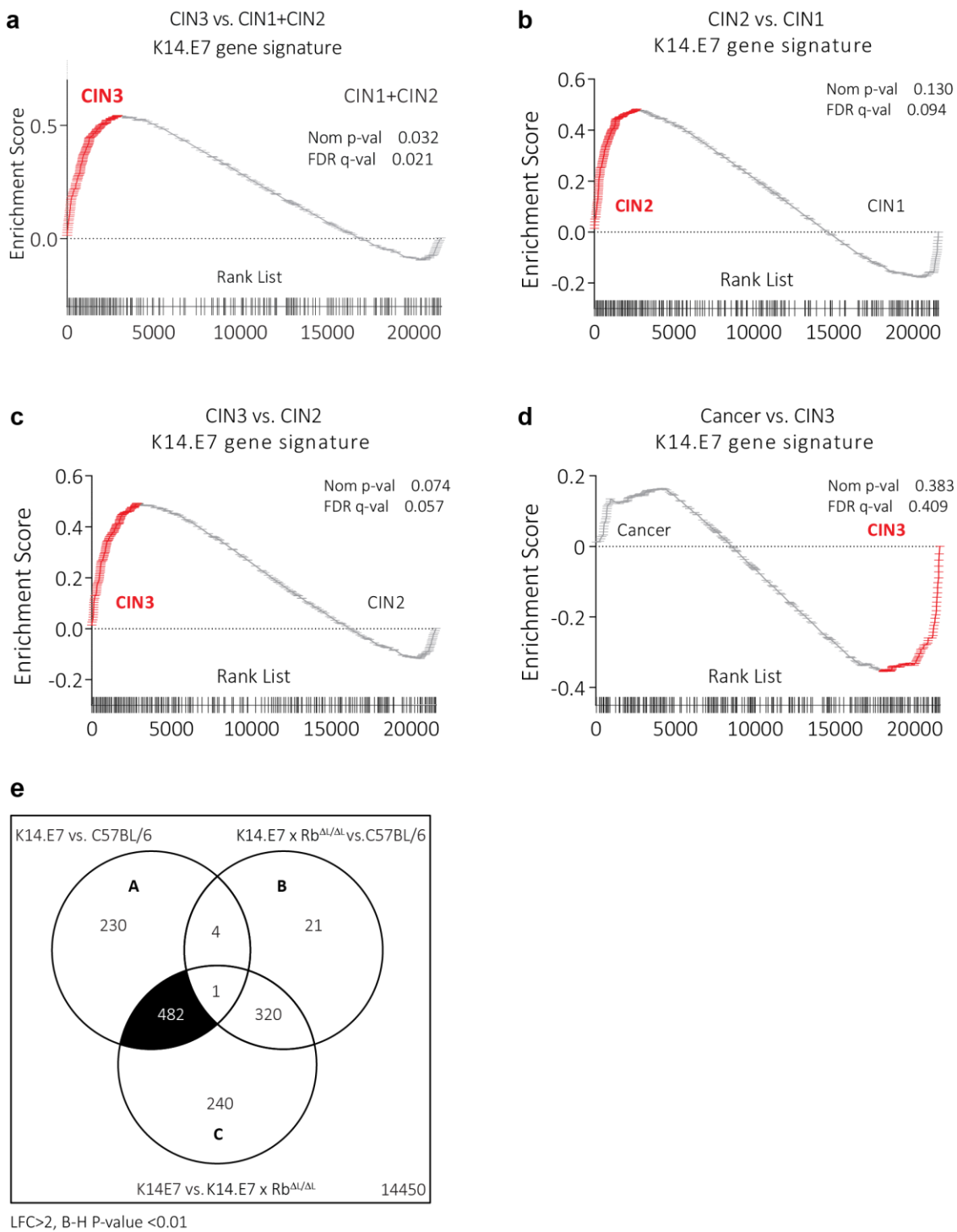
Figure S2.2.

(a-d) GSEA analysis of K14.E7 skin gene signature to CIN stages. Top 300 up-regulated genes in K14.E7 vs. C57BL/6 were identified as K14.E7 skin signature and projected onto ranked differential expression profiles. (a) CIN3 vs. CIN1/CIN2, (b) CIN2 vs. CIN1, (c) CIN3 vs. CIN and (d) Cancer vs. CIN3. Black lines indicate leading edge subset of the gene set. (e) Venn diagram of differentially expressed genes in indicated comparison.
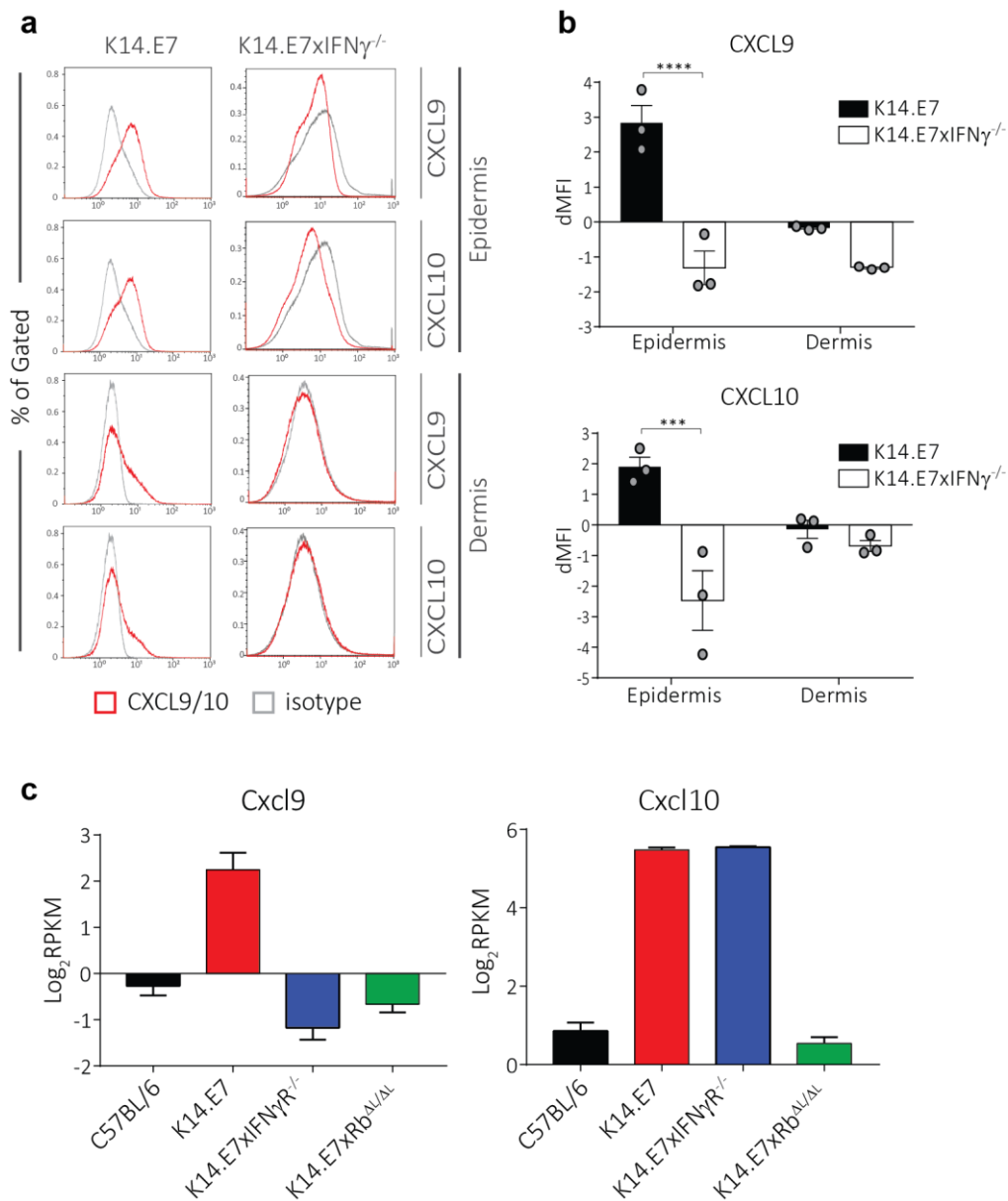
Figure S2.3.

(a) CXCL9 and CXCL10 expression level on CD45⁻ cells in skin of K14.E7 and K14.E7xIFNγKO. Black lines, signal staining; grey lines, isotype control. (b) Quantitative data of (a) showing ΔMFI, calculated by subtracting signal MFI from isotype control MFI. (c) Log₂RPKM of Cxcl9 and Cxcl10 expression level from whole skin RNA sequencing of C57BL/6, K14.E7, K14.E7xIFNgRKO and K14.E7xRb$^{ΔL/ΔL}$. Results showing one experiment with three biological replicates. Two independent experiments were done.
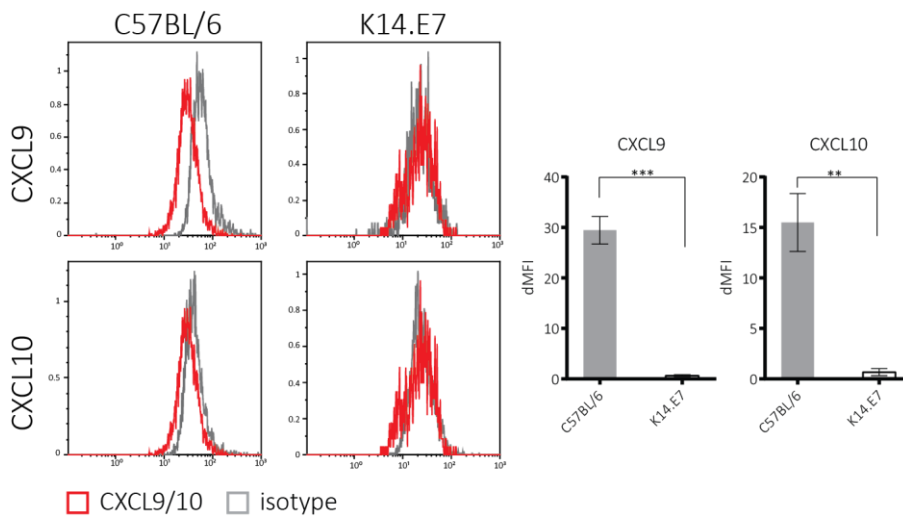
Figure S2.4.

CXCL9 and CXCL10 expression level on DCs (CD11c$^+$MHCII$^+$) in the epidermis of C57BL/6 and K14.E7 skin. Black lines, isotype control; grey lines, signal staining. Quantitative data showing ΔMFI, calculated by subtracting signal MFI from isotype control MFI. Results showing one experiment with three biological replicates. Two independent experiments were done.

Supplementary Tables

Table S2.1. ROAST and CAMERA analysis on CXCR3 pathway

ROAST (rotation gene set testing)	Testing whether genes are differentially expressed in gene sets					
K14.E7 vs C57BL/6	**NGenes**	**PropDown**	**PropUp**	**Direction (in K14.E7)**	**P-value**	**FDR**
PID_CXCR3_Pathway	43	0.2325581	0.5813953	Up	0.001	0.001
K14.E7 vs K14.E7 x Rb$^{\Delta L/\Delta L}$						
PID_CXCR3_Pathway	43	0.1860465	0.627907	Up	0.001	0.001

CAMERA (competitive gene set testing)	Testing whether the genes in the set are highly ranked in terms of differential expression relative to genes not in the set		
K14.E7 vs C57BL/6	**NGenes**	**Direction (in K14.E7)**	**P-value**
PID_CXCR3_Pathway	43	Up	0.09959264
K14.E7 vs K14.E7 x Rb$^{\Delta L/\Delta L}$			
PID_CXCR3_Pathway	43	Up	0.008101752

Table S2.2. Primers sequence

Gene Name	Forward primer (5'-3')	Reverse primer (5'-3')
Gapdh	TGACCACAGTCCATGCCATC	GACGGACACATTGGGGGTAG
Hprt	AGCGTCGTGATTAGCGATGA	CTCGAGCAAGTCTTTCAGTCCT
Hpv16e7	GACAAGCAGAACCGGACAGA	TTTCTGGGAACAGATGGGGC
Cxcl9	TGTGGAGTTCGAGGAACCCT	TGCCTCGGCTGGTGCTG
Cxcl10	AGTGCTGCCGTCATTTTCTG	ATTCTCACTGGCCCGTCAT

Additional data not described in article 1

Following the identification of that CXCR3+ T cells are required for K14.E7xRagKO skin graft rejection, we investigated whether CXCR3+ T cells are sufficient to enable K14.E7 skin graft clearance. To test this hypothesis, we grafted C57BL/6 skin alongside with K14.E7 skin on non-transgenic immunocompetent recipients. E7TCR269 mice were immunised with GF001 peptide and T cells were activated seven days after immunisation following protocol outlined in section 5.2 of chapter 5. FACS sorted CXCR3+ or CXCR3- T cells (200,000 per recipient) were transferred intravenously on day 14 (0 day post injection, DPI) and graft size was monitored until day 49 (35 DPI) (Figure 2.7a)[3]. No significant difference was observed between CXCR3+ or CXCR3- T cells receiving groups and no graft showed reduction in size at the end point of the experiment (Figure 2.7b). However, as shown in Figure 2.6, without this population, E7-expressing skin graft rejection can be prevented. This result suggests that CXCR3+ T cell alone is not sufficient, but is required, to induce K14.E7 skin graft rejection. As CXCR3 expression is dynamic, sorted CXCR3 positive or negative cells can down-regulate or upregulate this marker, respectively, upon transfer or being influenced by the in vivo environment. Potentially, the results showing in Figure 2.7 could be limited by the changing dynamics of CXCR3 expression. To circumvent this limitation, CXCR3 positive T cells can be obtained from T cell lines that express CXCR3 constitutively and CXCR3 negative T cells from CXCR3 knockout mice can be utilised.

---

[3] Detailed process for tracking sorted CXCR3+ and CXCR3- T cells in skin grafts is outlined in Chapter 5 section 5.
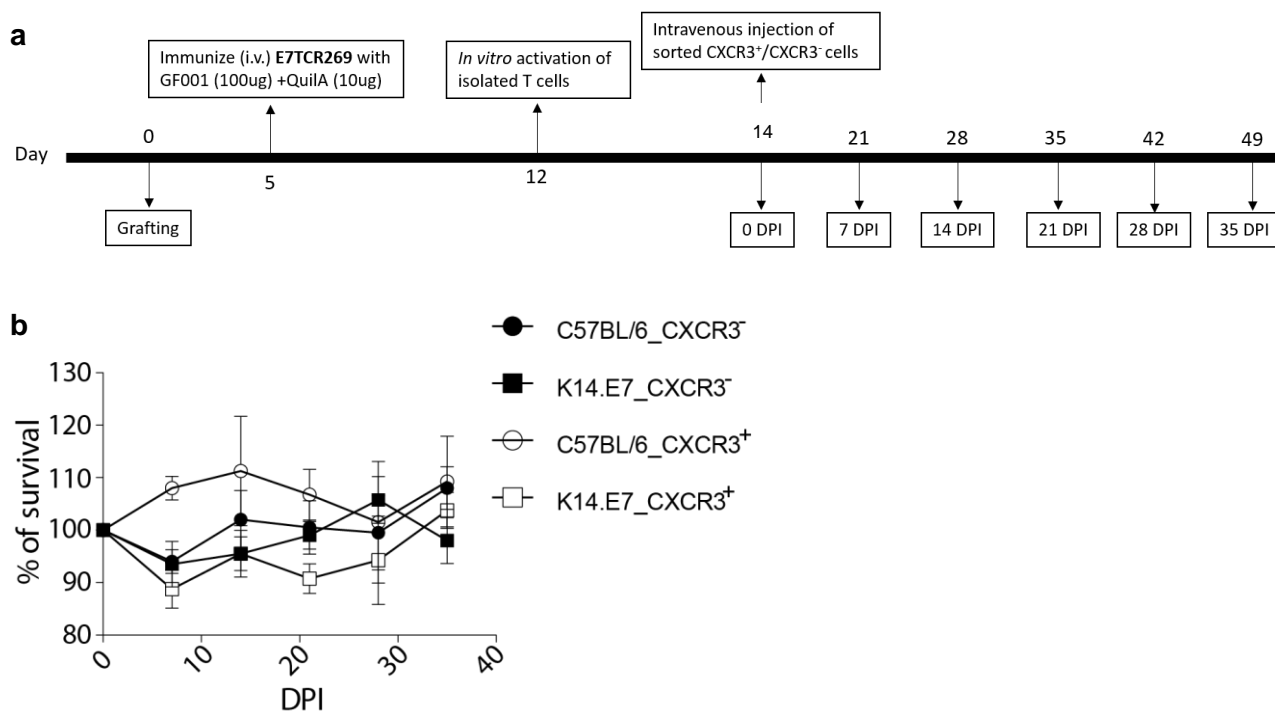
Figure 2.7 CXCR3$^+$ T cells are not sufficient to induce K14.E7 skin graft rejection

C57BL/6 and K14.E7 ear skin were grafted onto C57BL/6 recipients. Recipients receive either 200,000 CXCR3$^+$ or CXCR3$^-$ cells intravenously 14 days after grafting (0 DPI) and skin graft monitored until day 49 (35 DPI). Each experimental group includes five biological replicates. **(a)** experiment timeline. **(b)** percentage of graft survival. Graft size on the day of injection was set as 100%. Circle, C57BL/6 skin graft; square, K14.E7 skin graft; closed symbol, CXCR3$^-$ cell-receiving group; open symbol, CXCR3$^+$ cell- receiving group.

Chapter 3

Recruitment of APC to Skin Draining Lymph Node from HPV16E7-Expressing Skin Requires E7-Rb Interaction

3.1 Preface

This chapter covers two aims of the project- aim one and three. I characterized the immune responses of K14.E7xRb$^{\Delta L/\Delta L}$ upon immunization, grafted K14.E7xRb$^{\Delta L/\Delta L}$ skin on syngeneic immune competent recipients and examined the factors that influence the fate of the K14.E7xRb$^{\Delta L/\Delta L}$ skin graft. This chapter is written in manuscript format and will be submitted as an original research article.

3.2 Article 2

Original Article

Recruitment of APC to Skin Draining Lymph Node from HPV16E7-Expressing Skin Requires E7-Rb Interaction

Paula Kuo[1], Zewen K. Tuong[1], Siok Min Teoh[1], Ian H. Frazer[1]*, Stephen R. Mattarollo[1]*, Graham R. Leggatt[1]*

[1]The University of Queensland Diamantina Institute,

Translational Research Institute,

Woolloongabba, Queensland 4102, Australia

* These authors contributed equally and share last authorship

Correspondence:

Ian Frazer, The University of Queensland, Faculty of Medicine, The University of Queensland Diamantina Institute, Translational Research Institute

3.3 Abstract

"High-risk" human papillomaviruses (HPV) infect keratinocytes of squamous epithelia. The HPV16E7 protein induces epithelial hyperplasia by binding Rb family proteins and disrupting cell cycle termination. Murine skin expressing HPV16E7 as a transgene from a keratin 14 promoter (K14.E7) demonstrates epithelial hyperplasia, dysfunctional antigen presenting cells, ineffective antigen presentation by keratinocytes, and production of immunoregulatory cytokines. Furthermore, grafted K14.E7 skin is not rejected from immunocompetent non-transgenic recipient animals. To establish the contributions of E7, of E7-Rb interaction and of epithelial hyperplasia to altered local skin immunity, K14.E7 skin was compared with skin from K14.E7 mice heterozygous for a mutant Rb unable to bind E7 (K14.E7xRbΔL/ΔL mice), that have normoplastic epithelium. Previously, we demonstrated that E7-speicfic T cells do not accumulate in K14.E7xRbΔL/ΔL skin grafts. Here, we further show that K14.E7xRbΔL/ΔL skin, like K14.E7 skin, is not rejected by immunocompetent non-transgenic animals. There were fewer CD11b+ antigen presenting cells in skin draining lymph nodes from animals recipient of K14.E7xRbΔL/ΔL grafts, when compared with animals receiving K14.E7 grafts or K5mOVA grafts. Maturation of migratory DCs derived from K14.E7xRbΔL/ΔL grafts found in the draining lymph nodes is significantly lower than that of K14.E7 grafts. Surprisingly, K14.E7xRbΔL/ΔL keratinocytes, unlike K14.E7 keratinocytes, are susceptible to E7 directed CTL-mediated lysis in vitro. We conclude that E7-Rb interaction and its associated epithelial hyperplasia partially contribute to the suppressive local immune responses in area affected by HPV16E7 expression.

3.4 Introduction

Infection of the cervix with high-risk Human Papilloma Virus (HPV) accounts for ~100% of cervical cancer. While most high-risk HPV infections can be cleared spontaneously in immune competent individuals, 1-2 % of the infected subjects can progress to cervical intraepithelial neoplasia (CIN) and persist for decades before developing into cervical cancer (Centers for Disease Control and Prevention, 2017). A major risk factor for development of cervical premalignancy is immune response gene polymorphism (Leo et al., 2017), suggesting that an inadequate immune response is a determinant of development of premalignancy, but the basis of an inadequate immune response remains uncertain.

HPV specifically infects basal layer keratinocytes, and the virus life cycle is linked to keratinocyte differentiation (Stubenrauch and Laimins, 1999). Normally, keratinocytes are able to presenting antigen to primed T cells (Black et al., 2007; Kim et al., 2009; Zhou et al., 2011) However, HPV16 E7 transgenic primary keratinocytes are not susceptible to CTL-mediated lysis by E7-specific T cells *in vitro* (Leggatt et al., 2002). This defect of endogenous antigen presentation could be specific to the E7 antigen, as keratinocytes expressing OVA as transgenic antigen are sensitive to cell-mediated lysis by CD8^{+} OT-1 cells (Kim et al., 2009; Zhou et al., 2011), in a dendritic cell (DCs) and Langerhans cell-independent manner (Kim et al., 2009). In addition to *in vitro* studies using immortalized or primary keratinocytes, a transgenic mouse model expressing HPV16E7 protein controlled by keratin 14 (K14) promoter (K14.E7) has been used to study persisting HPV16 gene expression as this model harbors the molecular features of CIN3 tissue (Tuong et al., 2018). Multiple local factors including suppressive immunity mediated by CD4^{+}CD25^{+} cells against multiple immunogens (Narayan et al., 2009), IFNγ-producing NKT cells (Mattarollo et al., 2010a), impaired antigen processing and T cell activation by antigen-presenting cells (APCs) (Chandra et al., 2016) are observed in the skin of K14.E7 transgenic mice, and the ear skin of K14.E7 mice is not rejected when grafted to immunocompetent recipient mice (Matsumoto et al., 2004)., reflecting the failure of clearance of persistent HPV16 infection in human patients.

HPV16 E7 protein interacts with multiple proteins including γ-tubulin, p-600, Retinoblastoma (Rb) protein family, HDAC, E2F6, p21, and IRF1 (Moody and Laimins, 2010).The interaction between E7 and Rb disrupts normal cell cycle regulation, leading to epithelial hyper-proliferation, one of the major pathological phenotypes of CIN3 patients. However, it is unclear whether suppressed local immunity is a result of E7-associated hyperplasia or some other consequence of expression of the viral protein. To dissect this question, we utilized transgenic mice expressing the E7 protein and with a mutant Rb that is functional for cell cycle regulation but cannot bind E7 (K14.E7xRb$^{\Delta L/\Delta L}$) (Dick et al., 2000). Expressing comparable level of E7 transcript, the skin of K14.E7xRb$^{\Delta L/\Delta L}$ mice, whether homozygous or heterozygous for the Rb mutation, was found to closely resemble non-transgenic mouse skin (Choyce et al., 2013; Kuo et al., 2017). To test whether the local immune suppression observed in K14.E7 transgenic mouse skin was due to hyperproliferation or to some other action of E7 protein, we examined immune function in the skin of K14.E7 and K14.E7xRbΔL/ΔL mice. However, K14.E7xRbΔL/ΔL skin grafts were not rejected from naïve or E7 primed recipients, and this was associated with reduced numbers of CD11b+ DC, as well as the low expression of maturation markers- CD80 and CD86 on migratory DC subtypes in the skin draining lymph nodes. More importantly, adaptive immune responses to skin-directed antigen in K14.E7xRbΔL/ΔL mice were comparable to those in non-transgenic wild-type mice, and K14.E7xRbΔL/ΔL transgenic keratinocytes could present endogenous E7-antigen and be recognized by antigen specific CD8 T cells in vitro, unlike E7 transgenic keratinocytes.

3.5 Results

Disruption of E7-Rb interaction in E7 transgenic mice restores peripheral T cell response to that of non-transgenic animals

Mice expressing E7 as a transgene in epithelial cells have altered immune function locally in skin. The major effects of E7 in epithelial cells are mediated via binding to the Rb cell cycle regulatory protein. To determine whether disruption of E7-Rb interaction impacts on the altered immune response in E7 transgenic skin, we first examined induction of peripheral CD8 T cell responses, as these are impaired in E7 transgenic animals to multiple immunogens (Narayan et al., 2009). K14.E7 mice and K14.E7 x Rb$^{\Delta L/\Delta L}$ mice were immunised with ovalbumin intradermally, and IFNγ production by CD8 T cells from the draining lymph node in response to SIINFEKL was measured six days after immunisation. Re-stimulation with SIINFEKL resulted in IFNγ production by +0.11% of K14.E7xRb$^{\Delta L/\Delta L}$ CD8 T cells and +0.215% of C57BL/6 CD8 T cells compared to unstimulated control, significantly more than in K14E7 animals similarly immunised, which only showed a +0.035% increase in IFNγ CD8 T cells compare to unstimulated control (Figure 3.1). Thus, adaptive immune priming within K14.E7 x Rb$^{\Delta L/\Delta L}$ mice do not seem to be affected.

K14.E7xRb$^{\Delta L/\Delta L}$ skin is not rejected from immunocompetent syngeneic recipients

K14.E7xRb$^{\Delta L/\Delta L}$ mice and non-transgenic mice have similar composition of skin-infiltrating lymphocytes (Kuo et al., 2017), and exhibit similar local immunity (Figure 3.1), as well as a similar transcriptomic profile to a non-transgenic mouse skin (Kuo et al., 2017; Zhussupbekova et al., 2016). We therefore hypothesized that E7-expressing skin lacking hyperplasia might be susceptible to immune mediated rejection. To test this hypothesis, we grafted K14.E7xRb$^{\Delta L/\Delta L}$ skin onto syngeneic non-transgenic mice. As controls, we grafted hyperplastic NKT cell deficient Jα18KO x E7 skin, which is susceptible to rejection, (Mattarollo et al., 2010a) and K14.E7 skin, which is not. Jα18KO x E7 skin grafts showed rejection, defined as more than 50% shrinkage within 42 days (Figure 3.2a and b). However, both K14.E7xRb$^{\Delta L/\Delta L}$ and Rb$^{\Delta L/\Delta L}$ skin grafts showed no evidence of rejection (Figure 3.2a and b).

As there is no chemokine mediated accumulation of regulatory T cells in K14.E7xRb$^{\Delta L/\Delta L}$ skin, as observed in K14.E7 skin, a different mechanism must prevent E7 specific priming or effector functions where E7 transgenic grafts are not associated with hyperplasia. Passive transfer of sufficient E7-specific cytotoxic CD8 T cells enabled rejection of E7-

expressing skin grafts following immunization (Matsumoto et al., 2004). We therefore tested whether a similar~~this~~ approach would lead to rejection of K14.E7xRb$^{\Delta L/\Delta L}$ skin grafts. K14.E7 and K14.E7xRb$^{\Delta L/\Delta L}$ skin together were grafted on to the same E7TCR269 recipient~~recipients~~ that have an expanded E7-specific CD8 T cell repertoire (Narayan et al., 2009) (Supplementary Figure 1),~~,~~ and to non-transgenic recipients, with ~~or without~~ prior immunization with an H-2 D^b restricted peptide of E7 (GF001) (Figure 2c). Consistent with our previous findings, K14.E7 grafts showed ~40% reduction in size on immunized E7TCR269 recipients (Figure 2d and e). In contrast, K14.E7xRb$^{\Delta L/\Delta L}$ grafts showed no reduction in size on either C57BL/6 or E7TCR269 recipient mice. These data demonstrate that failure of E7 transgenic skin grafts to prime an E7-specific response is not the sole reason for failure of rejection of K14.E7xRb$^{\Delta L/\Delta L}$ grafts. As E7-expression levels are similar in K14.E7 and K14.E7xRb$^{\Delta L/\Delta L}$ skin (Kuo et al., 2017), it is unlikely that the expression level of the antigen influenced the fate of K14.E7xRb$^{\Delta L/\Delta L}$ skin grafts. Thus, we hypothesized three possibilities of why the K14.E7xRb$^{\Delta L/\Delta L}$ skin~~Thus, these~~ grafts are tolerated- i) K14.E7xRb$^{\Delta L/\Delta L}$ skin graft alone may not initiate sufficient skin antigen presenting cell migration and activation in the draining lymph nodes to prime T cells; ii) K14.E7xRb$^{\Delta L/\Delta L}$ skin grafts~~either~~ fail to attract effector cells, consistent with their lower expression of T cell attracting chemokines (Kuo et al. 2017); iii)~~), or~~ E7 transgenic KC fail to present antigen effectively in the absence of the local inflammatory signals (IL-1β, IL-17) that are a feature of K14.E7 skin (Tuong et al., 2018).

Limited presence of graft-derived dendritic cells in the draining lymph node was observed upon K14.E7xRb$^{\Delta L/\Delta L}$ skin grafting

We next investigated why E7-expressing skin, without the altered local immunity associated with hyperplasia (K14.E7xRb$^{\Delta L/\Delta L}$), was not rejected when grafted onto syngeneic background recipients. There are three critical steps involved in allogenic skin graft rejection. Firstly, antigen specific T cells are generated in the draining lymph node following migration of antigen-loaded dendritic cells from the skin. Secondly, primed T cells egress out of the lymph node are attracted to or retained in the targeted tissue. Lastly, effector T cells recognise the antigen and induce CTL-mediated killing.

We first determined whether K14.E7xRb$^{\Delta L/\Delta L}$ skin-derived dendritic cells could be found in the draining lymph node. K14.E7xRb$^{\Delta L/\Delta L}$ skin was transplanted onto congenic (CD45.1) recipients and draining lymph nodes (axillary and inguinal) from both grafted and non-grafted

flanks were harvested. To validate the separation of CD45.1 from CD45.2 lymphocytes, naïve lymph nodes from C57BL/6, B6.SJL.Ptprca, and 1:1 mixture of the two were stained with CD45.1 antibody (Figure S3.1a). Figure S3.1b shows the same gating strategy as Figure S3.1a. Lymph nodes were harvested and analysed 11 days post-grafting to minimise the effect caused by the surgical procedure. Differences in relative and absolute numbers of specific APC population in draining lymph nodes at this time point might reflect differences in migration, proliferation, maturation or turnover of skin-derived DCs. To establish the impact of the skin grafting procedure on APC migration, C57BL/6 skin was grafted as negative control, and to establish the profile of APC migration associated with skin graft rejection, skin expressing membrane-bound OVA driven by keratin 5 promoter (K5mOVA) was grafted (Azukizawa et al., 2003; Hadis et al., 2010) (Figure 3.3a). Percentage and total numbers of recipient-derived CD11c$^+$ cells between the grafted and non-grafted sides were similar in recipients bearing different types of skin grafts (Figure S3.2). Higher absolute number of graft-~~donor~~ derived CD11c$^+$ cells were found in the graft draining lymph node than in the contralateral node (Figure 3.3b). However, percentage of graft-derived CD11c$^+$ cells was significantly less in lymph nodes receiving C57BL/6, K14.E7xRb$^{\Delta L/\Delta L}$ and Rb$^{\Delta L/\Delta L}$ grafts than those bearing K5mOVA or K14.E7 skin grafts (Figure S3.1b and c). Significantly reduced numbers of graft-derived CD11c$^+$ cells was found in the draining lymph nodes of C57Bl/6, K14.E7xRb$^{\Delta L/\Delta L}$ and Rb$^{\Delta L/\Delta L}$ bearing recipients, when compared with K5mOVA recipients. K14.E7 skin grafts induced similar percentages of CD11c$^+$ cell in the draining lymph node to K5mOVA graft (Figure S3.1b), Graft-derived cells were further analysed based on CD11c and MHCII expression level to differentiate migratory DC (CD11c$^+$ MCHII^{hi} migDC) from resident DC (CD11c$^+$ MCHII^{int} ResDC). Significant amount of MigDC, but not ResDC, was found in the draining lymph nodes (Figure 3.3c), demonstrating the migratory property of cells were of skin graft origin. The number of migratory DC (CD11c$^+$ MCHII^{hi}) from K14.E7 grafts was similar to K5mOVA skin graft (Figure 3.3 c and d). The total amount of MigDC from K14.E7xRb$^{\Delta L/\Delta L}$ skin graft was significantly lower than the rejection control, K5mOVA, and the E7-expressing hyperplastic skin, K14.E7 (Figure 3.3d). Increased numbers of CD11b$^+$ migratory DCs but not CD103$^+$ DC or LC were found in the lymph nodes of K5mOVA and K14.E7 grafted animals (Figure 3.3f). Interestingly, significantly less K14.E7 skin-derived CD11b$^+$ migratory DC was found when compared to K5mOVA skin, but the number was still significantly higher than that derived from C57BL/6, K14.E7xRb$^{\Delta L/\Delta L}$ and Rb$^{\Delta L/\Delta L}$ skin graft.

Next, we further examined the maturation state of different subtypes of DC in the draining lymph nodes derived from either K14.E7 or K14.E7xRb$^{\Delta L/\Delta L}$ skin, based on the expression of CD80 and CD86. Analysed at the same time point, the percentage and MFI of CD80 and CD86 on migratory DC, including CD103$^+$ and CD11b$^+$ migratory DC, are significantly higher on cells derived from the K14.E7 skin graft (Figure 3.3g). No significant difference was observed in resident DC subtypes. This suggests that K14.E7xRb$^{\Delta L/\Delta L}$ skin graft-derived DC not only cannot sufficiently migrate to the draining lymph node, but also that the migrated DC are not mature DC. skin grafts. Together, these results suggest that grafting of K14.E7xRb$^{\Delta L/\Delta L}$ skin induces lesser numbers of skin-derived DCs to migrate to the draining lymph node when compared to grafts of K14.E7 or K5mOVA, skin and the number of K14.E7xRb$^{\Delta L/\Delta L}$ skin-DCs is similar to that from non-transgenic skin grafts, which potentially could explain the failure of rejection of K14.E7xRb$^{\Delta L/\Delta L}$ skin grafts.

Keratinocytes with disrupted E7-Rb interaction engage with antigen-specific CD8 T cells and enable CTL-mediated lysis

Previously, we have demonstrated that activated antigen-specific CD8 T cells can enter both hyperplastic (K14.E7) and normoplastic (K14.E7xRb$^{\Delta L/\Delta L}$) E7-expressing epidermis (Jazayeri et al., 2017). However, only a very low number of antigen-specific T cells can enter or be retained in the K14.E7xRb$^{\Delta L/\Delta L}$ epidermis. The final step of allograft rejection is the engagement of effector T cells and antigen expressing keratinocytes, followed by CTL-mediated lysis. An *in vitro* approach was therefore utilised to assess whether keratinocytes of K14.E7xRb$^{\Delta L/\Delta L}$ epidermis are susceptible to CTL-mediated lysis when sufficient antigen-specific effector cells are present. FACS sorted-keratinocytes of the epidermis were exposed to H-2 D^b restricted peptide of E7 (GF001) (Figure 3.4a), OVA (SIINFEKL) (Figure S3.4a) or not so exposed (Figure 3.4b), and were co-cultured with E7 peptide-specific effector T cells, or with SIINFEKL-specific OT-1 cells (Figure S3.4b-d) as controls. Consistent with previous findings, keratinocytes isolated from K14.E7 epithelium were susceptible to CTL-mediated lysis only when exposed to exogenous peptide antigen (Zhou et al., 2011) (Figure 3.4a and 3.4b). In contrast, keratinocytes of the K14.E7xRb$^{\Delta L/\Delta L}$ skin were susceptible to lysis without exogenous peptide provision, likely due to endogenous antigen presentation (Figure 3.4a and 3.4b). Target cell maximum release and spontaneous release of LDH are plotted in Figure S3.3. These results suggest that E7-Rb interaction or E7-induced cell proliferation interferes with effective MHC class I antigen presentation, and that disruption of E7-Rb interaction or of the resulting cellular proliferation can restore the

susceptibility of E7-expressing keratinocytes to cytotoxic T cell killing. Thus, E7 transgenic skin with no E7-Rb interaction demonstrates normal peripheral immunity but antigen expressing keratinocytes are not eliminated in vivo, though susceptible to lysis in vitro. This may reflect failure of skin-derived APC in the draining lymph node to prime or promote migration of effector T cells to the E7 transgenic skin.

3.6 Discussion

In this manuscript, we demonstrate that while E7-transgenic keratinocytes from normally proliferative epithelium are susceptible to immune lysis *in vitro*, unlike E7 transgenic keratinocytes from hyperproliferative epithelium, neither grafting induced nor vaccine induced immune responses can eliminate E7 transgenic grafts of normally proliferative epithelium. This was associated with lesser accumulation of CD11b$^+$ APC from the skin graft in the skin draining lymph nodes. The immune landscape of the tumour microenvironment is altered in association with enhanced cell proliferation. Suppressed local immunity has been extensively studied by our laboratory and others in hyperproliferative epithelium associated with expression of the HPV16E7 protein (Bergot et al., 2014; Chandra et al., 2016; Choyce et al., 2013; Gosmann et al., 2014b; Matsumoto et al., 2004; Mattarollo et al., 2010a). One of the mechanisms contributing to the suppressive immunity is that a different profile of cytokines and chemokines is generated, resulting in an altered balance in the hyperproliferative microenvironment that often favours the regulatory/inhibitory response (Kuo et al., 2017). Thus, targeting the hyperproliferation might rebalance the immune response in favour of elimination of HPV infected tissue.

As transplantation of the hyperproliferative K14.E7 skin results in graft tolerance (Matsumoto et al., 2004), we aimed to dissect the role of hyperplastic epithelium plays in determining the fate of E7-expressing skin grafts. Rejection of an allogeneic skin transplant is typically initiated by the migration of graft-derived DC to the draining lymph node, where they activate host T cells (Larsen et al., 1990; Richters et al., 1999). Meanwhile, the skin transplant provides allogeneic antigen, which can be processed and presented by the recipient's antigen presenting cells. Together, both sensitizations result in an influx of recipient CD4, CD8 T cells and CD11b$^+$ macrophages to the graft and graft rejection (Richters et al., 2005). Moreover, rejection of an allogeneic graft relies on the efficient presentation of the allogeneic antigen to the recruited cells to elicit antigen specific cytotoxic effect (Arnold et al., 1990; Gould and Auchincloss, 1999). Thus, i) T cell priming by antigen presenting cells in the lymph node, ii) influx of effector cells to the localized area and iii) engagement of cytotoxic T cells to the antigen are three critical aspects that determine the outcome of an allogeneic skin transplant.

Following skin grafting, we identified that the dendritic cells derived from the skin of K14.E7xRb$^{\Delta L/\Delta L}$ mice are of lower abundance in the draining lymph node, when compared to those derived from non-transgenic skin. Furthermore, the lower number of migratory

CD11b$^+$ DC derived from K14.E7xRb$^{\Delta L/\Delta L}$ skin was not due to the thickness of skin graft, as both K5mOVA and K14.E7xRb$^{\Delta L/\Delta L}$ skin are normoplastic. Failure of migration of adequate numbers of skin derived APC might result in an insufficient amount of primed T cells. The limited migration of K14.E7xRb$^{\Delta L/\Delta L}$ skin-derived DC could be due to their immaturity in K14.E7xRb$^{\Delta L/\Delta L}$ skin when compared with K.14E7 skin which demonstrates production of proinflammatory cytokines including IL-1β and IL-17 which would assist maturation of APCs. Antigens delivered though intradermal injection can be drained to the lymph node through lymphatic system and taken up by functional lymph node resident dendritic cells (Levin et al., 2017), bypassing the migration step of antigen-carrying skin-derived DC from skin to the draining lymph node. In this regard, intradermal immunisation is a better assessment for peripheral T cell response. We showed effective CD8 T cells response to intradermal OVA immunisation in K14.E7xRb$^{\Delta L/\Delta L}$ mice, suggesting a functional peripheral immunity in the K14.E7xRb$^{\Delta L/\Delta L}$ as opposed to K14.E7 animals (Malcolm et al., 2003). It is likely that the suppressed adaptive immunity in the HPV16E7 transgenic mice is dependent on the interaction between E7 and Rb.

Another reason for tolerance of the K14.E7xRb$^{\Delta L/\Delta L}$ skin could be the lack of antigen-specific effector T cell infiltration to the graft. In contrast to K14.E7xRb$^{\Delta L/\Delta L}$, the hyperplastic K14.E7 skin is able to induce trafficking of both antigen specific and non-specific effector T cells to the epidermis (Jazayeri et al., 2017). However, this does not confer graft rejection of K14.E7 grafts. It is likely that in the absence of epithelial hyperplasia in K14.E7xRb$^{\Delta L/\Delta L}$ epidermis results in insufficient signals produced to induce immunocyte trafficking to the local area (Kuo et al., 2017). We hypothesized that if the lack of localised recruitment of T cells was to be overcome by provision of sufficient antigen-specific effector T cells, antigen-bearing keratinocytes from the K14.E7xRb$^{\Delta L/\Delta L}$ skin could be lysed. We utilised *in vitro* CTL-mediated lysis assay to supply sufficient antigen-specific effector T cells. In contrast to K14.E7 keratinocytes, which are susceptible to lysis only if exogenous peptide is provided, keratinocytes from K14.E7xRb$^{\Delta L/\Delta L}$ animals are able to present endogenous antigen and are susceptible to CTL-mediated lysis *in vitro*. This finding is consistent with the observation that immunisation-induced immunity is ineffective in rejecting E7-expressing K14.E7xRb$^{\Delta L/\Delta L}$ skin as the lack of presentation of antigen by the skin-derived APC in the draining lymph node in the K14.E7xRb$^{\Delta L/\Delta L}$ mice fails to induce local inflammatory responses that are necessary for activation of effector T cells trafficking to the skin.

Recently, a small thiadiazolidinedione molecule binding to pRb through the LxCxE motif was identified and it was shown to selectively interfere with HPV16E7-Rb but not HPV18E7-Rb interaction (Fera et al., 2012). This small molecule interrupts the E7-Rb interaction the same manner as the K14.E7xRb$^{\Delta L/\Delta L}$ does. Moreover, this molecule demonstrated effects on cell cycle and reduced TC-1 tumour volume after treatment. However, the immune incompetent mouse model- NOD SCID mice were used for the tumour model, where the impact of immune response was not taken into account. Our results suggest that while the small molecule interruption of E7- Rb interactions may have similar impact to genetically mediated blockade and enable induction of effective peripheral immunity, it may not be sufficient to induce a sufficient response to clear E7 infected cells. A combination of a small molecule inhibitor of Rb-E7 interaction, combined with more effective antigen presentation through immunisation, might nevertheless represent a means to clear E7 infected tissues.

3.7 Materials and Methods

Mice

All mice were maintained in Translational Research Institute (TRI) Biological Research Facility (BRF) under specific pathogen free conditions. For experimental work, female mice were used at 8-12wk of age. C57BL/6 and B6.SJL.Ptprca mice were obtained from Animal Resources Centre (Perth, Australia) and OT-1 mice were purchased from The Jackson Laboratories (Bar Harbor, ME, USA). K14.E7 (Herber et al., 1996) and K5mOVA (Azukizawa et al., 2003) mice were maintained at the TRI-BRF. Heterozygous $Rb^{\Delta L/\Delta L}$ transgenic and NKT cell deficient $J\alpha18^{-/-}$ mice (Isaac et al., 2006) were obtained from Dr Fred Dick and Mark Smyth (Melbourne, Australia), respectively and maintained locally at TRI-BRF. $K14.E7xRb^{\Delta L/\Delta L}$ and $J\alpha18^{-/-}xE7$ mice were generated by mating heterozygous K14.E7 with heterozygous $Rb^{\Delta L/\Delta L}$ and homozygous $J\alpha18^{-/-}$, respectively. $K14.E7xRb^{\Delta L/\Delta L}$ mice have a single allele of E7 transgene and at least one allele of mutated Rb. OT-I mice were purchased from The Jackson Laboratories (Bar Harbor, ME, USA). E7TCR269 mice were bred as previously described (Narayan et al., 2009). All procedures were approved by the University of Queensland Animal Ethics Committee (UQDI/367/13/NHMRC and UQDI/452/16).

Immunisation

Immunisations were performed by injecting 5µg QuilA (Sigma-Aldrich, St. Louis, MO, USA) with 50µg OVA (A5503, Sigma-Aldrich, St. Louis, MO, USA) or E7 peptide-GF001 (RAHYNIVTF, synthesized by Auspep Pty Ltd, (Melbourne, Australia), with purity >80%) in 20µl PBS into one ear pinnae intradermally or 200µl PBS subcutaneously.

Isolation of cells from lymph node and spleen

The isolation was done as previously described (Kuo et al., 2017). Lymph nodes were digested with 1µg/ µl, of collagenase D (Roche) and 0.2µg/ µl of DNase, (Roche) for 30 minutes at 37ºC prior passing through the cell strainer.

FACS, antibodies and reagents

FACS analysis were undertaken as previously described (Mattarollo et al., 2010a). Foxp3 Fix/Perm Concentrate and Diluent kit was used for intracellular staining (eBioscience, San

Diego, USA). IFNγ was stained intracellularly. Anti-mouse monoclonal antibodies to CD45 (30-F11), CD45.1 (A20), CD8α (53-6.7), TCRβ (H57-597), CD4 (GK1.5), EpCAM (G8.8), I-A/I-E (MHCII) (M5/114.15.2), CD103 (M290), CD11c (HL3), CD11b (M1/70), IFNγ (XMG1.2) and the corresponding isotype antibodies were purchased from Biolegend (San Diego, USA), eBioscience (San Diego, USA), BD Bioscience (San Jose, USA)

In vitro cytotoxic T cell assay

Effector cells (E) were harvested from the spleen of E7TCR269 and OT-1 mice six days after GF001 and OVA immunisation, respectively. Splenocytes were cultured in standard RPMI and supplemented with IL-2 (1 U/mL, Peprotech, NJ, USA) overnight and CD8 T cells were enriched using biotinylated antibodies (Kuo et al., 2017). Target keratinocytes (T) were sorted using BD FACSAria Fusion Sorter and pulsed with 10 µg/mL of either GF001 or SIINFEKL (Sigma-Aldrich, St. Louis, MO, USA) peptide. Effector and target cells were co-cultured at 20:1, 10:1 or 2.5:1 ratio for 5 hours and cell-mediated cytotoxicity assay was performed using CytoTox 96® Non-Radioactive Cytotoxicity Assay kit (Promega, Madison, WI, USA) following manufacturer's instruction. Percentage of cytotoxicity was calculated as follow (each value calculated has been subtracted with medium background):

$$\% \ of \ Cytotoxicity =$$

$$\frac{(value \ of \ KC + E7TCR269 \ T \ cells \ at \ ratio \ x) - (mean \ value \ of \ KC \ with \ no \ peptide \ + \ OT-1 \ Tcells \ at \ ratio \ x)}{(KC \ maximum \ release) - (mean \ value \ of \ KC \ with \ no \ peptide \ + \ OT-1 \ Tcells \ at \ ratio \ x)} \ x \ 100\%$$

Skin grafting

Skin grafting was performed as previously described (Chakraborty et al., 2018). Briefly, skin graft recipients were shaved on the flank and shaved skin was cut out in the size that matches the donor skin. Ears from the donor mice were split into dorsal and ventral part and grafted onto recipient mice. Bactigras (Smith & Nephew, Australia) was placed, following by bandaging. The bandage was taken off seven days after the procedure. Day 21 post-grafting was set as baseline for comparison as the skin grafts are well-healed and no local inflammations were observed.

Statistical analysis

Prism 7 (GraphPad Software, La Jolla, CA) software was used for statistical analysis and to prepare the plots. Unless otherwise stated, all analyses were done using one-way ANOVA,

with Bonferroni's multiple comparison tests. Two-way ANOVA with Bonferroni's post-test analysis was used in Figure 3.3 and Figure 3.4. All plots show mean value with SEM. Paired-student t-test was used in Figure 3.3b. Result significance was shown, where $*p<0.05$, $**p<0.01$, $***p<0.001$ and $****p<0.0001$.
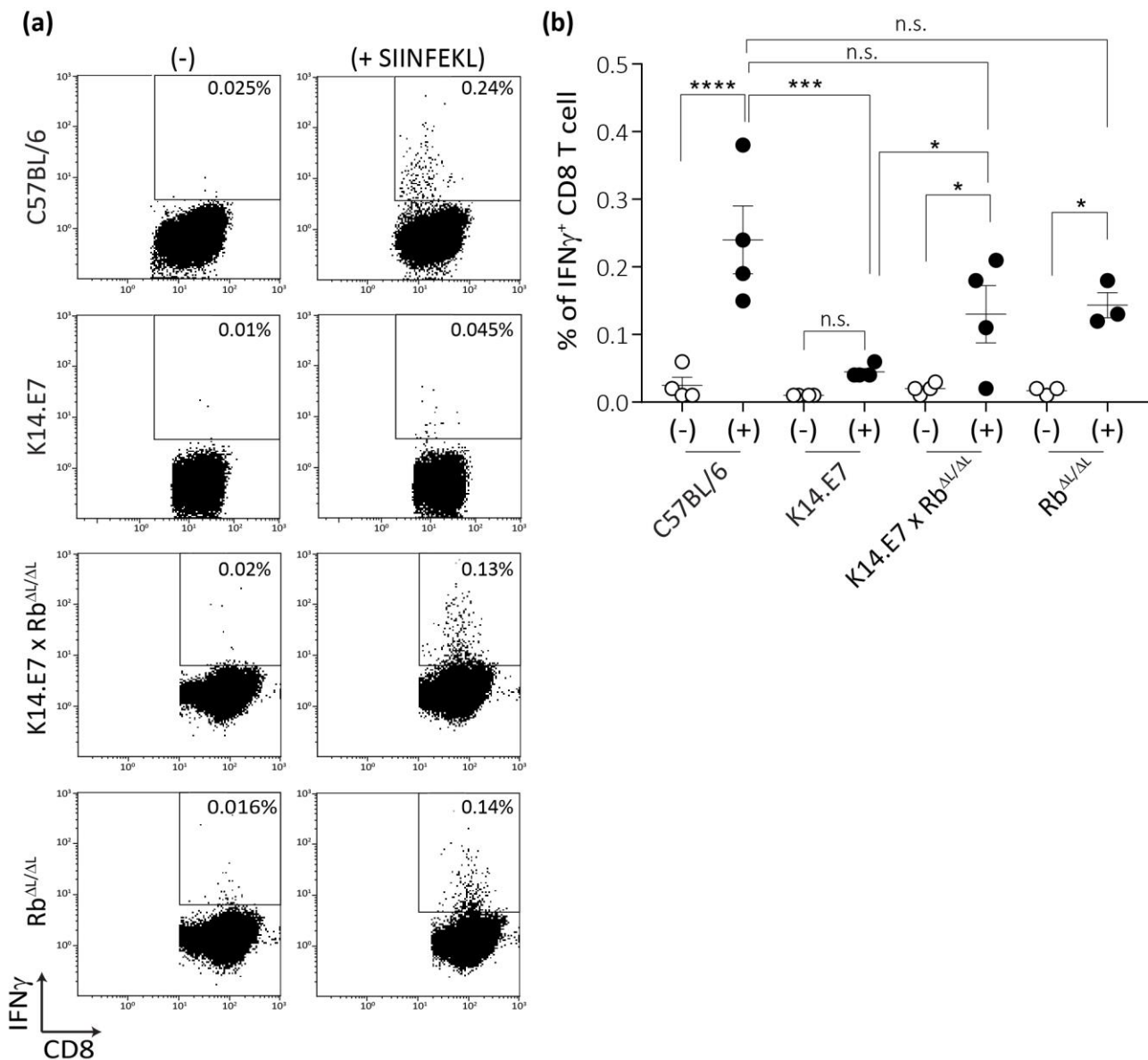
Figure 3.1. K14.E7xRb $^{\Delta L/\Delta L}$ and non-transgenic mice respond equally to intradermal immunisation

OVA specific CD8 T cell responses in the draining LN following intradermal immunisation were assessed as IFNγ production following in vitro re-stimulation. **(a)** Representative FACS plots pre-gated on TCRβ^{+} CD8 T cells showing IFNγ production with (+) or without (-) SIINFEKL re-stimulation. **(b)** Quantitative result showing mean+/-SEM with n>3 for each mouse type. Analyses were done using one-way ANOVA, with Bonferroni's multiple comparison tests. Result significance was shown, where *p<0.05, ***p<0.001 and ****p<0.0001.
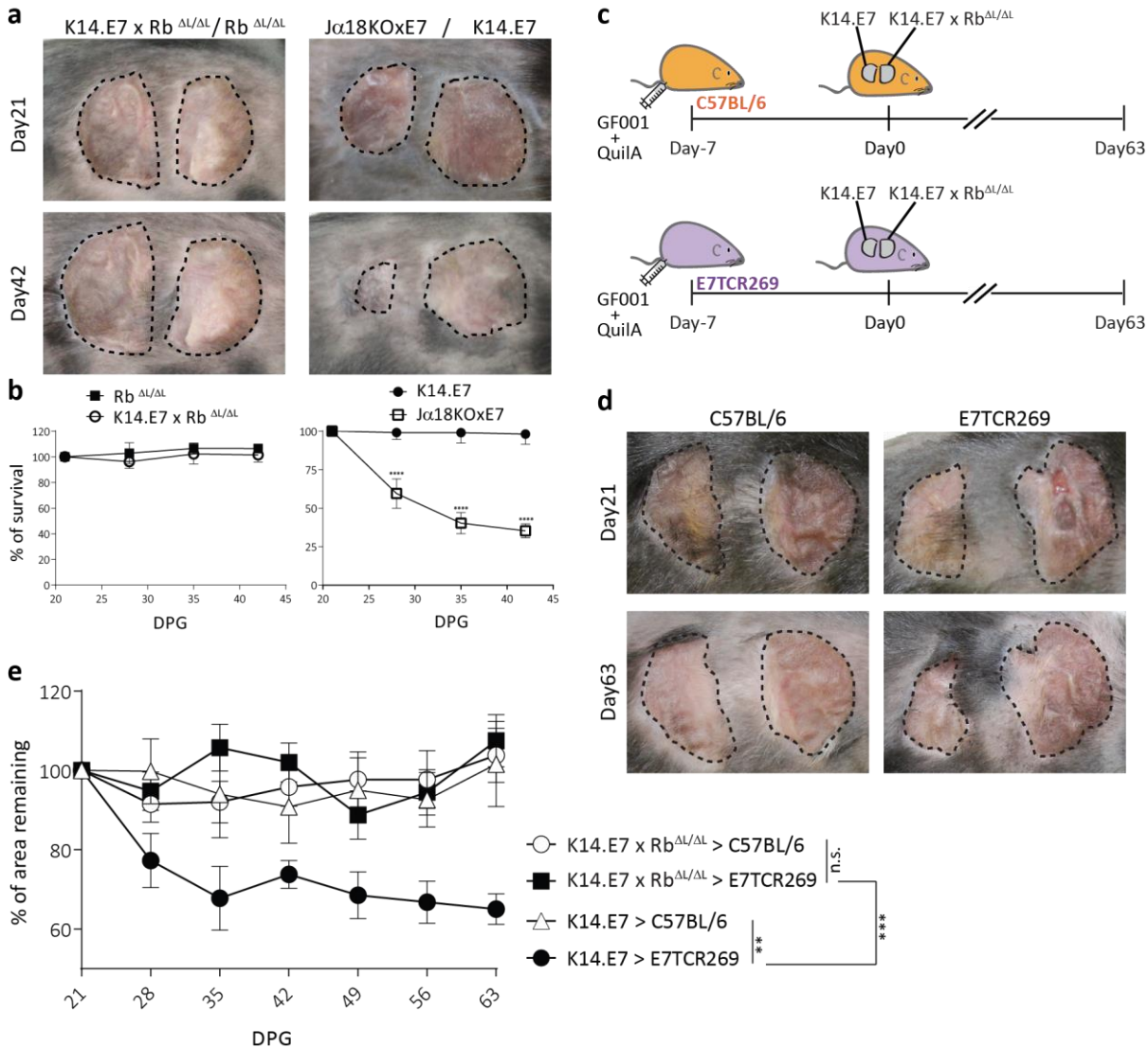
Figure 3.2. K14.E7xRb$^{\Delta L/\Delta L}$ skin grafts are not rejected from immunocompetent syngeneic recipients

(a) Grafts of donor ear skin, as shown, onto C57BL/6 recipients at 21 and 42-days post grafting. **(b)** Area remaining of graft at the indicated time points. **(c)** C57BL/6 and E7TCR269 recipients were immunised with GF001 (50 µg) and QuilA (5µg) subcutaneously seven days before grafting. **(d)** Representative photos of graft-bearing recipients on day21 and day63. K14.E7 skin (left) and K14.E7xRb$^{\Delta L/\Delta L}$ skin (right). **(e)** Area remaining of graft at the indicated time points, compared to the graft on day 21. DPG, day post grafting. Analyses were done using one-way ANOVA, with Bonferroni's multiple comparison tests. Error bars showing

mean+/-SEM with n≥3. Result significance was shown, where *p<0.05, **p<0.01, ***p<0.001

and ****p<0.0001.
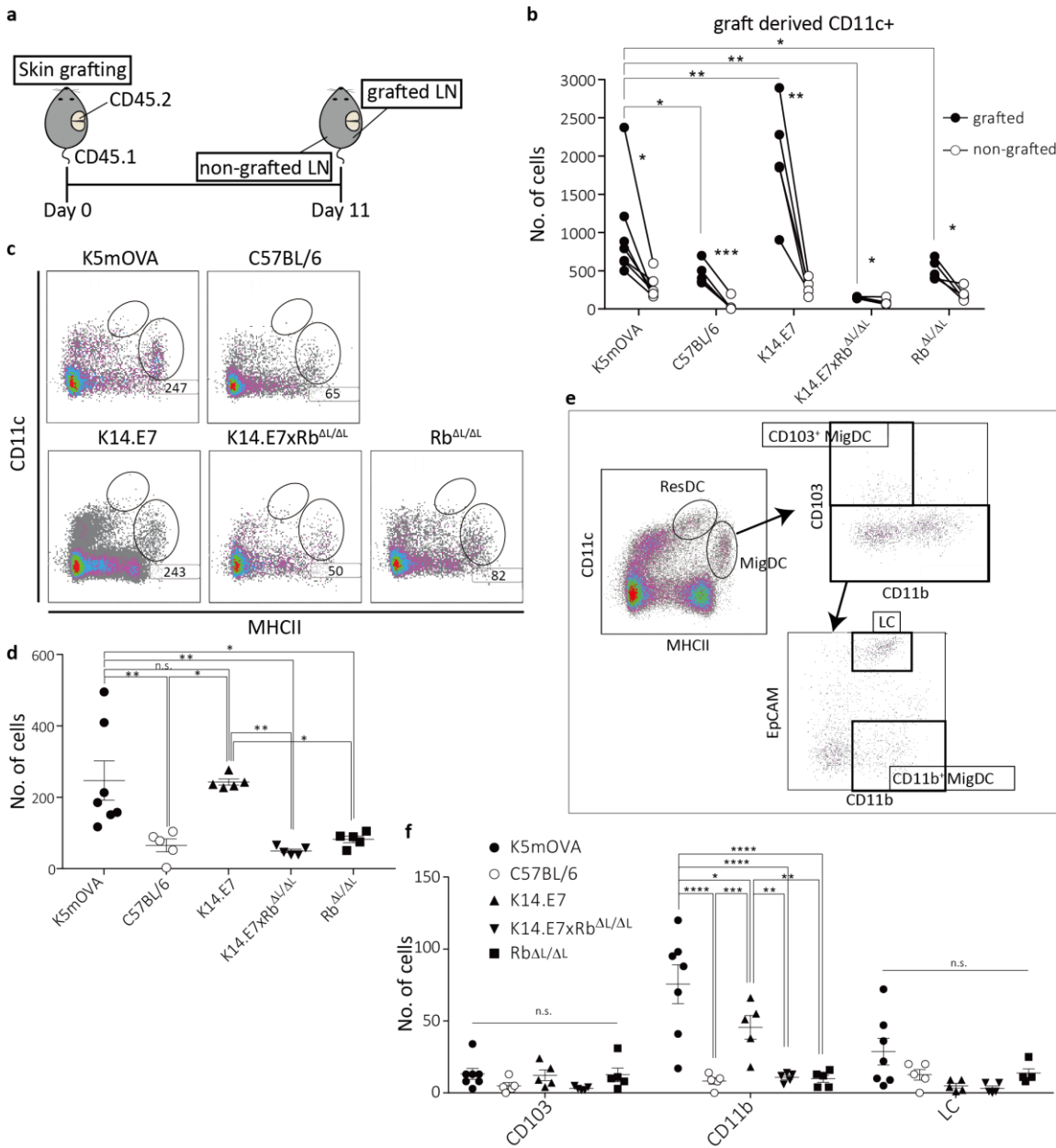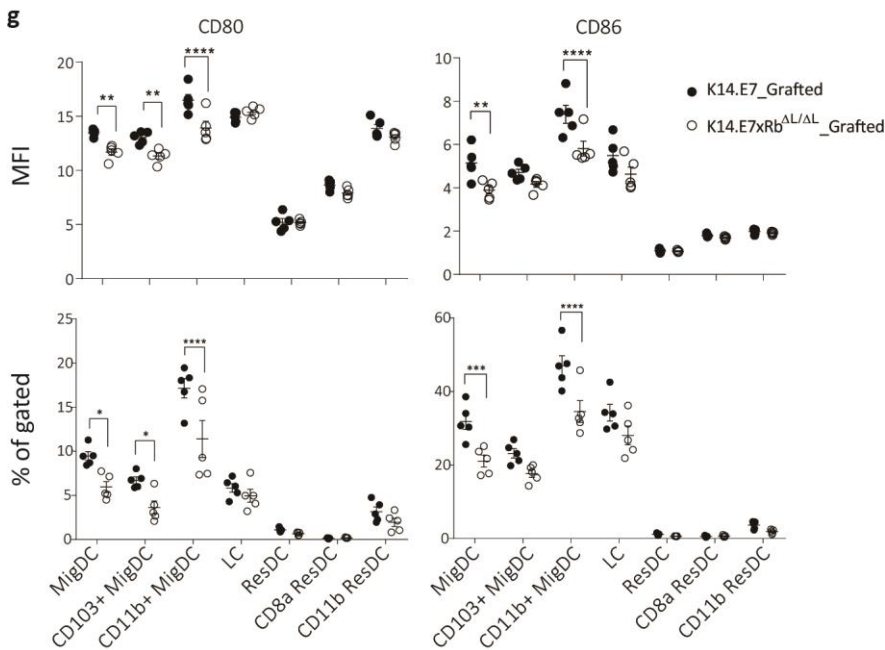
Figure 3.3. The presence of K14.E7xRb$^{\Delta L/\Delta L}$ and K14.E7 DCs from grafted skin in the draining lymph node

Skin-derived DC in graft draining and control lymph node of CD45.1 recipients receiving K5mOVA, C57BL/6, K14.E7, K14.E7xRb$^{\Delta L/\Delta L}$ or Rb$^{\Delta L/\Delta L}$ (CD45.2) skin grafts. **a)** experimental outline. Draining lymph nodes (axillary and iguanual) were harvested 11 days after grafting from either grafted side or non-grafted side of one graft recipient. **b)** total numbers of graft-derived cells (CD45.1$^-$), pre-gated on live CD11c$^+$ cells, in lymph nodes of grafted and non-grafted side. Paired student t-test applied. **c)** representative plots showing graft-derived migratory DC numbers under live CD45.1$^-$ gate. **d)** quantitative result of c). **e)** gating strategy of resident DC (ResDC), migratory DC (migDC) and DC subtypes. Representative plots from one recipient-derived live cell gate were shown. **f)** numbers of graft derived MigDC subtypes (CD103$^+$, CD11b$^+$ and LC) from lymph nodes of mice receiving indicated skin grafts. **g)** MFI (top panel) and percentage (bottom panel) of CD80 and CD86 positive cells of various DC subtypes in grafted-drianing lymph nodes receiving either K14.E7 (closed circle) or K14.E7xRb$^{\Delta L/\Delta L}$ (opened circle) skin graft. Statistics were done with one-way ANOVA test with Bonferroni post-test. Panel B was done by matched two-way ANOVA test. All plots show mean value with SEM, n>4. Result significance was shown, where *p<0.05, **p<0.01, ***p<0.001 and ****p<0.0001.

a

b
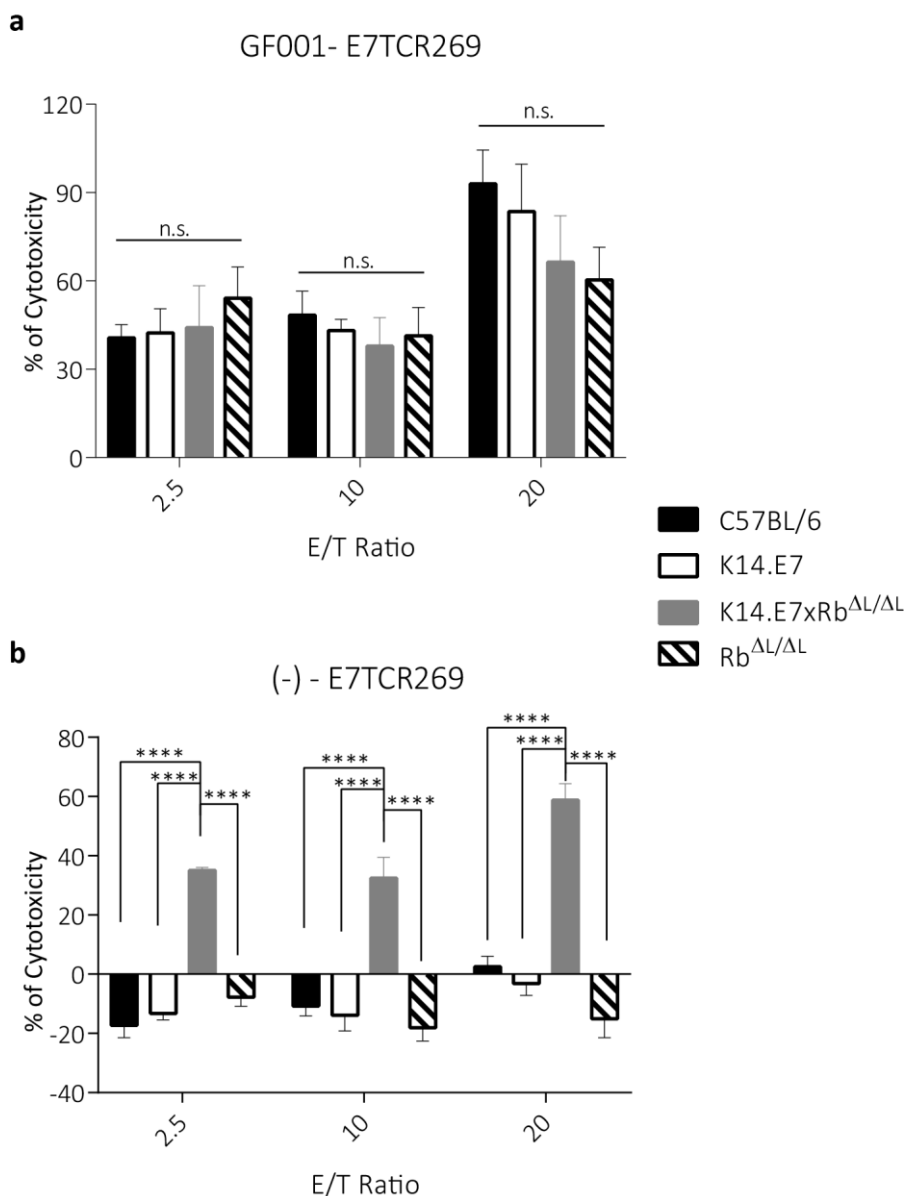
Figure 3.4. Keratinocytes from K14.E7xRb $^{\Delta L/\Delta L}$ skin present endogenous antigen and are susceptible to CTL-mediated lysis

Keratinocytes isolated from the epidermis of C57BL/6, K14.E7, K14.E7xRb$^{\Delta L/\Delta L}$, and Rb$^{\Delta L/\Delta L}$ mice were pulsed with a) GF001 peptide or b) without peptide and co-cultured with E7-specific effector T cells (E7TCR269) at the shown effector/target (E/T) ratios. Keratinocyte death was assessed as LDH release above background from no-peptide pulsed KC exposed to activated OT-1 T cells (see Methods section). Two independent experiments were done. Data analysed using two-way ANOVA and applied with Bonferroni post-test. Error bars showing mean+/- SEM with three biological replicates in each experimental group. Result significance was shown, where ****$p<0.0001$.

Supplementary Figures
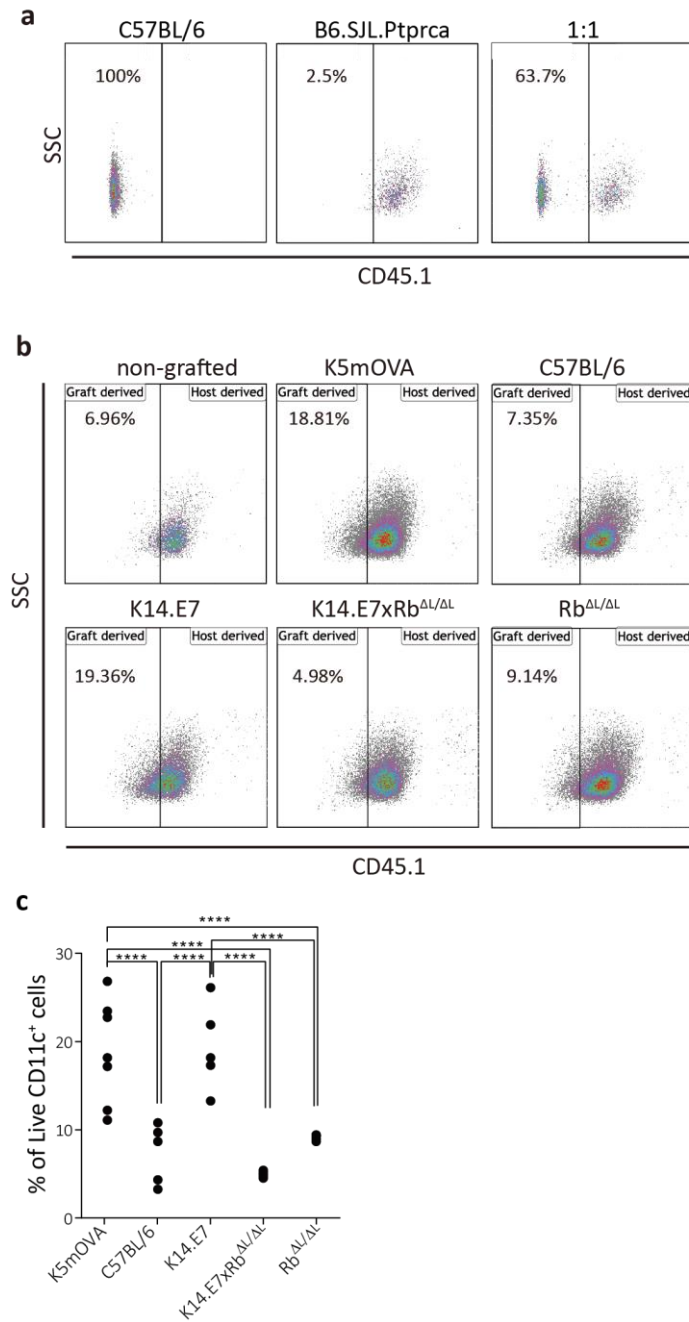
Figure S3.1

a) Naïve lymph node from C57BL/6, B6.SJL.Ptprca and 1:1 mixture stained with CD45.1 antibody to establish gating. Plots were pregated on live CD11c$^+$ cells. b) Skin-derived DC in graft draining and control lymph node of CD45.1 recipients receiving K5mOVA, C57BL/6, K14.E7, K14.E7xRb$^{\Delta L/\Delta L}$ or Rb$^{\Delta L/\Delta L}$ (CD45.2) skin grafts. Representative plots of graft-derived cells (CD45.1$^-$), pre-gated on live CD11c$^+$ cells. (c) Quantitative result showing mean value with SEM of graft-derived cells of b). Analyses were done using one-way ANOVA, with Bonferroni's multiple comparison tests. Result significance was shown, where ***p<0.001 and ****p<0.0001.

a

b
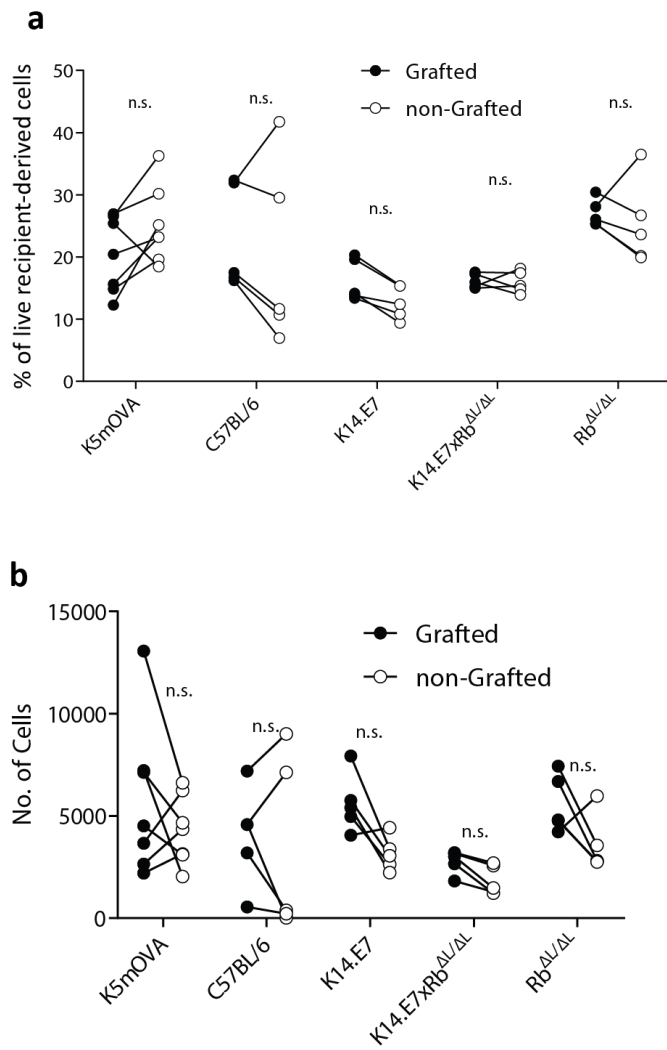
Figure S3.2

Percentage (a) and numbers (b) of recipient-derived CD11c$^+$ cells under live CD45.1$^+$ gate. Closed and open circle showing draining lymph nodes analysed from the grafted and non-grafted site, respectively.
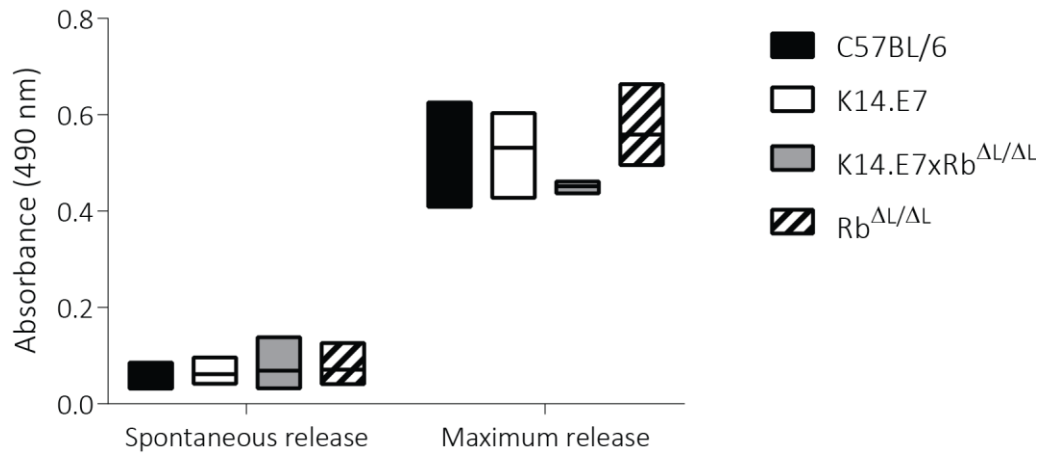
Figure S3.3

Target spontaneous and maximum LDH release at the same target cell number in Figure 3.4 Bar graph showing minimum and maximum absorbance at 490nm of three biological replicates.
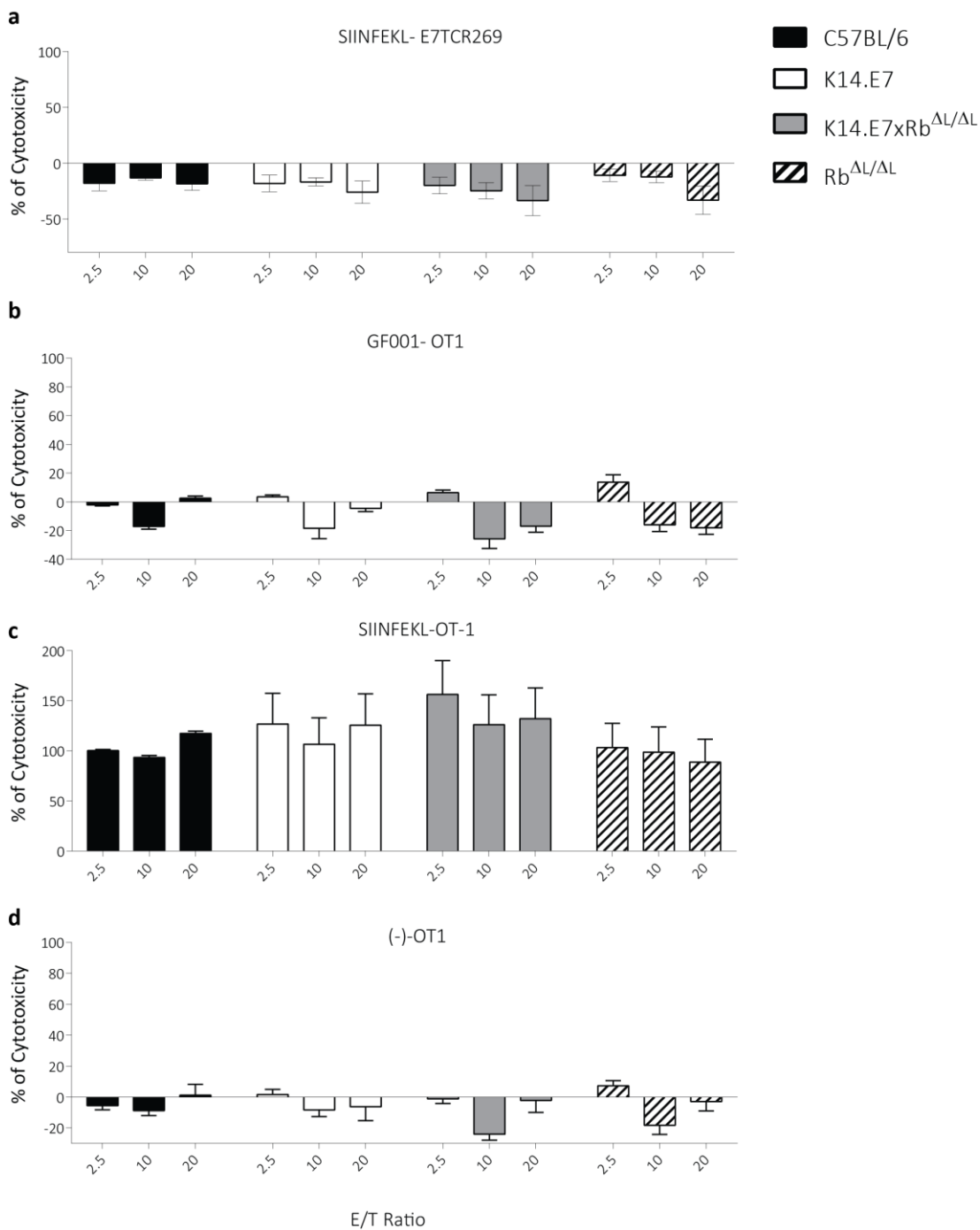
Figure S3.4

Control groups of antigen specific keratinocyte *in vitro* killing. Keratinocytes isolated from the epidermis of C57BL/6, K14.E7, K14.E7xRb$^{\Delta L/\Delta L}$, and Rb$^{\Delta L/\Delta L}$ mice were pulsed with GF001, SIINFEKL peptide or no peptide (-) and co-cultured with E7-specific effector T cells (E7TCR269) or SIINFEKL-specific effector T cells (OT-1) at the shown effector/target (E/T) ratios. Cytotoxicity is calculated with respect to keratinocyte death, which is assessed by LDH release using the following equation.

$$\% \ of \ Cytotoxicity = \frac{(mean \ read) - (effector \ spontaenous \ release) - (KC \ spontaneous \ release)}{(KC \ maximum \ release) - (KC \ spontaneous \ release)} \ x \ 100\%$$

Chapter 4

Discussions and Conclusion

4.1 Project summary

This project focuses on distinguishing the immunological phenotype and response in HPV16E7-expressing skin induced by E7-Rb interaction associated skin hyperplasia from E7 expression. Utilising both K14.E7 and K14.E7xRb$^{\Delta L/\Delta L}$ transgenic mice, I conclude that the hyperplastic skin environment induced by E7-Rb interaction, serves as an important factor that contributes to the suppressive local immunity in addition to the expression of viral oncoprotein E7.

In chapter 2, CXCR3$^+$ T cells are identified as a population that can facilitate E7-expressing skin graft rejection in the context of K14.E7xRag$^{-/-}$ skin graft. Chemokine ligands CXCL9 and CXCL10 are predominantly expressed by CD45$^-$ keratinocytes in the hyperplastic epithelium that direct the recruitment of CXCR3$^+$ T cells. Although, how this population interacts with other immunocytes that are mostly immunosuppressive in the context of K14.E7 skin still need to be explored, this is the first time an effector population has been identified to be involved in the process of skin graft rejection.

In chapter 3, I found that in the absence of E7-Rb interaction, the peripheral immune response is restored to a comparable level to non-transgenic wild-type. Moreover, this disruption allows endogenous antigen from the keratinocytes to be presented and induces CTL-mediated lysis *in vitro.* I assessed the ability of keratinocytes in presenting endogenous antigen by co-culturing keratinocytes, immediately after FACS sorting, with activated antigen-specific effector T cells. Although there are possibilities that proliferative cells (when E7-Rb interacts) are more insensitive/ sensitive to CTL-mediated lysis, the proliferation rate was not included as a factor of variables in this experiment. As keratinocytes from different transgenic animals were isolated the same way and co-cultured with T cells for five hours, which is shorter than average cell proliferation cycle, the results are conclusive. Despite that the keratinocytes from K14.E7xRb$^{\Delta L/\Delta L}$ skin can induce CTL-mediated lysis, disruption of E7-Rb interaction is unable to induce graft rejection. One of the possibilities that associates with skin transplant tolerance is that the lymph nodes draining K14.E7xRb$^{\Delta L/\Delta L}$ skin graft do not show increased K14.E7xRb$^{\Delta L/\Delta L}$ skin-derived DCs when compare to K14.E7 or K5mOVA skin. This may further impact on the efficiency of T cell priming in the lymph node. This part of the project suggests that interference of E7-Rb interaction can partially restore effective immune responses, but a combination triggering proper skin-derived APC function in the draining lymph node may be required if this was to be implemented clinically.

Figure 4.1 shows a graphical summary comparing the differences between K14.E7 and K14.E7xRb$^{\Delta L/\Delta L}$ skin phenotype.
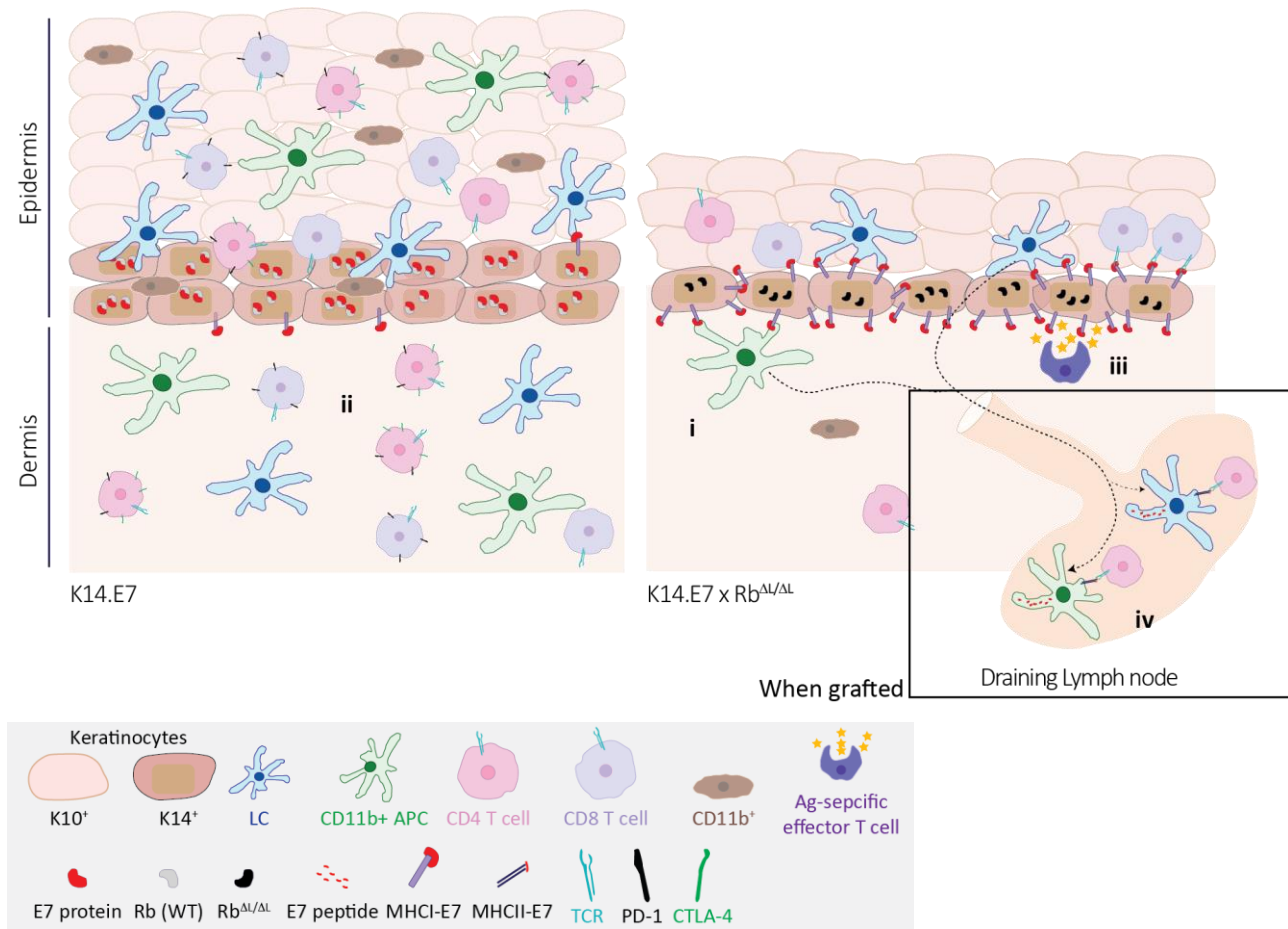
Figure 4.1 Comparison between K14.E7 skin and K14.E7xRb$^{\Delta L/\Delta L}$ skin.

The HPV16E7 protein interacts with cellular Rb and results in epithelial hyperplasia. i) In the hyperplastic K14.E7 skin, increased numbers of immunocytes including CD4, CD8 T cells, CD11b$^+$ non-DC, CD11b$^+$ DC and LC are found. ii) CD4 and CD8 T cells in the K14.E7 skin express higher level of co-inhibitory molecules, such as PD-1 and CTLA4. iii) Keratinocytes derived from the K14.E7xRb$^{\Delta L/\Delta L}$ skin are able to present endogenous antigens to antigen-specific effector T cells *in vitro* and induce cell-mediated lysis. iv) This part shows the non-transgenic recipient draining lymph node when grafted with K14.E7xRb$^{\Delta L/\Delta L}$ skin. Although the composition of DC subtypes in the K14.E7xRb$^{\Delta L/\Delta L}$ skin remained similar to non-transgenic skin, there was less CD11b$^+$ skin-derived DC in the draining lymph nodes when compared with immunogenic skin controls. This may result in insufficient T cell priming by the skin-derived DC and further restricts skin graft rejection.

4.2 Hyperplastic environment as a main force to influence the immune responses and phenotype of infiltrated lymphocytes

Persisting high-risk HPV infection in the cervix results in cervical intraepithelial neoplasia (CIN) and ultimately leads to cervical cancer. While spontaneous regression is observed at the early stages of CIN, the virus changes the microenvironment of the infected area during the course of persistent infection and evades immune surveillance through several mechanisms. The mechanisms include, but not restricted to, i) the preferred codon usage that are rarely used in mammalian cells and thus limited capsid proteins generation, which immune system can recognise (Zhou et al., 1999); ii) Failed maturation of HPV E7-loaded DC and therefore does not transmit immunogenic signal to T cells in the draining lymph node (Hemmi et al., 2001); iii) Regulatory T cells are generated by immature dendritic cells (Dhodapkar et al., 2001; Roncarolo et al., 2001) .

In the high-risk HPV genome, E6 and E7 proteins are the oncogenes that drive tumour development through the interaction with p53 and Rb, respectively. E6 and E7 impede effective immune responses mostly by changing the local environment as a consequence of uncontrolled cell growth. It has been widely characterized that the phenotype and function of tumour/hyperplasia infiltrating lymphocytes are shaped by the microenvironment, and the microenvironment in turn, changes the composition, as well as functions of tissue infiltrating lymphocytes. These changes of microenvironment induce i) a unique cytokine and chemokine secretion profile that alters the composition and function of immunocytes within the microenvironment and ii) expression of immune checkpoint molecules on tumour cells that attenuate effector function on lymphocytes. This project examines in details on the consequence of hyperproliferative epithelium, resulting from E7-Rb interaction, the immune environment including lymphocyte recruitment, phenotypic changes of skin infiltrating/resident lymphocytes and antigen presentation of the keratinocytes.

Keratinocytes in the epidermis change the cytokine and chemokine secretion profile in response to injuries, infections, as well as the proliferation and differentiation of keratinocytes (Bourke et al., 2015; Mckay and Leigh, 1991; Tuzun et al., 2007). These events that involve tissue structure alterationsoften lead to the overexpression of stress keratins, a phenotype which was also observed in the epidermis of K14.E7 (Zhussupbekova et al., 2016). Pro-inflammatory cytokines including IL-1, 6, 7, 10, 15, tumour necrosis factor α (TNFα), IFNα, β and γ are also produced (Blauvelt et al., 1996; Fujisawa et al., 1997; Grewe et al., 1995; Heufler et al., 1993; Howie et al., 1996; Kock et al., 1990; Kupper and

Groves, 1995; Oxholm et al., 1991). These cytokines and chemokines together recruit and activate immunocytes, therefore, change the local immune response. In addition, chemokines are also produced to attract leukocytes possessing cognate chemokine receptors to the site of inflammation (Nedoszytko et al., 2014). However, these changes can be reversed back to the level comparable to non-transgenic wild type when E7 can no longer interact with Rb. Thus, the cytokine and chemokine secretion in the epidermis of a persistent HPV infection mouse model, according to this study, is dependent on the interaction between E7 and Rb protein and the associated epidermal hyperplasia.

Previous studies showed that a range of pro-inflammatory cytokines, such as IFNγ, secreted by NKT cells, (Mattarollo et al., 2010a), IL-17, secreted by CD4 and γδ T cells, (Gosmann et al., 2014b) and IL-18, which is induced by IFNγ secreting NKT cells (Gosmann et al., 2014a) play immune suppressive roles in E7-associated hyperplasia. It is very likely that the microenvironment imposes strong influence on the recruitment of these particular cell types and forms a positive loop that reinforce on the suppressive immunity. Other possible mechanisms contributing to the suppressive immunity are i) PD-L1 and/ or PD-L2 expression on keratinocytes and/ or dendritic cells (Chandra et al., 2016) attenuate the effector T cell function; ii) IFNγ produced by the recruited immunocytes induces more expression of PD-L1 and PD-L2 (Garcia-Diaz et al., 2017); iii) IFNγ produced by NKT cells plays immunosuppressive role, as the E7-expressing transplants can only be rejected in the absence of IFNγ or NKT cells (Mattarollo et al., 2010a); iv) effector function of chemokine-recruited T cells, such as CXCR3^{+} T cells, could be influenced and suppressed by cytokines secreted by other cell types within the environment ; v) CXCR3 is expressed on both effector and regulatory T cells, and thus despite the recruitment of CXCR3^{+} T cell to the hyperplastic epithelium, no inflammatory response or skin graft rejection was observed; and vi) antigen presentation in both keratinocytes and DCs could be impaired at any step of the antigen presenting process as a result of E7 expression (Li et al., 2006; Li et al., 2009; Park et al., 2000).

4.3 Clinical relevance

This study provides a greater insight to HPV16E7-associated epithelial hyperplasia in addition to the expression of E7 protein itself. More importantly, it is identified in this project that an effector population can be recruited to the E7-expressing hyperplastic epithelium and the signal for this lymphocyte recruitment is provided by the proliferative epithelium. CXCL9 and CXCL10 production can be induced by type I interferons locally through topical imiquimod application and draw in effector cells with boosted immune response in a melanoma clinical study (Mauldin et al., 2016). Imiquimod has been widely used to treat genital warts (Skinner, 2003) and was on a phase II trial in combination with protein based HPV therapeutic vaccine for grade 2 and 3 vulval intraepithelial neoplasia (VIN) (Daayana et al., 2010). The trial result shows significant CD4$^+$ and CD8$^+$ T cells infiltration and antigen specific proliferation in responders. As shown in Figure 2.6d, CXCR3+ CD4+ T cells are preferentially recruited to the K14.E7 skin graft at the experiment endpoint. It is likely that this population contributes highly to skin graft tolerance. Depleting CD4 T cells could then, in some degree, induce clearance of skin graft. Given the observations and findings in this project, CXCR3 signal agonists or topical imiquimod to recruit substantial amount of effector T cells could be implemented in conjunction with E7-targeting therapeutic vaccines for late stage CIN treatment.

In chapter 3, we showed that disruption of E7-Rb interaction was unable to induce skin graft rejection, which is a critical measurement for lesion clearance. Possible explanations to the tolerance are i) low immunogenicity of E7 protein and ii) low level of antigen specific effector cell recruitment or retention in the localised area. Michal Šmahel et al., showed that vaccination with E7 DNA containing point mutations that disrupts the Rb-binding site can induce protection against TC-1 tumour only when it is fused with E. coli β-glucuronidase (GUS), suggesting low immunogenicity of E7 (Smahel et al., 2004). Furthermore, in the E7-expressing normoplastic skin, low level of vascularisation as well as cytokine and chemokine production were observed, which are important for recruiting and retaining cytotoxic T cells. On the other hand, as abrogation of E7-Rb interaction significantly improved immune responses against vaccination and the local environment exhibited similar molecular and phenotypic profile to normal tissue, it is still of great potential that this could be implemented as one of the therapeutic strategies for persistent HPV infection. In fact, a small molecule antagonising Rb inactivation by HPVE7 protein has been identified (Fera et al., 2012). This small molecule inhibits Rb and E7 interaction by competing the Rb binding site with E7 and is able to selectively induce effective E7$^+$ cell death *in vitro*. However, the

anti-tumour effect of this molecule was only tested in TC-1 tumour bearing NOD SCID model, which lacks competent immune system. Taken together, E7-Rb interaction and the associated hyperplasia can be a potential therapeutic target but may require further combinatorial treatment to achieve promising outcome.

Current therapeutic strategies for late stage CIN or HPV-induced cervical cancer focuses on targeting the E7 antigen along with inducing more tissue-homing cytotoxic T cells. Some of the main drawbacks from current therapeutic vaccines are the concurrent recruitment of regulatory or suppressive lymphocytes (Welters et al., 2008) and also the lack of significant lesion regression when compared to spontaneous clearance (Einstein et al., 2007). This implies that simply targeting E7 antigen may not be enough to generate sufficient immunity to eradicate persistent infection. One promising therapy under phase 3 clinical trial is VGX-3100, a DNA vaccine targeting E6 and E7 of HPV16 and HPV18developed by Inovio Pharmaceuticals, Inc (Morrow et al., 2016; Trimble et al., 2015). In phase 2b trial (NCT01304524), 40% of vaccinated women showed lesion regression, whereas only 14.3% regression was observed in the placebo treated group (Morrow et al., 2018). Although the vaccine is effective in terms of successful lesion regression and viral clearance, 60% of the patients were not responsive to the vaccine. This suggests that the suppressive immunity may still plays a significant role controlling the outcome of therapeutic effectiveness. Interestingly, a follow up study of this clinical trial showed a number of findings and prediction of clinical outcomes that coincide with the findings in the K14.E7 mouse model. In the VGX-3100 trial study, infiltration of CD8^{+} cells, FoxP3^{+} cells, the CD8/Foxp3 ratio, or PD-L1 expression in cervical epithelial tissue prior to treatment do not predict the clinical response. After final treatment with VGX-3100 but before the trial end point, increased number of T cell co-stimulatory marker 4-1BB^{+} (CD137^{+}) CD8 T cells expressing GrzA, GrzB and Prf specific for the infected HPV type from the peripheral blood can be good predictive markers for responsive outcome. In relation to this, the K14.E7 skin has significant CD137^{+}CD8^{+} T cells infiltration (Choyce et al., 2013) (and data not shown) and PD-L1 expression (Chandra et al., 2016). Moreover, depletion of FoxP3 expressing cells did not enable graft rejection, indicating that these cells are not critical populations contributing to skin graft tolerance (Mattarollo et al., 2011). These results further strengthen and support this transgenic mouse as a suitable model to study the suppressive immunity in persistent HPV infection and to improve our understanding to the therapeutic vaccine non-responders.

4.4 Concluding remark and future prospect

This project reported that the local immune environment and responses in a persistent HPV16 infected model are mostly, but not all, the result of the HPV16E7-Rb interaction-induced epithelial hyperplasia. This study provides a potential strategy for treatment of HPV related CIN. To resolve persistent HPV infection, localised effector T cells infiltration and antigen specific resident memory T cells establishment could be promising for future studies on therapeutic vaccine development.

The following questions could be addressed in prospective studies:

1. What are the immunocytes and/or secretory factors that positively contribute to HPV16E7-expressing skin graft rejection?

The Frazer lab together has identified immunocytes and secretory factors that contribute to K14.E7 skin graft rejection (see Chapter 1 introduction). It was found that adoptive transfer of E7-specific CD8 T cells plus E7 immunisation are necessary to induce IFNγ secretion by antigen-specific CD8$^+$ T cells and K14.E7 skin graft rejection (Matsumoto et al., 2004). In contrast to adoptive transfer, one positive regulator identified in this project that, without adoptive transfer or immunisation, facilitates HPV16E7-expressing skin graft clearance is the CXCR3$^+$ T cell subset. In chapter 2, inhibiting the infiltration of this T cell subset was shown to alter the fate of hyperplastic E7-expressing skin, when no other T or B cells are present (K14.E7xRagKO), turning the rejection to tolerance. However, when sorted CXCR3$^+$ T cells were transferred to immunocompetent recipients grafted with K14.E7 skin (shown in additional data, chapter 2), both control and K14.E7 skin grafts are tolerated. This indicates that CXCR3$^+$ T cell alone is not sufficient, or not the dominant population, to induce K14.E7 skin graft clearance. It would be clinically important to identify which immune population and/or secretory factors alone or in cooperation with CXCR3$^+$ T cell that can actively reject K14.E7 skin grafts.

2. Evaluate the clinical value of combining CXCR3+ T cell transfer and small molecule disruption of the E7-Rb interaction in treating late stage CIN.

In chapter 2, CXCR3$^+$ T cells are identified as an effector population that positively contribute to E7-expressing skin graft clearance in the absence of other lymphocytes. In chapter 3, although DC from the K14.E7xRb$^{\Delta L/\Delta L}$ skin has limited abundance in draining lymph node, the *in vitro* result showed that keratinocytes with disrupted E7-Rb interaction can be lysed in a CTL-mediated fashion when sufficient effector T cells are supplied. Providing sufficient

effector lymphocytes to the localised area combining with E7-Rb interaction inhibitor could then become a possible therapeutic method to enable HPV16E7-expressing lesion clearance.

Chapter 5

Appendix-
Optimisation Experiments and Extended Methods

5.1 Preface

This project aims to differentiate the immune responses induced by the expression of HPV16E7 from the associated hyperproliferative environment. The main approach is utilising the K14.E7 and K14.E7xRb$^{\Delta L/\Delta L}$ mice for transcriptomic and immunological analysis. To further investigate the impact of the HPV16E7-associated epidermal hyperplasia, some functional assays were designed. This chapter includes three key optimisation experiments, which were then further served as standard procedures in the main experiments mentioned in chapter 2. Also, this chapter includes one experiment, which resulted in a change of experimental approach due to technical difficulties. In addition to the experimental optimisation, this chapter also includes a section to explain the exclusions and limitations regarding the transgenic mouse model used.

5.2 Enrichment of T cells and induction of CXCR3 expression *in vitro*

Corresponding to Figure 2.5 in chapter 2- *in vitro* trans-well migration

The aim of the trans-well migration is to assess whether supernatants from different skin explant culture attract different numbers of CXCR3$^+$ T cells as a result of the chemokines contained in the supernatants. To test this, equal amount of sorted CXCR3$^+$ cells were seeded at the start of the experiment. Although, CXCR3$^+$ T cells can be sorted directly from the spleen of a naïve non-transgenic animal, the total number of cells that can be obtained is not enough for a comprehensive trans-well migration experiment. Therefore, an alternative method was developed to obtain optimal number and consistent CXCR3-expressing T cells. This section contains two parts- enrichment of T cells, and the induction of CXCR3 expression on the enriched T cells *in vitro*.

Enrichment of T cells from naïve non-transgenic spleen using a novel antibody cocktail

The concept of this enrichment assay is negative selection. Single cell suspension from the spleen was obtained with standard procedure. For one reaction, 1 x 10^8 cells was incubated with an 1 mL cocktail containing 5% rat serum, biotin-conjugated antibodies- CD19 (clone 6D5, Biolegend, San Diego, USA), CD11b (clone M1/70, Biolegend, San Diego, USA) and CD11c (clone N418, Biolegend, San Diego, USA) in 1:200 dilution in FACS buffer for 15 minutes at room temperature. Strepavidin beads (EasySep™ Streptavidin RapidSpheres™ 50001, STEMCELL technologies, Canada) were mixed thoroughly and 75 µl was added into each 1ml reaction and let sit at room temperature for 2 minutes. FACS buffer was added to top up the volume to 2.5 ml/reaction before placed in the EasySep™ Magnet (STEMCELL technologies, Canada). T cells were extracted from the unbound portion and were counted for further use.

The enrichment increased the T cell population to 93% from 54% per spleen (about 72 % efficiency) (Figure 5.1). Also, non-T cell population decreased, from 39% to 7% (about 82% reduction efficiency). This showed that the assay has successfully enriched a pool of T cells from a naïve non-transgenic spleen.

pre-gated on live cells
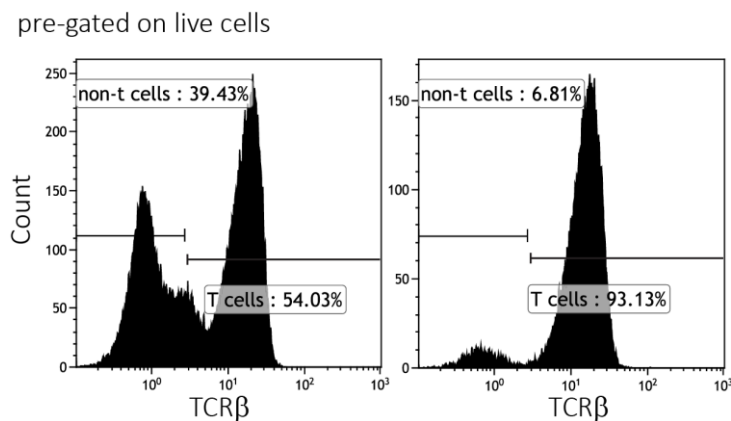
Figure 5.1 T cell percentage before and after enrichment with homemade antibody cocktail

Splenocytes were purified as described above and analysed under live cell gate. TCRβ was used as T cell marker. Left, before enrichment; Right, after enrichment.

Induction of CXCR3 expression on enriched T cells

The main purpose of inducing CXCR3 expression is to test how many cells are attracted by various skin explant supernatant. Consistent CXCR3 expression on T cells is required to assess the variability of ligands in different supernatants. As CXCR3 is a chemokine receptor that is expressed on activated T cells, *in vitro* activation of enriched T cells with various methods were employed. As described before, CXCR3 expression does not coincide with the expression level of known activation markers (CD69 and CD44) (Nakajima et al., 2002). Therefore, different time points were analysed to find out the optimal time point where a larger percentage of cells expressing CXCR3 were identified. A table below summarises the conditions tested.

Table 5.1 Conditions tested for optimal CXCR3 expression on enriched T cells

(In each 48-well, 2 x 10^5 cells were seeded; all condition contains IL-2)

Group	Condition	Time point	Activation markers used
A	No treatment (-)	1 Day	CD69
B	No treatment (-)	2 Days	CD69
C	No treatment (-)	7 Days	CD44
D	PMA/ Ion	1 Day	CD69
E	PMA/ Ion	2 Days	CD69
F	PMA/ Ion	7 Days	CD44
G	anti-CD3/28	1 Day	CD69
H	anti-CD3/28	2 Days	CD69
I	anti-CD3/28	7 Days	CD44

PMA 25 ng/mL; Ionomycin (Ion) 1 µg/mL; anti-CD3 2 µg/mL; anti-CD28 2 µg/mL; IL-2 5 ng/mL

The result showed that after 2-days stimulation (Figure 5.2-B, E and H), a larger proportion of CXCR3$^+$ cells can be detected when compared with 1-day (Figure 5.2-A, D and G) and 7-days (Figure 5.2-C, F and I) stimulation. Surprisingly, non-stimulated group (B) has higher percentage of CXCR3$^+$ cells, when compared with other stimulations, but with limited activation marker expression. While CXCR3 was expressed on cells receiving no stimulation, the viability under this condition was lower than those receiving activation. Therefore, this condition was not considered optimal. Stimulation with PMA/Ion (group E) and anti-CD3/28 antibody (group H) generate similar amount of total CXCR3$^+$ cells on day 5. As anti-CD3/28 treatment resulted in more CXCR3$^+$CD69$^+$ cells, indicating more activation, this condition was chosen as the optimal condition among those tested.
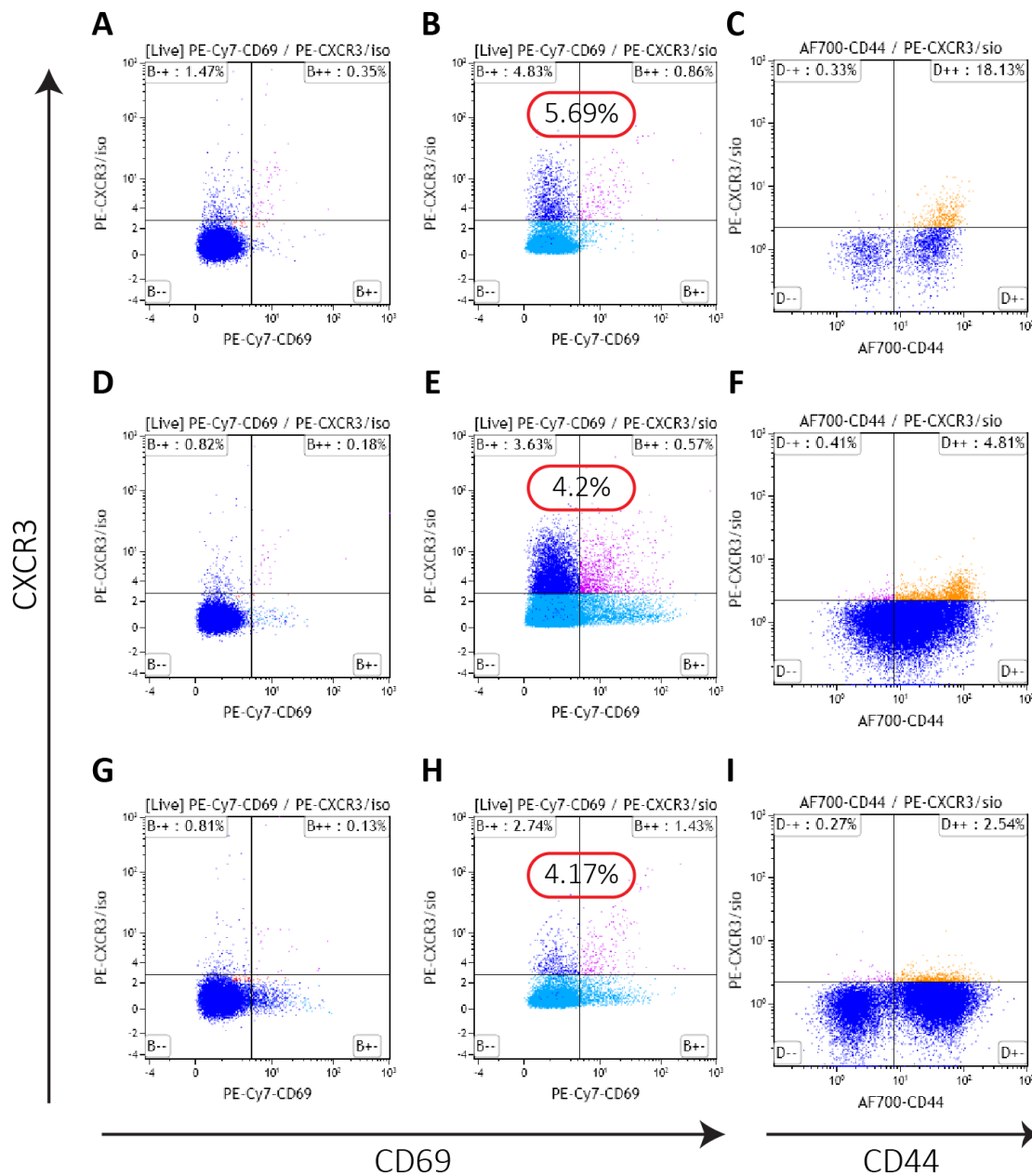
Figure 5.2 Induction CXCR3 expression with various *in vitro* stimulation.
Enriched T cells were stimulated with PMA/Ion (D, E and F) or anti-CD3/28 (G, H and I) or without stimulation (A, B and C). The panels in this figure are outlined in Table 5.1. All analysis were done on live cells. Isotype controls were used for gating.

      The strategy employed above was repeated twice and the results were consistent. However, less than 5% recovery from live cells was not ideal nor efficient. According to Nakajima et al. (Nakajima et al., 2002), CXCR3 expression can be induced on T cells from lymph node with immobilised anti-CD3/28 stimulation following with one day of stimulant withdraw. To test this protocol, 24-well plate was coated with anti-CD3/28 (both at 5 µg/mL) in Tris buffer (pH=9.4) at 4°C overnight. Splenic T cells were enriched using homemade

antibody cocktail. The coated plate was washed with PBS and T cells were seeded at 2.5 x 10^6 cells/ well. The plate was centrifuged at 350g for 5 minutes to allow T cells contacting the coated surface. The cells were cultured for 48 or 72 hours with various conditions. The conditions tested are as below:

Table 5.2 Conditions tested for optimal CXCR3 expression using immobilised antibodies		
Group	0 to 48 hours	48 to 72 hours
A	No stimulant (-)	N/A
B	anti-CD3/28	N/A
C	No stimulant (-)	No stimulant (-)
D	anti-CD3/28	anti-CD3/28
E	anti-CD3/28	No stimulant (-)

In group B, 48 hours of immobilised antibody stimulation generated 2% CXCR3$^+$ T cells of live cells, which was less than 72 hours of continuous stimulation (4.1% of live cells in group D). By plating cells to fresh complete RPMI after 48-hour culture for another 24-hour (group E), the percentage increased up to 29%, which was more than 6-fold higher compared to the previous method and to group D in this same experiment. Therefore, this condition was chosen to induce surface CXCR3 expression on enriched T cells as standard procedure for further experiments.
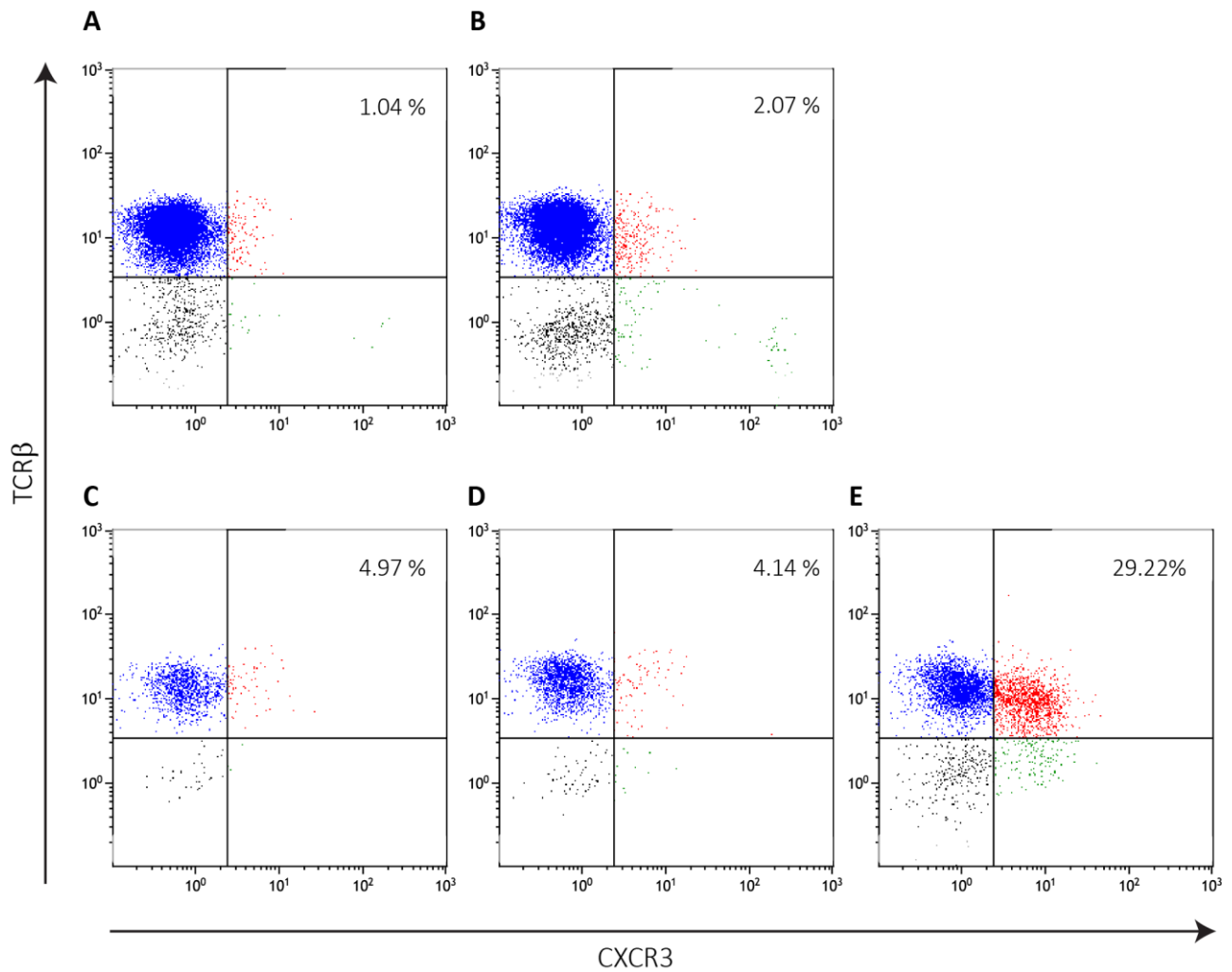
Figure 5.3 Induction CXCR3 expression with immobilised antibody *in vitro* stimulation
Enriched T cells were used for stimulation. The panels in this figure are outlined in Table 5.2
and all analysed on live cells. Isotype controls were used for gating.

5.3 Establishing positive controls and neutralising antibody dose for in vitro chemotaxis

The following experiment outlines how the concentration of recombinant CXCL9 (Murine MIG, 250-18, Lonza, Basel, Switzerland) and CXCL10 (Murine IP-10, 250-16, Lonza, Basel, Switzerland) was determined as chemotaxis positive control, as well as the concentration required for the neutralising antibody to capture the CXCL9 and CXCL10 existed in the skin culture supernatant (correspond to in vitro trans-well migration assay in chapter 2).

The receptor CXCR3 internalises when it engages with its ligands. Given this nature, the amount of recombinant ligands required to achieve receptor internalisation can be determined by the amount of surface CXCR3. Using the optimised protocol outlined in section 4.2 and 4.3, CXCR3$^+$ T cells were sorted and incubated with ligand or ligand/ neutralising antibody containing medium. Conditions tested are outlined in the table below:

Table 5.3 Concentration tested to establish positive controls and neutralising antibody dose		
Ligand	Ligand concentration	Ligand to nAb ratio
CXCL9	0 nM	n/a
	10 nM	n/a
	50 nM	n/a
	100 nM	n/a
	50 nM	1:10
	50 nM	1:25
CXCL10	0 nM	n/a
	10 nM	n/a
	50 nM	n/a
	100 nM	n/a
	50 nM	1:10
	50 nM	1:25

Neutralising antibody (nAb) to CXCL9 (AF-492-NA, R&D, MN, USA), CXCL10 (AF-466-NA, R&D, MN, USA) isotype antibody (Goat IgG, AB-108-C, R&D, MN, USA) were used. Concentration of the nAb was tested with two different ratios: 1 ng of antibody neutralises 10 ng of ligand (1:10) or 1 ng of antibody neutralises 25 ng of ligand (1:25).

Sorted CXCR3^{+} T cells were incubated with the medium at density $3x10^5$/ 96-well 37°C for 60 minutes. Surface CXCR3 was then stained after culture. The surface CXCR3 decreased as the amount of ligand increased. A sharp descend of surface CXCR3 was observed when cultured with 50nM CXCL9 and 10 nM CXCL10. Therefore, these two concentrations were used as positive controls for trans-well migration experiment. nAb against CXCL9 used at ratio 1:10 successfully blocked the ligand and receptor binding and restored the surface CXCR3 to a level comparable to 0 nM. Although the nAb against CXCL10 did not fully restore surface CXCR3 at 1:10 ratio, this was considered effective, mainly because isotype control at the same ratio showed the same level of internalisation to that of 50nM ligand. Thus, ratio 1:10 was chosen as neutralizing condition.

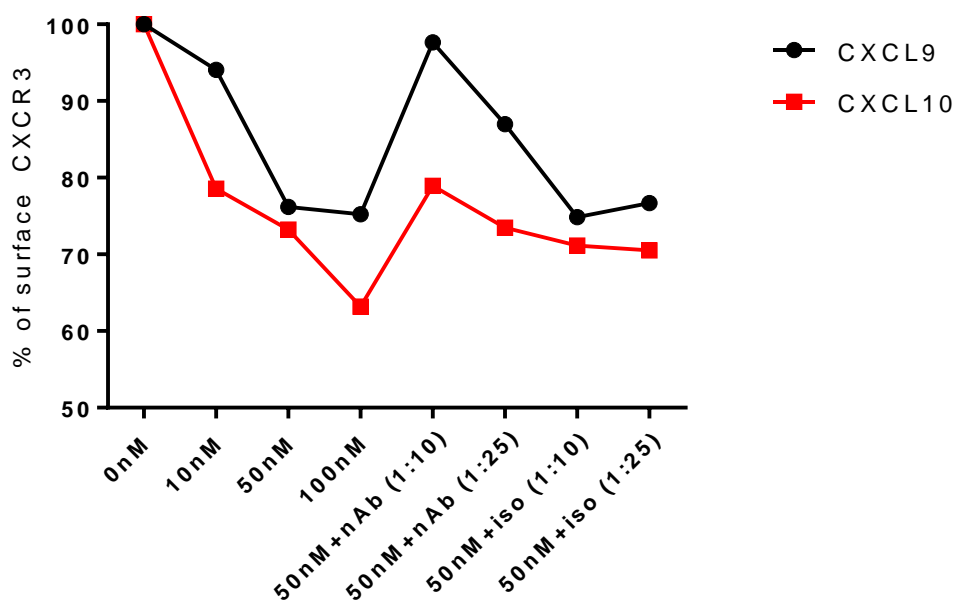**Figure 5.4 Percentage of surface CXCR3 after culture with ligand or ligand/ nAb containing medium.**

Sorted CXCR3^{+} T cells were incubated with either CXCL9 or CXCL10 at different concentration with or without neutralising antibody (nAb) or isotype control antibody at different ratio. The mean fluorescent intensity (MFI) of 0nM was set as 100%. MFI from every other condition was compared to 0nM.

5.4 Estimation of the amount of CXCL9 and CXCL10 present in K14.E7 skin explant culture supernatant

As the neutralising antibody was meant to neutralise the existing ligands contained in the K14.E7 skin supernatant, it was required to determine how much ligand was present in the supernatant. Combining the result of this section with section 5.3, which tells the ratio of ligands to nAb, the amount of nAb to be used can thus be finalised. Although the amount of CXCL9 and CXCL10 can be determined using ELISA, which requires larger volume of supernatant in total from more animals, due to the limitation on the numbers of animals granted in the ethics, an alternative method was utilised.

The same culture experiment, as described in section 5.3, was used. Additional conditions where K14.E7 skin explant culture supernatant was diluted with complete RPMI as culture medium were added. The supernatant used here was a pooled sample from three supernatant. The rest of the un-pooled supernatant aliquots were kept for further experimental use to minimise the amount of experimental animals required. Without dilution, K14.E7 skin supernatant induced around 25% surface CXCR3 internalisation. As the supernatant diluted, the amount of surface CXCR3 increased, indicating less ligands in the medium. To conclude, there is approximately 100nM of CXCL9 and 50nM of CXCL10 in the K14.E7 skin supernatant.
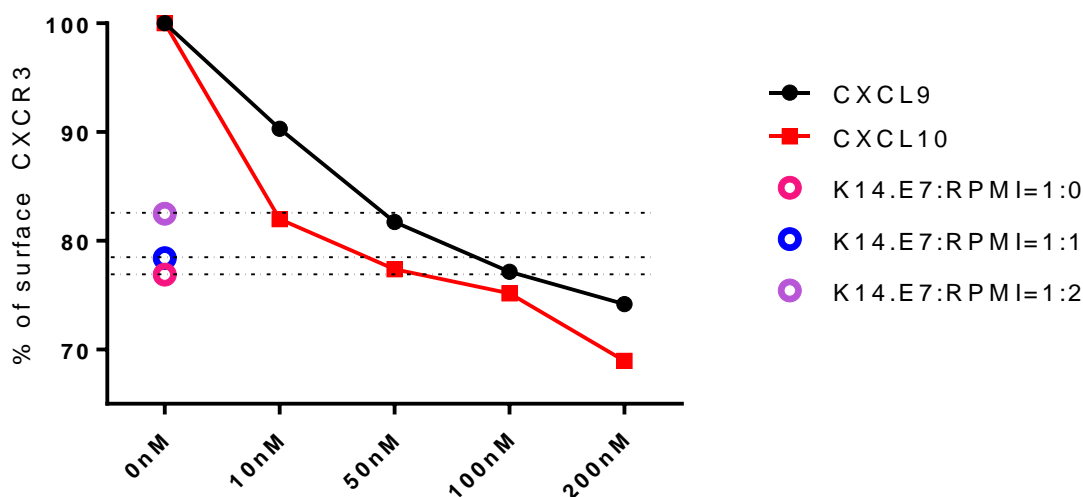

Figure 5.5 Percentage of surface CXCR3 after culture with K14.E7 skin explant culture supernatant at various dilution.

Sorted CXCR3$^+$ T cells were incubated with either CXCL9 or CXCL10 at different concentration or with pooled K14.E7 skin culture supernatant. K14.E7 skin supernatant was

diluted with complete RPMI in 1 to 0 (pink), 1 to 1 (blue) and 1 to 2 (purple) ratio. MFI from every condition was compared to 0nM, which was set as 100%.

5.5 *In vivo* transfer of sorted CXCR3$^+$ T cells and track the migration of transferred cells

In chapter 2, we observed increased expression of CXCL9 and CXCL10 in the skin of K14.E7. We therefore wonder what the main function of CXCR3+ T cells is once they get into the K14.E7 skin. The approach was to coat sorted CXCR3$^+$ T cells (congenic background expressing CD45.1), generated *in vitro* using the procedure outlined in section 5.2, with traceable fluorescent dye, transfer them to K14.E7 mice intravenously and track the transferred cells at various time points in spleen, lymph nodes and ear skin. A more detailed procedure is outlined below.

In vitro induction of CXCR3 following method developed in section 4.2 were performed using splenocytes from B6.SJL.Ptprca mice and sorted into two populations- CXCR3$^+$TCRβ$^+$ and CXCR3$^-$ TCRβ$^+$ using BD FACSAria Fusion sorter (BD Biosciences, NJ, USA). Figure 5.6 showing representative results, which CXCR3$^+$TCRβ$^+$ and CXCR3$^-$ TCRβ$^+$ can be sorted at percentages 5.2% and 52% of total events, respectively. CXCR3$^+$TCRβ$^+$ and CXCR3$^-$ TCRβ$^+$ population were then coated with fluorescent dye eFluor 670 (65-0840-85, eBioscience, ThermoFisher, MA, USA) and CFSE (65-0850-84, eBioscience, ThermoFisher, MA, USA), respectively. Figure 5.7 showing representative plots immediately after coating. Coated cells were then mix at 1:1 ratio and 500,000 cells in total were injected to each recipient. Spleen, lymph nodes and ear skin were harvested on day 5, day 8 and day 10 for further analysis.
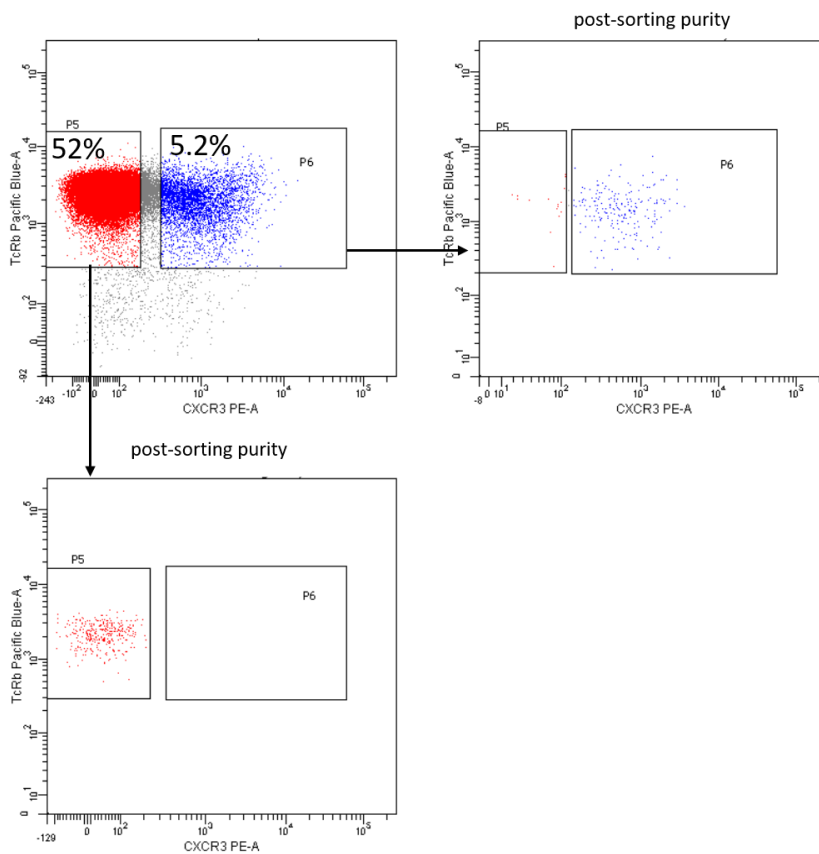
Figure 5.6 Representative CXCR3 and TCRβ sorting result.

Pre-gated on live cells, CXCR3$^+$TCRβ$^+$ (P6 gate) and CXCR3$^-$ TCRβ$^+$ (P5 gate) population were sorted. Post-sorting purity of both populations are >90%.
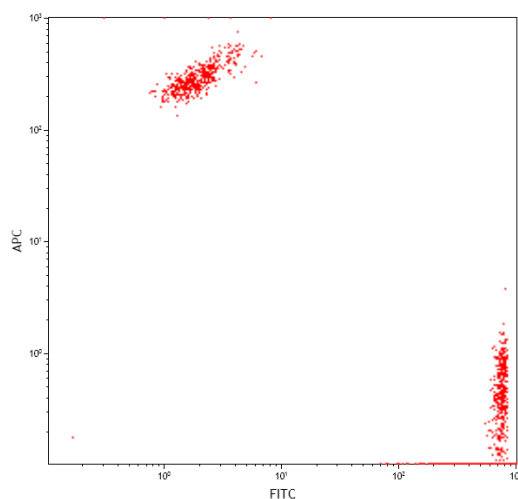
Figure 5.7 Fluorescent dye coating on sorted CXCR3$^+$TCRβ$^+$ and CXCR3$^-$ TCRβ$^+$ mixture before injection.

eFluor 670 coated CXCR3$^+$TCRβ$^+$ and CFSE coated CXCR3$^-$ TCRβ$^+$ cells were detected by APC and FITC channel, respectively. The two sorted populations were mixed after coating separately in 1:1 ratio and analysed by FACS prior to injection.
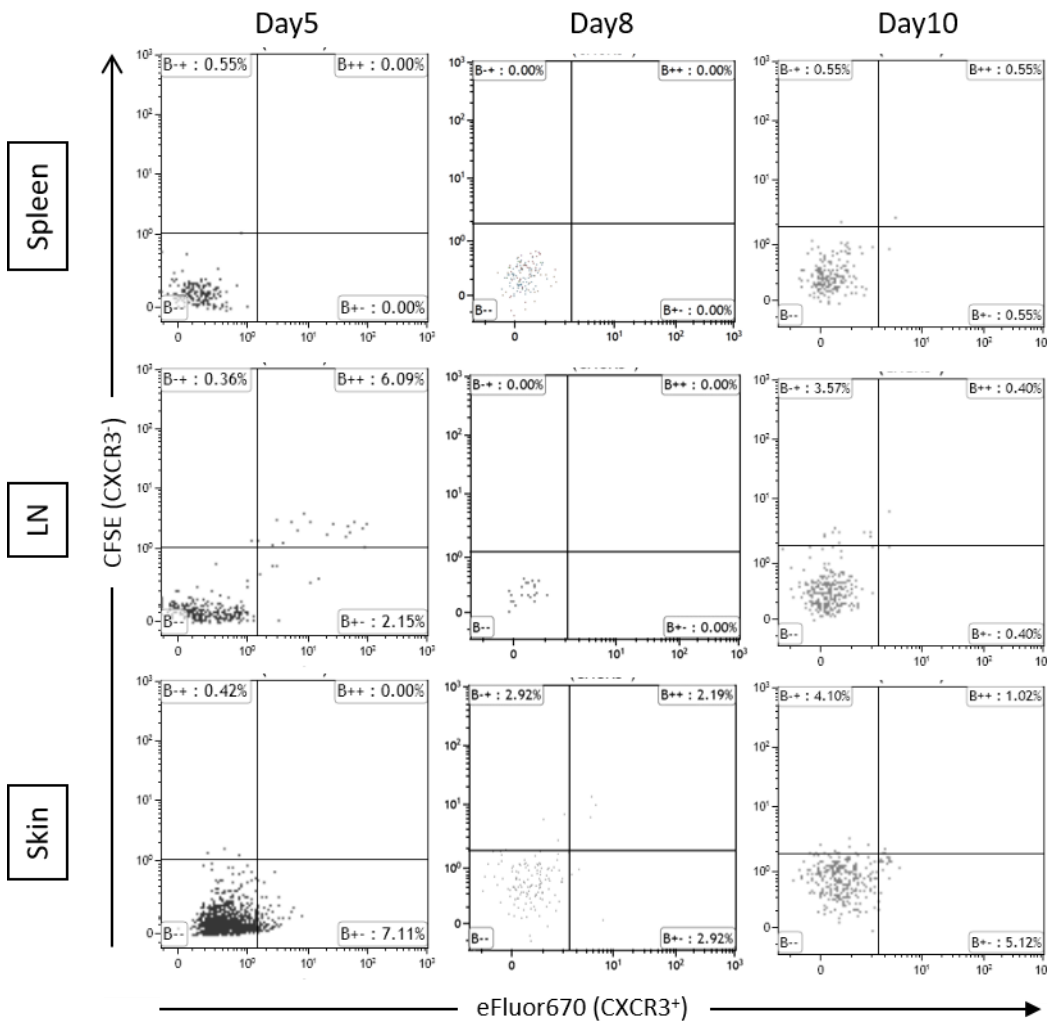
Figure 5.8 Representative plots showing analysis on transferred CXCR3+ and CXCR3-cells of recipient spleen, lymph node and ear skin.

Sorted cells were coated with fluorescent dye (CXCR3+-eFluor 670; CXCR3⁻CFSE), mixed at 1:1 ratio in a total of 500,000 cells and transferred intravenously to congenic recipients (CD45.2). Tissues from the recipients were harvested 5, 8 and 10 days after transfer. All plots were pre-gated on live CD45.1 T cells.

From nine donor mice, after T cell enrichment, *in vitro* stimulation and sorting for CXCR3 expression, about 2×10^6 of CXCR3+ T cells could be obtained. Each recipient received 250,000 CXCR3+ T cells and a total of eight mice can be transferred. The spleen, lymph node and skin of the recipient mice were collected 5, 9 and 10 days after cell transfer and analysed under CD45.1 T cell gate (Figure 5.8). The fluorescent coating was mostly not detectable at any time point experimented, suggesting that the transferred cells might have proliferated or the fluorescent coating is no longer detectable. Moreover, the amount of cells is insufficient for further analysis at any given time point in the skin of the recipient mice. The

reason might be that the transferred cells travel and can be recruited to any area of the skin, but only ear skin can be further analysed using the establish protocol. As a result, the events acquired are not enough to be analysed properly. Due to the technical difficulty and low cost-effective outcome of this experiment, an alternative method was sought. Splenocytes from congenic donor were injected, without sorting, into recipients bearing skin grafts along with either vehicle or CXCR3-antagonist treatment. This allows a localised area, the skin graft, to be analysed and direct comparison between different skin grafts side by side, as well as different lymphoid organs. Moreover, the specific recruitment of CXCR3$^+$ T cells can be distinguished by CXCR3-antagonist treatment, following by FACS analysis. This alternative approach and results are included in Figure 5 of chapter 2.

5.6 Exclusions and limitations

In this section, I address some exclusions and limitations for the project due to animal breeding difficulties in this project.

The Rb mutant mice used in this project are mostly heterozygotes, with only one allele that has the mutated E7-interaction site. The female breeders tend not to keep homozygotic Rb mutant pups during the weaning process, which includes less milk feeding and nursing, eventually these pups do no survive the weaning process. This made it difficult to obtain sufficient mature animals for experiments. With a few homozygotic animals obtained, I analysed and compared the skin histology between them and heterozygotes. At the molecular level, heterozygous Rb mutant provides one copy of Rb to interact with E7, but the thickness of the skin between homozygotes and heterozygotes remains similar. Phenotypically, the composition of the immunocytes in the skin showed no difference between homozygotic and heterozygotic Rb mutant in E7-expressing transgenic mice. This suggests that E7-induced hyperproliferation could be suppressed with only disrupting a single copy of E7-Rb interaction. In fact, it is expected that with one copy of Rb still functioning, without E7-induced degradation, the cell cycle should remain controlled. Figure 5.9 and Figure 5.10 showing the analysis of immunocyte subpopulations in the epidermis and dermis, respectively, by FACS. In the epidermis, $CD3\varepsilon^+$ cells, including $\alpha\beta$ T cells and $\gamma\delta$ T cells, and $CD11b^+$ myeloid cells were analysed under live $CD45^+$ gate, showing little and insignificant differences in percentage of gated. $CD11c^+$ and $MHCII^+$ DC was analysed under $CD3\varepsilon^-$ cell gate. Gated on EpCAM, LC also showed insignificant difference between homozygotic and heterzygotic $K14.E7xRb^{\Delta L/\Delta L}$ skin. Dermal immunocyte populations including $CD3\varepsilon^+$ T cells, DC, LC, macrophages, and $Ly6C^+$ and $Gr1^+$ monocytes were analysed. As there were no major phenotypic differences, homozygotic Rb mutant mice were not separated from heterozygotes Rb mutant mice and the two genotypes were combined to provide sufficient biological replicates in every experiment.

Epidermis
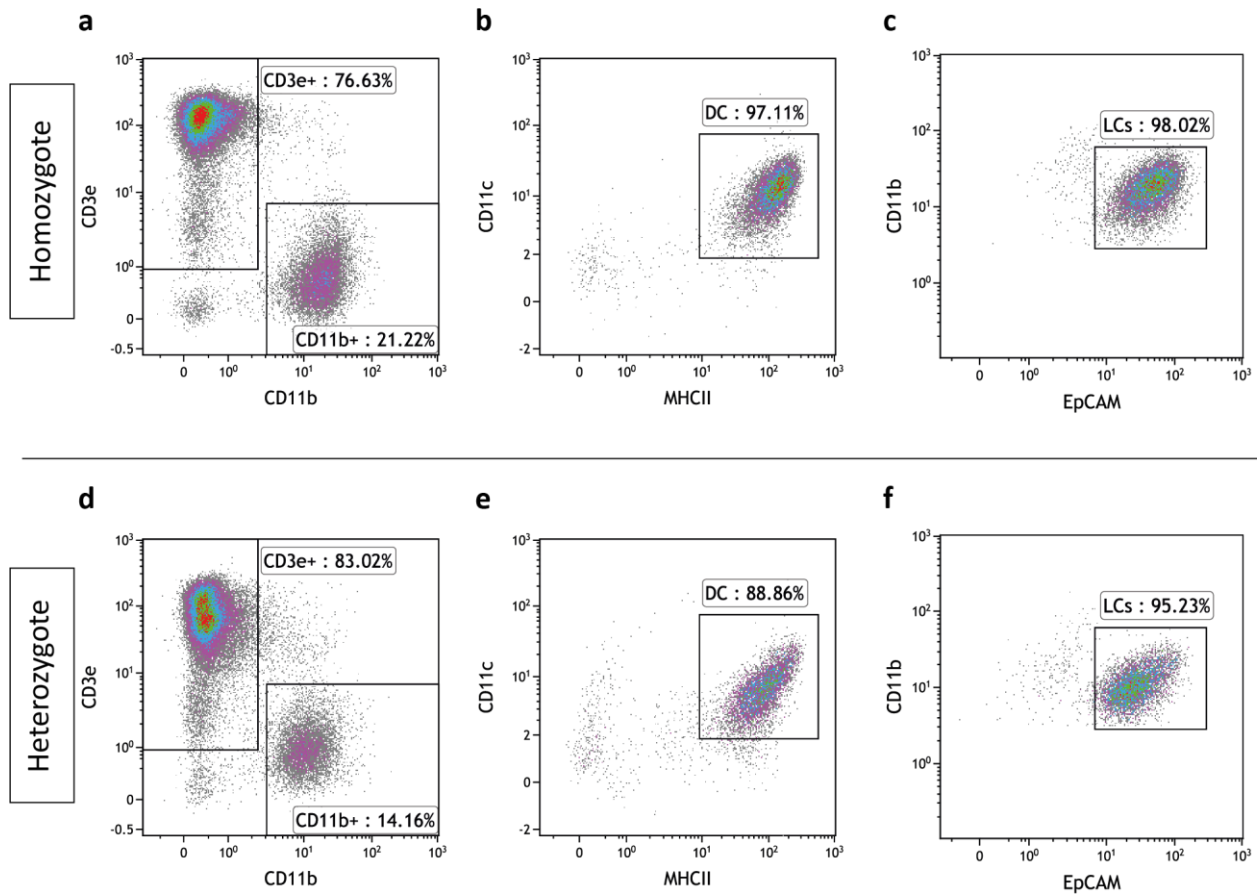
Figure 5.9 Representative plot of epidermal immunocyte composition in homozygotic and heterozygotic K14.E7xRb$^{\Delta L/\Delta L}$ skin

Composition of immunocytes in the epidermis. a and d) CD3ε^+ and CD11b$^+$ cells gated under live CD45$^+$ gate. b and e) CD11c$^+$ and MHCII$^+$ DC gated on CD3ε^- cells. c and f) LC gated under DC gate.
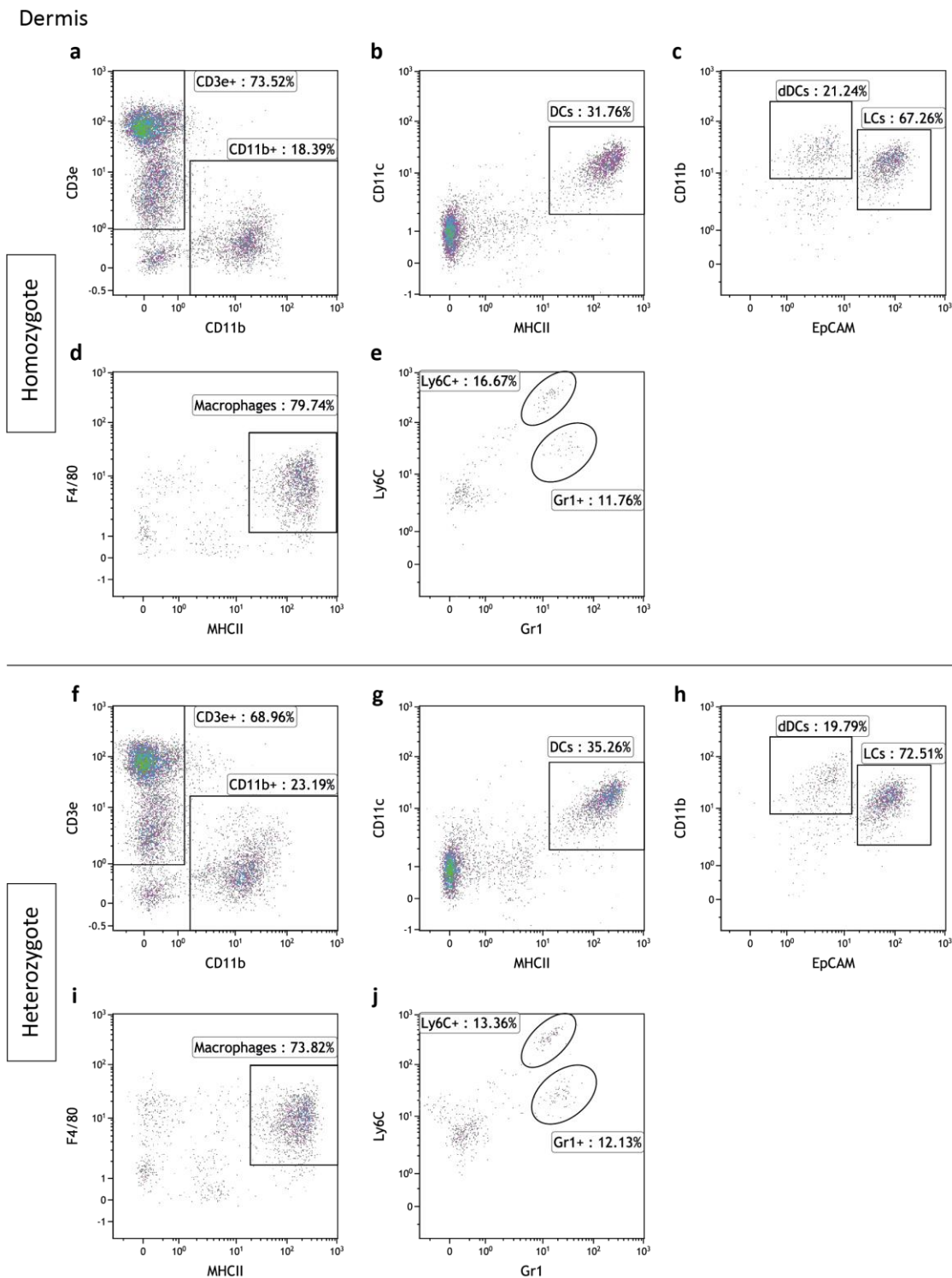
Figure 5.10 Representative plot of dermal immunocyte composition in homozygotic and heterozygotic K14.E7xRb$^{\Delta L/\Delta L}$ skin

a and f) gated under live CD45$^+$ cell gate. b and g) CD11c$^+$ and MHCII$^+$ DC gated on CD3ϵ^- cells. c and h) LC and dermal DC (CD11b$^+$ EpCAM$^-$) were analysed under DC gate in b and g, respectively. d and i) Macrophages were analysed under CD11b+ gate in a and f, respectively. e and j) F4/80$^-$ cells were further analysed based on expression of Ly6C and Gr1.

References

Adurthi, S., S. Krishna, G. Mukherjee, U.D. Bafna, U. Devi, and R.S. Jayshree. 2008. Regulatory T cells in a spectrum of HPV-induced cervical lesions: cervicitis, cervical intraepithelial neoplasia and squamous cell carcinoma. *Am. J. Reprod. Immunol.* 60:55-65.

Antinore, M.J., M.J. Birrer, D. Patel, L. Nader, and D.J. McCance. 1996. The human papillomavirus type 16 E7 gene product interacts with and trans-activates the AP1 family of transcription factors. *EMBO J.* 15:1950-1960.

Antonelli, A., P. Fallahi, A. Delle Sedie, S.M. Ferrari, M. Maccheroni, S. Bombardieri, L. Riente, and E. Ferrannini. 2008. High values of alpha (CXCL10) and beta (CCL2) circulating chemokines in patients with psoriatic arthritis, in presence or absence of autoimmune thyroiditis. *Autoimmunity* 41:537-542.

Arany, I., A. Goel, and S.K. Tyring. 1995. Interferon response depends on viral transcription in human papillomavirus-containing lesions. *Anticancer Res.* 15:2865-2869.

Arbeit, J.M., K. Munger, P.M. Howley, and D. Hanahan. 1994. Progressive squamous epithelial neoplasia in K14-human papillomavirus type 16 transgenic mice. *J. Virol.* 68:4358-4368.

Arnold, B., M. Messerle, L. Jatsch, G. Kublbeck, and U. Koszinowski. 1990. Transgenic mice expressing a soluble foreign H-2 class I antigen are tolerant to allogeneic fragments presented by self class I but not to the whole membrane-bound alloantigen. *Proc. Natl. Acad. Sci. U. S. A.* 87:1762-1766.

Awwad, M., and R.J. North. 1988. Immunologically mediated regression of a murine lymphoma after treatment with anti-L3T4 antibody. A consequence of removing L3T4+ suppressor T cells from a host generating predominantly Lyt-2+ T cell-mediated immunity. *J. Exp. Med.* 168:2193-2206.

Azukizawa, H., H. Kosaka, S. Sano, W.R. Heath, I. Takahashi, X.H. Gao, Y. Sumikawa, M. Okabe, K. Yoshikawa, and S. Itami. 2003. Induction of T-cell-mediated skin disease specific for antigen transgenically expressed in keratinocytes. *Eur. J. Immunol.* 33:1879-1888.

Bagarazzi, M.L., J. Yan, M.P. Morrow, X. Shen, R.L. Parker, J.C. Lee, M. Giffear, P. Pankhong, A.S. Khan, K.E. Broderick, C. Knott, F. Lin, J.D. Boyer, R. Draghia-Akli, C.J. White, J.J. Kim, D.B. Weiner, and N.Y. Sardesai. 2012. Immunotherapy against HPV16/18 generates potent TH1 and cytotoxic cellular immune responses. *Sci. Transl. Med.* 4:155ra138.

Balkwill, F. 2003. Chemokine biology in cancer. *Semin. Immunol.* 15:49-55.

Balkwill, F. 2004. Cancer and the chemokine network. *Nat. Rev. Cancer* 4:540-550.

Balsitis, S., F. Dick, D. Lee, L. Farrell, R.K. Hyde, A.E. Griep, N. Dyson, and P.F. Lambert. 2005. Examination of the pRb-dependent and pRb-independent functions of E7 in vivo. *J. Virol.* 79:11392-11402.

Balsitis, S.J., J. Sage, S. Duensing, K. Munger, T. Jacks, and P.F. Lambert. 2003. Recapitulation of the effects of the human papillomavirus type 16 E7 oncogene on mouse epithelium by somatic Rb deletion and detection of pRb-independent effects of E7 in vivo. *Mol. Cell. Biol.* 23:9094-9103.

Bergot, A.S., N. Ford, G.R. Leggatt, J.W. Wells, I.H. Frazer, and M.A. Grimbaldeston. 2014. HPV16-E7 expression in squamous epithelium creates a local immune suppressive environment via CCL2- and CCL5- mediated recruitment of mast cells. *PLoS Pathog.* 10:e1004466.

Bermudez-Morales, V.H., L.X. Gutierrez, J.M. Alcocer-Gonzalez, A. Burguete, and V. Madrid-Marina. 2008. Correlation between IL-10 gene expression and HPV infection

in cervical cancer: a mechanism for immune response escape. *Cancer Invest.* 26:1037-1043.

Bernat, A., N. Avvakumov, J.S. Mymryk, and L. Banks. 2003. Interaction between the HPV E7 oncoprotein and the transcriptional coactivator p300. *Oncogene* 22:7871-7881.

Bjerke, J.R. 1982. Subpopulations of mononuclear cells in lesions of psoriasis, lichen planus and discoid lupus erythematosus studied using monoclonal antibodies. *Acta Derm. Venereol.* 62:477-483.

Black, A.P., M.R. Ardern-Jones, V. Kasprowicz, P. Bowness, L. Jones, A.S. Bailey, and G.S. Ogg. 2007. Human keratinocyte induction of rapid effector function in antigen-specific memory CD4+ and CD8+ T cells. *Eur. J. Immunol.* 37:1485-1493.

Blauvelt, A., H. Asada, V. KlausKovtun, D.J. Altman, D.R. Lucey, and S.I. Katz. 1996. Interleukin-15 mRNA is expressed by human keratinocytes, Langerhans cells, and blood-derived dendritic cells and is downregulated by ultraviolet B radiation. *J. Invest. Dermatol.* 106:1047-1052.

Bourke, C.D., C.T. Prendergast, D.E. Sanin, T.E. Oulton, R.J. Hall, and A.P. Mountford. 2015. Epidermal keratinocytes initiate wound healing and pro-inflammatory immune responses following percutaneous schistosome infection. *Int. J. Parasitol.* 45:215-224.

Bouvard, V., A. Storey, D. Pim, and L. Banks. 1994. Characterization of the human papillomavirus E2 protein: evidence of trans-activation and trans-repression in cervical keratinocytes. *EMBO J.* 13:5451-5459.

Brandt, D., M. Sergon, S. Abraham, K. Mabert, and C.M. Hedrich. 2017. TCR+CD3+CD4-CD8- effector T cells in psoriasis. *Clin. Immunol.* 181:51-59.

Broom, J.K., A.M. Lew, H. Azukizawa, T.J. Kenna, G.R. Leggatt, and I.H. Frazer. 2010. Antigen-specific CD4 cells assist CD8 T-effector cells in eliminating keratinocytes. *J. Invest. Dermatol.* 130:1581-1589.

Brown, C.A., J. Bogers, S. Sahebali, C.E. Depuydt, F. De Prins, and D.P. Malinowski. 2012. Role of protein biomarkers in the detection of high-grade disease in cervical cancer screening programs. *J Oncol* 2012:289315.

Campanella, G.S., B.D. Medoff, L.A. Manice, R.A. Colvin, and A.D. Luster. 2008. Development of a novel chemokine-mediated in vivo T cell recruitment assay. *J. Immunol. Methods* 331:127-139.

Carrero, Y., D. Callejas, F. Alana, C. Silva, R. Mindiola, and J. Mosquera. 2009. Increased vascular endothelial growth factor expression, CD3-positive cell infiltration, and oxidative stress in premalignant lesions of the cervix. *Cancer* 115:3680-3688.

Centers for Disease Control and Prevention, U. 2017. Genital HPV infection-CDC Fact Sheet. *National Center for Immunization and Respiratory Diseases*

Chakraborty, R., J. Chandra, S. Cui, L. Tolley, M.A. Cooper, M. Kendall, and I.H. Frazer. 2018. CD8(+) lineage dendritic cells determine adaptive immune responses to inflammasome activation upon sterile skin injury. *Exp. Dermatol.* 27:71-79.

Chandra, J., Y. Miao, N. Romoff, and I.H. Frazer. 2016. Epithelium Expressing the E7 Oncoprotein of HPV16 Attracts Immune-Modulatory Dendritic Cells to the Skin and Suppresses Their Antigen-Processing Capacity. *PLoS ONE* 11:e0152886.

Chow, M.T., and A.D. Luster. 2014. Chemokines in cancer. *Cancer Immunol Res* 2:1125-1131.

Choyce, A., M. Yong, S. Narayan, S.R. Mattarollo, A. Liem, P.F. Lambert, I.H. Frazer, and G.R. Leggatt. 2013. Expression of a single, viral oncoprotein in skin epithelium is sufficient to recruit lymphocytes. *PLoS ONE* 8:e57798.

Cicchini, L., J.A. Westrich, T. Xu, D.W. Vermeer, J.N. Berger, E.T. Clambey, D. Lee, J.I. Song, P.F. Lambert, R.O. Greer, J.H. Lee, and D. Pyeon. 2016. Suppression of Antitumor Immune Responses by Human Papillomavirus through Epigenetic Downregulation of CXCL14. *MBio* 7:

Clark, W.H., Jr., D.E. Elder, D.t. Guerry, L.E. Braitman, B.J. Trock, D. Schultz, M. Synnestvedt, and A.C. Halpern. 1989. Model predicting survival in stage I melanoma based on tumor progression. *J. Natl. Cancer Inst.* 81:1893-1904.

Clemente, C.G., M.C. Mihm, Jr., R. Bufalino, S. Zurrida, P. Collini, and N. Cascinelli. 1996. Prognostic value of tumor infiltrating lymphocytes in the vertical growth phase of primary cutaneous melanoma. *Cancer* 77:1303-1310.

Cobrinik, D., S.F. Dowdy, P.W. Hinds, S. Mittnacht, and R.A. Weinberg. 1992. The retinoblastoma protein and the regulation of cell cycling. *Trends Biochem. Sci.* 17:312-315.

Corona Gutierrez, C.M., A. Tinoco, T. Navarro, M.L. Contreras, R.R. Cortes, P. Calzado, L. Reyes, R. Posternak, G. Morosoli, M.L. Verde, and R. Rosales. 2004. Therapeutic vaccination with MVA E2 can eliminate precancerous lesions (CIN 1, CIN 2, and CIN 3) associated with infection by oncogenic human papillomavirus. *Hum. Gene Ther.* 15:421-431.

Cortes-Malagon, E.M., J. Bonilla-Delgado, J. Diaz-Chavez, A. Hidalgo-Miranda, S. Romero-Cordoba, A. Uren, H. Celik, M. McCormick, J.A. Munguia-Moreno, E. Ibarra-Sierra, J. Escobar-Herrera, P.F. Lambert, D. Mendoza-Villanueva, R.M. Bermudez-Cruz, and P. Gariglio. 2013. Gene expression profile regulated by the HPV16 E7 oncoprotein and estradiol in cervical tissue. *Virology* 447:155-165.

Curiel, T.J., G. Coukos, L. Zou, X. Alvarez, P. Cheng, P. Mottram, M. Evdemon-Hogan, J.R. Conejo-Garcia, L. Zhang, M. Burow, Y. Zhu, S. Wei, I. Kryczek, B. Daniel, A. Gordon, L. Myers, A. Lackner, M.L. Disis, K.L. Knutson, L. Chen, and W. Zou. 2004. Specific recruitment of regulatory T cells in ovarian carcinoma fosters immune privilege and predicts reduced survival. *Nat. Med.* 10:942-949.

Daayana, S., E. Elkord, U. Winters, M. Pawlita, R. Roden, P.L. Stern, and H.C. Kitchener. 2010. Phase II trial of imiquimod and HPV therapeutic vaccination in patients with vulval intraepithelial neoplasia. *Br. J. Cancer* 102:1129-1136.

Daniel, D., N. Meyer-Morse, E.K. Bergsland, K. Dehne, L.M. Coussens, and D. Hanahan. 2003. Immune enhancement of skin carcinogenesis by CD4+ T cells. *J. Exp. Med.* 197:1017-1028.

de Visser, K.E., L.V. Korets, and L.M. Coussens. 2005. De novo carcinogenesis promoted by chronic inflammation is B lymphocyte dependent. *Cancer Cell* 7:411-423.

Devalaraja, R.M., L.B. Nanney, J. Du, Q. Qian, Y. Yu, M.N. Devalaraja, and A. Richmond. 2000. Delayed wound healing in CXCR2 knockout mice. *J. Invest. Dermatol.* 115:234-244.

Dhodapkar, M.V., R.M. Steinman, J. Krasovsky, C. Munz, and N. Bhardwaj. 2001. Antigen-specific inhibition of effector T cell function in humans after injection of immature dendritic cells. *J. Exp. Med.* 193:233-238.

Dick, F.A., E. Sailhamer, and N.J. Dyson. 2000. Mutagenesis of the pRB pocket reveals that cell cycle arrest functions are separable from binding to viral oncoproteins. *Mol Cell Biol* 20:3715-3727.

Durst, M., L. Gissmann, H. Ikenberg, and H. zur Hausen. 1983. A papillomavirus DNA from a cervical carcinoma and its prevalence in cancer biopsy samples from different geographic regions. *Proc. Natl. Acad. Sci. U. S. A.* 80:3812-3815.

Einstein, M.H., A.S. Kadish, R.D. Burk, M.Y. Kim, S. Wadler, H. Streicher, G.L. Goldberg, and C.D. Runowicz. 2007. Heat shock fusion protein-based immunotherapy for treatment of cervical intraepithelial neoplasia III. *Gynecol. Oncol.* 106:453-460.

Fera, D., D.C. Schultz, S. Hodawadekar, M. Reichman, P.S. Donover, J. Melvin, S. Troutman, J.L. Kissil, D.M. Huryn, and R. Marmorstein. 2012. Identification and characterization of small molecule antagonists of pRb inactivation by viral oncoproteins. *Chem. Biol.* 19:518-528.

Flier, J., D.M. Boorsma, P.J. van Beek, C. Nieboer, T.J. Stoof, R. Willemze, and C.P. Tensen. 2001. Differential expression of CXCR3 targeting chemokines CXCL10, CXCL9, and CXCL11 in different types of skin inflammation. *J. Pathol.* 194:398-405.

Foguel, D., J.L. Silva, and G. de Prat-Gay. 1998. Characterization of a partially folded monomer of the DNA-binding domain of human papillomavirus E2 protein obtained at high pressure. *J. Biol. Chem.* 273:9050-9057.

Frazer, I.H. 2004. Prevention of cervical cancer through papillomavirus vaccination. *Nat. Rev. Immunol.* 4:46-54.

Frazer, I.H., R. De Kluyver, G.R. Leggatt, H.Y. Guo, L. Dunn, O. White, C. Harris, A. Liem, and P. Lambert. 2001. Tolerance or immunity to a tumor antigen expressed in somatic cells can be determined by systemic proinflammatory signals at the time of first antigen exposure. *J. Immunol.* 167:6180-6187.

Frigerio, S., T. Junt, B. Lu, C. Gerard, U. Zumsteg, G.A. Hollander, and L. Piali. 2002. Beta cells are responsible for CXCR3-mediated T-cell infiltration in insulitis. *Nat. Med.* 8:1414-1420.

Fujisawa, H., S. Kondo, B.H. Wang, G.M. Shivji, and D.N. Sauder. 1997. The expression and modulation of IFN-alpha and IFN-beta in human keratinocytes. *J. Interferon Cytokine Res.* 17:721-725.

Garcia-Diaz, A., D.S. Shin, B.H. Moreno, J. Saco, H. Escuin-Ordinas, G.A. Rodriguez, J.M. Zaretsky, L. Sun, W. Hugo, X. Wang, G. Parisi, C.P. Saus, D.Y. Torrejon, T.G. Graeber, B. Comin-Anduix, S. Hu-Lieskovan, R. Damoiseaux, R.S. Lo, and A. Ribas. 2017. Interferon Receptor Signaling Pathways Regulating PD-L1 and PD-L2 Expression. *Cell Rep* 19:1189-1201.

Garcia-Hernandez, E., J.L. Gonzalez-Sanchez, A. Andrade-Manzano, M.L. Contreras, S. Padilla, C.C. Guzman, R. Jimenez, L. Reyes, G. Morosoli, M.L. Verde, and R. Rosales. 2006. Regression of papilloma high-grade lesions (CIN 2 and CIN 3) is stimulated by therapeutic vaccination with MVA E2 recombinant vaccine. *Cancer Gene Ther.* 13:592-597.

Gawkrodger, D.J., M.M. Carr, E. McVittie, K. Guy, and J.A. Hunter. 1987. Keratinocyte expression of MHC class II antigens in allergic sensitization and challenge reactions and in irritant contact dermatitis. *J. Invest. Dermatol.* 88:11-16.

Gillison, M.L., L. Alemany, P.J. Snijders, A. Chaturvedi, B.M. Steinberg, S. Schwartz, and X. Castellsague. 2012. Human papillomavirus and diseases of the upper airway: head and neck cancer and respiratory papillomatosis. *Vaccine* 30 Suppl 5:F34-54.

Gillison, M.L., X. Castellsague, A. Chaturvedi, M.T. Goodman, P. Snijders, M. Tommasino, M. Arbyn, and S. Franceschi. 2014. Eurogin Roadmap: comparative epidemiology of HPV infection and associated cancers of the head and neck and cervix. *Int. J. Cancer* 134:497-507.

Gillitzer, R., and M. Goebeler. 2001. Chemokines in cutaneous wound healing. *J. Leukoc. Biol.* 69:513-521.

Godfrey, D.I., and M. Kronenberg. 2004. Going both ways: immune regulation via CD1d-dependent NKT cells. *J. Clin. Invest.* 114:1379-1388.

Godfrey, D.I., H.R. MacDonald, M. Kronenberg, M.J. Smyth, and L. Van Kaer. 2004. NKT cells: what's in a name? *Nat. Rev. Immunol.* 4:231-237.

Gosmann, C., I.H. Frazer, S.R. Mattarollo, and A. Blumenthal. 2014a. IL-18, but not IL-12, induces production of IFN-gamma in the immunosuppressive environment of HPV16 E7 transgenic hyperplastic skin. *J. Invest. Dermatol.* 134:2562-2569.

Gosmann, C., S.R. Mattarollo, J.A. Bridge, I.H. Frazer, and A. Blumenthal. 2014b. IL-17 suppresses immune effector functions in human papillomavirus-associated epithelial hyperplasia. *J. Immunol.* 193:2248-2257.

Gould, D.S., and H. Auchincloss, Jr. 1999. Direct and indirect recognition: the role of MHC antigens in graft rejection. *Immunol. Today* 20:77-82.

Grewe, M., K. Gyufko, and J. Krutmann. 1995. Interleukin-10 Production by Cultured Human Keratinocytes - Regulation by Ultraviolet-B and Ultraviolet A1 Radiation. *J. Invest. Dermatol.* 104:3-6.

Groom, J.R., and A.D. Luster. 2011. CXCR3 ligands: redundant, collaborative and antagonistic functions. *Immunol. Cell Biol.* 89:207-215.

Hadis, U., G.R. Leggatt, R. Thomas, I.H. Frazer, and E.M. Kovacs. 2010. IL-1 signalling determines the fate of skin grafts expressing non-self protein in keratinocytes. *Exp. Dermatol.* 19:723-729.

Hallez, S., P. Simon, F. Maudoux, J. Doyen, J.C. Noel, A. Beliard, X. Capelle, F. Buxant, I. Fayt, A.C. Lagrost, P. Hubert, C. Gerday, A. Burny, J. Boniver, J.M. Foidart, P. Delvenne, and N. Jacobs. 2004. Phase I/II trial of immunogenicity of a human papillomavirus (HPV) type 16 E7 protein-based vaccine in women with oncogenic HPV-positive cervical intraepithelial neoplasia. *Cancer Immunol Immunother* 53:642-650.

Harper, E.G., C. Guo, H. Rizzo, J.V. Lillis, S.E. Kurtz, I. Skorcheva, D. Purdy, E. Fitch, M. Iordanov, and A. Blauvelt. 2009. Th17 cytokines stimulate CCL20 expression in keratinocytes in vitro and in vivo: implications for psoriasis pathogenesis. *J. Invest. Dermatol.* 129:2175-2183.

Hasan, U.A., C. Zannetti, P. Parroche, N. Goutagny, M. Malfroy, G. Roblot, C. Carreira, I. Hussain, M. Muller, J. Taylor-Papadimitriou, D. Picard, B.S. Sylla, G. Trinchieri, R. Medzhitov, and M. Tommasino. 2013. The human papillomavirus type 16 E7 oncoprotein induces a transcriptional repressor complex on the Toll-like receptor 9 promoter. *J. Exp. Med.* 210:1369-1387.

Heath, W.R., and F.R. Carbone. 2009. Dendritic cell subsets in primary and secondary T cell responses at body surfaces. *Nat. Immunol.* 10:1237-1244.

Hemmi, H., M. Yoshino, H. Yamazaki, M. Naito, T. Iyoda, Y. Omatsu, S. Shimoyama, J.J. Letterio, T. Nakabayashi, H. Tagaya, T. Yamane, M. Ogawa, S. Nishikawa, K. Ryoke, K. Inaba, S. Hayashi, and T. Kunisada. 2001. Skin antigens in the steady state are trafficked to regional lymph nodes by transforming growth factor-beta1-dependent cells. *Int. Immunol.* 13:695-704.

Herber, R., A. Liem, H. Pitot, and P.F. Lambert. 1996. Squamous epithelial hyperplasia and carcinoma in mice transgenic for the human papillomavirus type 16 E7 oncogene. *J. Virol.* 70:1873-1881.

Heufler, C., G. Topar, A. Grasseger, U. Stanzl, F. Koch, N. Romani, A.E. Namen, and G. Schuler. 1993. Interleukin-7 Is Produced by Murine and Human Keratinocytes. *J. Exp. Med.* 178:1109-1114.

Howie, S.E.M., R.D. Aldridge, E. McVittie, R.J. Forsey, C. Sands, and J.A.A. Hunter. 1996. Epidermal keratinocyte production of interferon-gamma immunoreactive protein and mRNA is an early event in allergic contact dermatitis. *J. Invest. Dermatol.* 106:1218-1223.

Huang da, W., B.T. Sherman, and R.A. Lempicki. 2009. Systematic and integrative analysis of large gene lists using DAVID bioinformatics resources. *Nat. Protoc.* 4:44-57.

Huibregtse, J.M., M. Scheffner, and P.M. Howley. 1993. Cloning and expression of the cDNA for E6-AP, a protein that mediates the interaction of the human papillomavirus E6 oncoprotein with p53. *Mol. Cell. Biol.* 13:775-784.

Isaac, C.E., S.M. Francis, A.L. Martens, L.M. Julian, L.A. Seifried, N. Erdmann, U.K. Binne, L. Harrington, P. Sicinski, N.G. Berube, N.J. Dyson, and F.A. Dick. 2006. The retinoblastoma protein regulates pericentric heterochromatin. *Mol. Cell. Biol.* 26:3659-3671.

Ishii, T., T. Ishida, A. Utsunomiya, A. Inagaki, H. Yano, H. Komatsu, S. Iida, K. Imada, T. Uchiyama, S. Akinaga, K. Shitara, and R. Ueda. 2010. Defucosylated humanized

anti-CCR4 monoclonal antibody KW-0761 as a novel immunotherapeutic agent for adult T-cell leukemia/lymphoma. *Clin. Cancer Res.* 16:1520-1531.

Jacks, T., A. Fazeli, E.M. Schmitt, R.T. Bronson, M.A. Goodell, and R.A. Weinberg. 1992. Effects of an Rb mutation in the mouse. *Nature* 359:295-300.

Jazayeri, S.D., P.T. Kuo, G.R. Leggatt, and I.H. Frazer. 2017. HPV16-E7-Specific Activated CD8 T Cells in E7 Transgenic Skin and Skin Grafts. *Front Immunol* 8:524.

Karin, N., G. Wildbaum, and M. Thelen. 2015. Biased signaling pathways via CXCR3 control the development and function of CD4+ T cell subsets. *J. Leukoc. Biol.*

Kashiwagi, M., J. Hosoi, J.F. Lai, J. Brissette, S.F. Ziegler, B.A. Morgan, and K. Georgopoulos. 2017. Direct control of regulatory T cells by keratinocytes. *Nat. Immunol.* 18:334-343.

Kenter, G.G., M.J. Welters, A.R. Valentijn, M.J. Lowik, D.M. Berends-van der Meer, A.P. Vloon, F. Essahsah, L.M. Fathers, R. Offringa, J.W. Drijfhout, A.R. Wafelman, J. Oostendorp, G.J. Fleuren, S.H. van der Burg, and C.J. Melief. 2009. Vaccination against HPV-16 oncoproteins for vulvar intraepithelial neoplasia. *N. Engl. J. Med.* 361:1838-1847.

Khan, I.A., J.A. MacLean, F.S. Lee, L. Casciotti, E. DeHaan, J.D. Schwartzman, and A.D. Luster. 2000. IP-10 is critical for effector T cell trafficking and host survival in Toxoplasma gondii infection. *Immunity* 12:483-494.

Kim, B.S., F. Miyagawa, Y.H. Cho, C.L. Bennett, B.E. Clausen, and S.I. Katz. 2009. Keratinocytes function as accessory cells for presentation of endogenous antigen expressed in the epidermis. *J. Invest. Dermatol.* 129:2805-2817.

Kobayashi, A., V. Weinberg, T. Darragh, and K. Smith-McCune. 2008. Evolving immunosuppressive microenvironment during human cervical carcinogenesis. *Mucosal Immunol.* 1:412-420.

Koch, A.E. 2005. Chemokines and their receptors in rheumatoid arthritis: future targets? *Arthritis Rheum.* 52:710-721.

Koch, M.A., G. Tucker-Heard, N.R. Perdue, J.R. Killebrew, K.B. Urdahl, and D.J. Campbell. 2009. The transcription factor T-bet controls regulatory T cell homeostasis and function during type 1 inflammation. *Nat. Immunol.* 10:595-602.

Kock, A., T. Schwarz, R. Kirnbauer, A. Urbanski, P. Perry, J.C. Ansel, and T.A. Luger. 1990. Human keratinocytes are a source for tumor necrosis factor alpha: evidence for synthesis and release upon stimulation with endotoxin or ultraviolet light. *J. Exp. Med.* 172:1609-1614.

Kuo, P., Z.K. Tuong, S.M. Teoh, I.H. Frazer, S. Mattarollo, and G.R. Leggatt. 2017. HPV16E7 Induced Hyperplasia Promotes CXCL9/10 Expression and Induces CXCR3(+) T cell Migration to Skin. *J. Invest. Dermatol.*

Kupper, T.S., and R.C. Fuhlbrigge. 2004. Immune surveillance in the skin: mechanisms and clinical consequences. *Nat. Rev. Immunol.* 4:211-222.

Kupper, T.S., and R.W. Groves. 1995. The interleukin-1 axis and cutaneous inflammation. *J. Invest. Dermatol.* 105:62S-66S.

Lampert, I.A., G. Janossy, A.J. Suitters, M. Bofill, S. Palmer, E. Gordon-Smith, H.G. Prentice, and J.A. Thomas. 1982. Immunological analysis of the skin in graft versus host disease. *Clin. Exp. Immunol.* 50:123-131.

Larsen, C.P., R.M. Steinman, M. Witmer-Pack, D.F. Hankins, P.J. Morris, and J.M. Austyn. 1990. Migration and maturation of Langerhans cells in skin transplants and explants. *J. Exp. Med.* 172:1483-1493.

Lee, J.H., S.M. Yi, M.E. Anderson, K.L. Berger, M.J. Welsh, A.J. Klingelhutz, and M.A. Ozbun. 2004. Propagation of infectious human papillomavirus type 16 by using an adenovirus and Cre/LoxP mechanism. *Proc. Natl. Acad. Sci. U. S. A.* 101:2094-2099.

Leggatt, G.R., L.A. Dunn, R.L. De Kluyver, T. Stewart, and I.H. Frazer. 2002. Interferon-gamma enhances cytotoxic T lymphocyte recognition of endogenous peptide in

keratinocytes without lowering the requirement for surface peptide. *Immunol. Cell Biol.* 80:415-424.

Leo, P.J., M.M. Madeleine, S. Wang, S.M. Schwartz, F. Newell, U. Pettersson-Kymmer, K. Hemminki, G. Hallmans, S. Tiews, W. Steinberg, J.S. Rader, F. Castro, M. Safaeian, E.L. Franco, F. Coutlee, C. Ohlsson, A. Cortes, M. Marshall, P. Mukhopadhyay, K. Cremin, L.G. Johnson, C.L. Trimble, S. Garland, S.N. Tabrizi, N. Wentzensen, F. Sitas, J. Little, M. Cruickshank, I.H. Frazer, A. Hildesheim, and M.A. Brown. 2017. Defining the genetic susceptibility to cervical neoplasia-A genome-wide association study. *PLoS Genet* 13:e1006866.

Levin, C., O. Bonduelle, C. Nuttens, C. Primard, B. Verrier, A. Boissonnas, and B. Combadiere. 2017. Critical Role for Skin-Derived Migratory DCs and Langerhans Cells in TFH and GC Responses after Intradermal Immunization. *J. Invest. Dermatol.* 137:1905-1913.

Li, H., X. Ou, J.H. Xiong, and T.X. Wang. 2006. HPV16E7 mediates HADC chromatin repression and downregulation of MHC class I genes in HPV16 tumorigenic cells through interaction with an MHC class I promoter. *Biochem. Biophys. Res. Commun.* 349:1315-1321.

Li, H., T.L. Zhan, C. Li, M.G. Liu, and Q.K. Wang. 2009. Repression of MHC class I transcription by HPV16E7 through interaction with a putative RXR beta motif and NF-kappa B cytoplasmic sequestration. *Biochem. Biophys. Res. Commun.* 388:383-388.

Lord, G.M., R.M. Rao, H. Choe, B.M. Sullivan, A.H. Lichtman, F.W. Luscinskas, and L.H. Glimcher. 2005. T-bet is required for optimal proinflammatory CD4+ T-cell trafficking. *Blood* 106:3432-3439.

Luster, A.D. 1998. Chemokines--chemotactic cytokines that mediate inflammation. *N. Engl. J. Med.* 338:436-445.

Maarsingh, H., J. Zaagsma, and H. Meurs. 2009. Arginase: a key enzyme in the pathophysiology of allergic asthma opening novel therapeutic perspectives. *Br. J. Pharmacol.* 158:652-664.

Malcolm, K.M., J. Gill, G.R. Leggatt, R. Boyd, P. Lambert, and I.H. Frazer. 2003. Expression of the HPV16E7 oncoprotein by thymic epithelium is accompanied by disrupted T cell maturation and a failure of the thymus to involute with age. *Clin. Dev. Immunol.* 10:91-103.

Mantovani, A., P. Allavena, S. Sozzani, A. Vecchi, M. Locati, and A. Sica. 2004. Chemokines in the recruitment and shaping of the leukocyte infiltrate of tumors. *Semin. Cancer Biol.* 14:155-160.

Martin-Fontecha, A., L.L. Thomsen, S. Brett, C. Gerard, M. Lipp, A. Lanzavecchia, and F. Sallusto. 2004. Induced recruitment of NK cells to lymph nodes provides IFN-gamma for T(H)1 priming. *Nat. Immunol.* 5:1260-1265.

Martinez, F.O., A. Sica, A. Mantovani, and M. Locati. 2008. Macrophage activation and polarization. *Front. Biosci.* 13:453-461.

Matsumoto, K., G.R. Leggatt, J. Zhong, X. Liu, R.L. de Kluyver, T. Peters, G.J. Fernando, A. Liem, P.F. Lambert, and I.H. Frazer. 2004. Impaired antigen presentation and effectiveness of combined active/passive immunotherapy for epithelial tumors. *J. Natl. Cancer Inst.* 96:1611-1619.

Mattarollo, S.R., A. Rahimpour, A. Choyce, D.I. Godfrey, G.R. Leggatt, and I.H. Frazer. 2010a. Invariant NKT cells in hyperplastic skin induce a local immune suppressive environment by IFN-gamma production. *J. Immunol.* 184:1242-1250.

Mattarollo, S.R., M. Yong, C. Gosmann, A. Choyce, D. Chan, G.R. Leggatt, and I.H. Frazer. 2011. NKT cells inhibit antigen-specific effector CD8 T cell induction to skin viral proteins. *J. Immunol.* 187:1601-1608.

Mattarollo, S.R., M. Yong, L. Tan, I.H. Frazer, and G.R. Leggatt. 2010b. Secretion of IFN-gamma but not IL-17 by CD1d-restricted NKT cells enhances rejection of skin grafts expressing epithelial cell-derived antigen. *J. Immunol.* 184:5663-5669.

Mauldin, I.S., N.A. Wages, A.M. Stowman, E. Wang, W.C. Olson, D.H. Deacon, K.T. Smith, N. Galeassi, J.E. Teague, M.E. Smolkin, K.A. Chianese-Bullock, R.A. Clark, G.R. Petroni, F.M. Marincola, D.W. Mullins, and C.L. Slingluff, Jr. 2016. Topical treatment of melanoma metastases with imiquimod, plus administration of a cancer vaccine, promotes immune signatures in the metastases. *Cancer Immunol. Immunother.* 65:1201-1212.

McGuire, H.M., A. Vogelzang, C.S. Ma, W.E. Hughes, P.A. Silveira, S.G. Tangye, D. Christ, D. Fulcher, M. Falcone, and C. King. 2011. A subset of interleukin-21+ chemokine receptor CCR9+ T helper cells target accessory organs of the digestive system in autoimmunity. *Immunity* 34:602-615.

Mckay, I.A., and I.M. Leigh. 1991. Epidermal Cytokines and Their Roles in Cutaneous Wound-Healing. *Br. J. Dermatol.* 124:513-518.

Medoff, B.D., J.C. Wain, E. Seung, R. Jackobek, T.K. Means, L.C. Ginns, J.M. Farber, and A.D. Luster. 2006. CXCR3 and its ligands in a murine model of obliterative bronchiolitis: regulation and function. *J. Immunol.* 176:7087-7095.

Meiron, M., Y. Zohar, R. Anunu, G. Wildbaum, and N. Karin. 2008. CXCL12 (SDF-1alpha) suppresses ongoing experimental autoimmune encephalomyelitis by selecting antigen-specific regulatory T cells. *J. Exp. Med.* 205:2643-2655.

Mittal, D., A.J. Kassianos, L.S. Tran, A.S. Bergot, C. Gosmann, J. Hofmann, A. Blumenthal, G.R. Leggatt, and I.H. Frazer. 2013. Indoleamine 2,3-dioxygenase activity contributes to local immune suppression in the skin expressing human papillomavirus oncoprotein e7. *J. Invest. Dermatol.* 133:2686-2694.

Moody, C.A., and L.A. Laimins. 2010. Human papillomavirus oncoproteins: pathways to transformation. *Nat. Rev. Cancer* 10:550-560.

Morrow, M.P., K.A. Kraynyak, A.J. Sylvester, M. Dallas, D. Knoblock, J.D. Boyer, J. Yan, R. Vang, A.S. Khan, L. Humeau, N.Y. Sardesai, J.J. Kim, S. Plotkin, D.B. Weiner, C.L. Trimble, and M.L. Bagarazzi. 2018. Clinical and Immunologic Biomarkers for Histologic Regression of High-Grade Cervical Dysplasia and Clearance of HPV16 and HPV18 after Immunotherapy. *Clin. Cancer Res.* 24:276-294.

Morrow, M.P., K.A. Kraynyak, A.J. Sylvester, X. Shen, D. Amante, L. Sakata, L. Parker, J. Yan, J. Boyer, C. Roh, L. Humeau, A.S. Khan, K. Broderick, K. Marcozzi-Pierce, M. Giffear, J. Lee, C.L. Trimble, J.J. Kim, N.Y. Sardesai, D.B. Weiner, and M.L. Bagarazzi. 2016. Augmentation of cellular and humoral immune responses to HPV16 and HPV18 E6 and E7 antigens by VGX-3100. *Mol Ther Oncolytics* 3:16025.

Morrow, M.P., J. Yan, and N.Y. Sardesai. 2013. Human papillomavirus therapeutic vaccines: targeting viral antigens as immunotherapy for precancerous disease and cancer. *Expert Rev. Vaccines* 12:271-283.

Mulligan, A.M., D. Pinnaduwage, S. Tchatchou, S.B. Bull, and I.L. Andrulis. 2016. Validation of Intratumoral T-bet+ Lymphoid Cells as Predictors of Disease-Free Survival in Breast Cancer. *Cancer Immunol Res* 4:41-48.

Munger, K., M. Scheffner, J.M. Huibregtse, and P.M. Howley. 1992. Interactions of HPV E6 and E7 oncoproteins with tumour suppressor gene products. *Cancer Surv.* 12:197-217.

Muniz-Medina, V.M., S. Jones, J.M. Maglich, C. Galardi, R.E. Hollingsworth, W.M. Kazmierski, R.G. Ferris, M.P. Edelstein, K.E. Chiswell, and T.P. Kenakin. 2009. The relative activity of "function sparing" HIV-1 entry inhibitors on viral entry and CCR5 internalization: is allosteric functional selectivity a valuable therapeutic property? *Mol. Pharmacol.* 75:490-501.

Nakajima, C., T. Mukai, N. Yamaguchi, Y. Morimoto, W.R. Park, M. Iwasaki, P. Gao, S. Ono, H. Fujiwara, and T. Hamaoka. 2002. Induction of the chemokine receptor CXCR3 on TCR-stimulated T cells: dependence on the release from persistent TCR-triggering and requirement for IFN-gamma stimulation. *Eur. J. Immunol.* 32:1792-1801.

Narayan, S., A. Choyce, R. Linedale, N.A. Saunders, A. Dahler, E. Chan, G.J. Fernando, I.H. Frazer, and G.R. Leggatt. 2009. Epithelial expression of human papillomavirus type 16 E7 protein results in peripheral CD8 T-cell suppression mediated by CD4+CD25+ T cells. *Eur. J. Immunol.* 39:481-490.

Natale, C., T. Giannini, A. Lucchese, and D. Kanduc. 2000. Computer-assisted analysis of molecular mimicry between human papillomavirus 16 E7 oncoprotein and human protein sequences. *Immunol. Cell Biol.* 78:580-585.

Nedoszytko, B., M. Sokolowska-Wojdylo, K. Ruckemann-Dziurdzinska, J. Roszkiewicz, and R.J. Nowicki. 2014. Chemokines and cytokines network in the pathogenesis of the inflammatory skin diseases: atopic dermatitis, psoriasis and skin mastocytosis. *Postepy Dermatol Alergol* 31:84-91.

Nevins, J.R. 1992. E2F: a link between the Rb tumor suppressor protein and viral oncoproteins. *Science* 258:424-429.

Oxholm, A., M. Diamant, P. Oxholm, and K. Bendtzen. 1991. Interleukin-6 and Tumor-Necrosis-Factor-Alpha Are Expressed by Keratinocytes but Not by Langerhans Cells. *APMIS* 99:58-64.

Pacini, L., C. Savini, R. Ghittoni, D. Saidj, J. Lamartine, U.A. Hasan, R. Accardi, and M. Tommasino. 2015. Downregulation of Toll-Like Receptor 9 Expression by Beta Human Papillomavirus 38 and Implications for Cell Cycle Control. *J. Virol.* 89:11396-11405.

Park, J.S., E.J. Kim, H.J. Kwon, E.S. Hwang, S.E. Namkoong, and S.J. Um. 2000. Inactivation of interferon regulatory factor-1 tumor suppressor protein by HPV E7 oncoprotein. Implication for the E7-mediated immune evasion mechanism in cervical carcinogenesis. *J. Biol. Chem.* 275:6764-6769.

Poulter, L.W., G.J. Seymour, O. Duke, G. Janossy, and G. Panayi. 1982. Immunohistological analysis of delayed-type hypersensitivity in man. *Cell. Immunol.* 74:358-369.

Prathapam, T., C. Kuhne, and L. Banks. 2001. The HPV-16 E7 oncoprotein binds Skip and suppresses its transcriptional activity. *Oncogene* 20:7677-7685.

Proudfoot, A.E. 2002. Chemokine receptors: multifaceted therapeutic targets. *Nat. Rev. Immunol.* 2:106-115.

Qin, S., J.B. Rottman, P. Myers, N. Kassam, M. Weinblatt, M. Loetscher, A.E. Koch, B. Moser, and C.R. Mackay. 1998. The chemokine receptors CXCR3 and CCR5 mark subsets of T cells associated with certain inflammatory reactions. *J. Clin. Invest.* 101:746-754.

Reboldi, A., C. Coisne, D. Baumjohann, F. Benvenuto, D. Bottinelli, S. Lira, A. Uccelli, A. Lanzavecchia, B. Engelhardt, and F. Sallusto. 2009. C-C chemokine receptor 6-regulated entry of TH-17 cells into the CNS through the choroid plexus is required for the initiation of EAE. *Nat. Immunol.* 10:514-523.

Reiter, E., S. Ahn, A.K. Shukla, and R.J. Lefkowitz. 2012. Molecular mechanism of beta-arrestin-biased agonism at seven-transmembrane receptors. *Annu. Rev. Pharmacol. Toxicol.* 52:179-197.

Richters, C.D., M.J. Hoekstra, J.S. du Pont, R.W. Kreis, and E.W. Kamperdijk. 2005. Immunology of skin transplantation. *Clin. Dermatol.* 23:338-342.

Richters, C.D., E. van Gelderop, J.S. du Pont, M.J. Hoekstra, R.W. Kreis, and E.W. Kamperdijk. 1999. Migration of dendritic cells to the draining lymph node after allogeneic or congeneic rat skin transplantation. *Transplantation* 67:828-832.

Roncarolo, M.G., M.K. Levings, and C. Traversari. 2001. Differentiation of T regulatory cells by immature dendritic cells. *J. Exp. Med.* 193:F5-9.

Ronco, L.V., A.Y. Karpova, M. Vidal, and P.M. Howley. 1998. Human papillomavirus 16 E6 oncoprotein binds to interferon regulatory factor-3 and inhibits its transcriptional activity. *Genes Dev.* 12:2061-2072.

Rosenblum, J.M., N. Shimoda, A.D. Schenk, H. Zhang, D.D. Kish, K. Keslar, J.M. Farber, and R.L. Fairchild. 2010. CXC chemokine ligand (CXCL) 9 and CXCL10 are antagonistic costimulation molecules during the priming of alloreactive T cell effectors. *J. Immunol.* 184:3450-3460.

Sallusto, F., D. Lenig, C.R. Mackay, and A. Lanzavecchia. 1998. Flexible programs of chemokine receptor expression on human polarized T helper 1 and 2 lymphocytes. *J. Exp. Med.* 187:875-883.

Salomon, I., N. Netzer, G. Wildbaum, S. Schif-Zuck, G. Maor, and N. Karin. 2002. Targeting the function of IFN-gamma-inducible protein 10 suppresses ongoing adjuvant arthritis. *J. Immunol.* 169:2685-2693.

Samama, P., S. Cotecchia, T. Costa, and R.J. Lefkowitz. 1993. A mutation-induced activated state of the beta 2-adrenergic receptor. Extending the ternary complex model. *J. Biol. Chem.* 268:4625-4636.

Satoh, M., S. Iida, and K. Shitara. 2006. Non-fucosylated therapeutic antibodies as next-generation therapeutic antibodies. *Expert Opin. Biol. Ther.* 6:1161-1173.

Sheets, E.E., R.G. Urban, C.P. Crum, M.L. Hedley, J.A. Politch, M.A. Gold, L.I. Muderspach, G.A. Cole, and P.A. Crowley-Nowick. 2003. Immunotherapy of human cervical high-grade cervical intraepithelial neoplasia with microparticle-delivered human papillomavirus 16 E7 plasmid DNA. *Am. J. Obstet. Gynecol.* 188:916-926.

Shehadeh, N., S. Pollack, G. Wildbaum, Y. Zohar, I. Shafat, R. Makhoul, E. Daod, F. Hakim, R. Perlman, and N. Karin. 2009. Selective autoantibody production against CCL3 is associated with human type 1 diabetes mellitus and serves as a novel biomarker for its diagnosis. *J. Immunol.* 182:8104-8109.

Shojaei, F., X. Wu, X. Qu, M. Kowanetz, L. Yu, M. Tan, Y.G. Meng, and N. Ferrara. 2009. G-CSF-initiated myeloid cell mobilization and angiogenesis mediate tumor refractoriness to anti-VEGF therapy in mouse models. *Proceedings of the National Academy of Sciences of the United States of America* 106:6742-6747.

Shojaei, F., X. Wu, C. Zhong, L. Yu, X.H. Liang, J. Yao, D. Blanchard, C. Bais, F.V. Peale, N. van Bruggen, C. Ho, J. Ross, M. Tan, R.A. Carano, Y.G. Meng, and N. Ferrara. 2007. Bv8 regulates myeloid-cell-dependent tumour angiogenesis. *Nature* 450:825-831.

Siegel, C.T., K. Schreiber, S.C. Meredith, G.B. Beck-Engeser, D.W. Lancki, C.A. Lazarski, Y.X. Fu, D.A. Rowley, and H. Schreiber. 2000. Enhanced growth of primary tumors in cancer-prone mice after immunization against the mutant region of an inherited oncoprotein. *J. Exp. Med.* 191:1945-1956.

Skinner, R.B., Jr. 2003. Imiquimod. *Dermatol. Clin.* 21:291-300.

Slebos, R.J., M.H. Lee, B.S. Plunkett, T.D. Kessis, B.O. Williams, T. Jacks, L. Hedrick, M.B. Kastan, and K.R. Cho. 1994. p53-dependent G1 arrest involves pRB-related proteins and is disrupted by the human papillomavirus 16 E7 oncoprotein. *Proc. Natl. Acad. Sci. U. S. A.* 91:5320-5324.

Smahel, M., D. Pokorna, J. Mackova, and J. Vlasak. 2004. Enhancement of immunogenicity of HPV16 E7 oncogene by fusion with E. coli beta-glucuronidase. *J. Gene Med.* 6:1092-1101.

Spranger, S., D. Dai, B. Horton, and T.F. Gajewski. 2017. Tumor-Residing Batf3 Dendritic Cells Are Required for Effector T Cell Trafficking and Adoptive T Cell Therapy. *Cancer Cell* 31:711-723 e714.

Stanley, M.A., M.R. Pett, and N. Coleman. 2007. HPV: from infection to cancer. *Biochem. Soc. Trans.* 35:1456-1460.

Stoermer, K.A., A. Burrack, L. Oko, S.A. Montgomery, L.B. Borst, R.G. Gill, and T.E. Morrison. 2012. Genetic ablation of arginase 1 in macrophages and neutrophils enhances clearance of an arthritogenic alphavirus. *J. Immunol.* 189:4047-4059.

Stoolman, L.M. 1989. Adhesion molecules controlling lymphocyte migration. *Cell* 56:907-910.

Stubenrauch, F., and L.A. Laimins. 1999. Human papillomavirus life cycle: active and latent phases. *Semin. Cancer Biol.* 9:379-386.

Subramanian, A., P. Tamayo, V.K. Mootha, S. Mukherjee, B.L. Ebert, M.A. Gillette, A. Paulovich, S.L. Pomeroy, T.R. Golub, E.S. Lander, and J.P. Mesirov. 2005. Gene set enrichment analysis: a knowledge-based approach for interpreting genome-wide expression profiles. *Proc. Natl. Acad. Sci. U. S. A.* 102:15545-15550.

Thapa, M., and D.J. Carr. 2008. Chemokines and Chemokine Receptors Critical to Host Resistance following Genital Herpes Simplex Virus Type 2 (HSV-2) Infection. *Open Immunol. J.* 1:33-41.

Thapa, M., R.S. Welner, R. Pelayo, and D.J. Carr. 2008. CXCL9 and CXCL10 expression are critical for control of genital herpes simplex virus type 2 infection through mobilization of HSV-specific CTL and NK cells to the nervous system. *J. Immunol.* 180:1098-1106.

Thomas, M., D. Pim, and L. Banks. 1999. The role of the E6-p53 interaction in the molecular pathogenesis of HPV. *Oncogene* 18:7690-7700.

Tikhonova, A.N., F. Van Laethem, K. Hanada, J. Lu, L.A. Pobezinsky, C. Hong, T.I. Guinter, S.K. Jeurling, G. Bernhardt, J.H. Park, J.C. Yang, P.D. Sun, and A. Singer. 2012. alphabeta T cell receptors that do not undergo major histocompatibility complex-specific thymic selection possess antibody-like recognition specificities. *Immunity* 36:79-91.

Tindle, R.W. 2002. Immune evasion in human papillomavirus-associated cervical cancer. *Nat. Rev. Cancer* 2:59-65.

Tran le, S., D. Mittal, S.R. Mattarollo, and I.H. Frazer. 2015. Interleukin-17A Promotes Arginase-1 Production and 2,4-Dinitrochlorobenzene-Induced Acute Hyperinflammation in Human Papillomavirus E7 Oncoprotein-Expressing Skin. *J. Innate Immun.* 7:392-404.

Tran, L.S., A.S. Bergot, S.R. Mattarollo, D. Mittal, and I.H. Frazer. 2014. Human Papillomavirus E7 Oncoprotein Transgenic Skin Develops an Enhanced Inflammatory Response to 2,4-Dinitrochlorobenzene by an Arginase-1-Dependent Mechanism. *J. Invest. Dermatol.*

Trimble, C.L., M.P. Morrow, K.A. Kraynyak, X. Shen, M. Dallas, J. Yan, L. Edwards, R.L. Parker, L. Denny, M. Giffear, A.S. Brown, K. Marcozzi-Pierce, D. Shah, A.M. Slager, A.J. Sylvester, A. Khan, K.E. Broderick, R.J. Juba, T.A. Herring, J. Boyer, J. Lee, N.Y. Sardesai, D.B. Weiner, and M.L. Bagarazzi. 2015. Safety, efficacy, and immunogenicity of VGX-3100, a therapeutic synthetic DNA vaccine targeting human papillomavirus 16 and 18 E6 and E7 proteins for cervical intraepithelial neoplasia 2/3: a randomised, double-blind, placebo-controlled phase 2b trial. *Lancet* 386:2078-2088.

Tuong, Z.K., K. Noske, P. Kuo, A.A. Bashaw, S.M. Teoh, and I.H. Frazer. 2018. Murine HPV16 E7-expressing transgenic skin effectively emulates the cellular and molecular features of human high-grade squamous intraepithelial lesions *Papillomavirus Research* 5:6-20.

Tuzun, Y., M. Antonov, N. Dolar, and R. Wolf. 2007. Keratinocyte cytokine and chemokine receptors. *Dermatol. Clin.* 25:467-476, vii.

Ustav, M., E. Ustav, P. Szymanski, and A. Stenlund. 1991. Identification of the origin of replication of bovine papillomavirus and characterization of the viral origin recognition factor E1. *EMBO J.* 10:4321-4329.

Van Doorslaer, K., L.L. Reimers, Y.Y. Studentsov, M.H. Einstein, and R.D. Burk. 2010. Serological response to an HPV16 E7 based therapeutic vaccine in women with high-grade cervical dysplasia. *Gynecol. Oncol.* 116:208-212.

Van Laethem, F., S.D. Sarafova, J.H. Park, X. Tai, L. Pobezinsky, T.I. Guinter, S. Adoro, A. Adams, S.O. Sharrow, L. Feigenbaum, and A. Singer. 2007. Deletion of CD4 and CD8 coreceptors permits generation of alphabetaT cells that recognize antigens independently of the MHC. *Immunity* 27:735-750.

Villarroel, V.A., N. Okiyama, G. Tsuji, J.T. Linton, and S.I. Katz. 2014. CXCR3-mediated skin homing of autoreactive CD8 T cells is a key determinant in murine graft-versus-host disease. *J. Invest. Dermatol.* 134:1552-1560.

Wang, J., A. Sampath, P. Raychaudhuri, and S. Bagchi. 2001. Both Rb and E7 are regulated by the ubiquitin proteasome pathway in HPV-containing cervical tumor cells. *Oncogene* 20:4740-4749.

Ward, P.L., H.K. Koeppen, T. Hurteau, D.A. Rowley, and H. Schreiber. 1990. Major histocompatibility complex class I and unique antigen expression by murine tumors that escaped from CD8+ T-cell-dependent surveillance. *Cancer Res.* 50:3851-3858.

Watson, C., S. Jenkinson, W. Kazmierski, and T. Kenakin. 2005. The CCR5 receptor-based mechanism of action of 873140, a potent allosteric noncompetitive HIV entry inhibitor. *Mol. Pharmacol.* 67:1268-1282.

Welters, M.J., G.G. Kenter, S.J. Piersma, A.P. Vloon, M.J. Lowik, D.M. Berends-van der Meer, J.W. Drijfhout, A.R. Valentijn, A.R. Wafelman, J. Oostendorp, G.J. Fleuren, R. Offringa, C.J. Melief, and S.H. van der Burg. 2008. Induction of tumor-specific CD4+ and CD8+ T-cell immunity in cervical cancer patients by a human papillomavirus type 16 E6 and E7 long peptides vaccine. *Clin. Cancer Res.* 14:178-187.

Wildbaum, G., N. Netzer, and N. Karin. 2002. Plasmid DNA encoding IFN-gamma-inducible protein 10 redirects antigen-specific T cell polarization and suppresses experimental autoimmune encephalomyelitis. *J. Immunol.* 168:5885-5892.

Winkler, A.E., J.J. Brotman, M.E. Pittman, N.P. Judd, J.S. Lewis, Jr., R.D. Schreiber, and R. Uppaluri. 2011. CXCR3 enhances a T-cell-dependent epidermal proliferative response and promotes skin tumorigenesis. *Cancer Res.* 71:5707-5716.

Wood, A., and D. Armour. 2005. The discovery of the CCR5 receptor antagonist, UK-427,857, a new agent for the treatment of HIV infection and AIDS. *Prog. Med. Chem.* 43:239-271.

WORLD HEALTH ORGANIZATION International Agency for Research on Cancer Multicenter Cervical Cancer Study, G. 2007. Human Papillomaviruses. *IARC Monogr. Eval. Carcinog. Risks Hum.* 90:

Xie, J.H., N. Nomura, M. Lu, S.L. Chen, G.E. Koch, Y. Weng, R. Rosa, J. Di Salvo, J. Mudgett, L.B. Peterson, L.S. Wicker, and J.A. DeMartino. 2003. Antibody-mediated blockade of the CXCR3 chemokine receptor results in diminished recruitment of T helper 1 cells into sites of inflammation. *J. Leukoc. Biol.* 73:771-780.

Yamazaki, T., X.O. Yang, Y. Chung, A. Fukunaga, R. Nurieva, B. Pappu, N. Martin-Orozco, H.S. Kang, L. Ma, A.D. Panopoulos, S. Craig, S.S. Watowich, A.M. Jetten, Q. Tian, and C. Dong. 2008. CCR6 regulates the migration of inflammatory and regulatory T cells. *J. Immunol.* 181:8391-8401.

Yang, L., L.M. DeBusk, K. Fukuda, B. Fingleton, B. Green-Jarvis, Y. Shyr, L.M. Matrisian, D.P. Carbone, and P.C. Lin. 2004. Expansion of myeloid immune suppressor Gr+CD11b+ cells in tumor-bearing host directly promotes tumor angiogenesis. *Cancer Cell* 6:409-421.

Yates, C.C., D. Whaley, S. Hooda, P.A. Hebda, R.J. Bodnar, and A. Wells. 2009. Delayed reepithelialization and basement membrane regeneration after wounding in mice lacking CXCR3. *Wound Repair Regen.* 17:34-41.

Yellin, M., I. Paliienko, A. Balanescu, S. Ter-Vartanian, V. Tseluyko, L.A. Xu, X. Tao, P.M. Cardarelli, H. Leblanc, G. Nichol, C. Ancuta, R. Chirieac, and A. Luo. 2012. A phase II, randomized, double-blind, placebo-controlled study evaluating the efficacy and safety of MDX-1100, a fully human anti-CXCL10 monoclonal antibody, in combination with methotrexate in patients with rheumatoid arthritis. *Arthritis Rheum.* 64:1730-1739.

Yoon, S.H., S.O. Yun, J.Y. Park, H.Y. Won, E.K. Kim, H.J. Sohn, H.I. Cho, and T.G. Kim. 2009. Selective addition of CXCR3(+) CCR4(-) CD4(+) Th1 cells enhances generation of cytotoxic T cells by dendritic cells in vitro. *Exp. Mol. Med.* 41:161-170.

Zhang, L., J.R. Conejo-Garcia, D. Katsaros, P.A. Gimotty, M. Massobrio, G. Regnani, A. Makrigiannakis, H. Gray, K. Schlienger, M.N. Liebman, S.C. Rubin, and G. Coukos. 2003. Intratumoral T cells, recurrence, and survival in epithelial ovarian cancer. *N. Engl. J. Med.* 348:203-213.

Zhang, W., B. Baban, M. Rojas, S. Tofigh, S.K. Virmani, C. Patel, M.A. Behzadian, M.J. Romero, R.W. Caldwell, and R.B. Caldwell. 2009. Arginase activity mediates retinal inflammation in endotoxin-induced uveitis. *Am. J. Pathol.* 175:891-902.

Zhang, Z.X., K. Young, and L. Zhang. 2001. CD3+CD4-CD8- alphabeta-TCR+ T cell as immune regulatory cell. *J Mol Med (Berl)* 79:419-427.

Zhou, F., G.R. Leggatt, and I.H. Frazer. 2011. Human papillomavirus 16 E7 protein inhibits interferon-gamma-mediated enhancement of keratinocyte antigen processing and T-cell lysis. *FEBS J.* 278:955-963.

Zhou, J., W.J. Liu, S.W. Peng, X.Y. Sun, and I. Frazer. 1999. Papillomavirus capsid protein expression level depends on the match between codon usage and tRNA availability. *J. Virol.* 73:4972-4982.

Zhussupbekova, S., R. Sinha, P. Kuo, P.F. Lambert, I.H. Frazer, and Z.K. Tuong. 2016. A Mouse Model of Hyperproliferative Human Epithelium Validated by Keratin Profiling Shows an Aberrant Cytoskeletal Response to Injury. *EBioMedicine* 9:314-323.

Zohar, Y., G. Wildbaum, R. Novak, A.L. Salzman, M. Thelen, R. Alon, Y. Barsheshet, C.L. Karp, and N. Karin. 2014. CXCL11-dependent induction of FOXP3-negative regulatory T cells suppresses autoimmune encephalomyelitis. *J. Clin. Invest.* 124:2009-2022.

zur Hausen, H. 2001. Cervical carcinoma and human papillomavirus: on the road to preventing a major human cancer. *J. Natl. Cancer Inst.* 93:252-253.

Zweemer, A.J., J. Toraskar, L.H. Heitman, and I.J. AP. 2014. Bias in chemokine receptor signalling. *Trends Immunol.* 35:243-252.